Gamma-Interferon Attenuates Yellow Fever Virus Vaccine Strain 17D

by

Long Kwan Metthew Lam

Bachelor of Science, Washington State University, 2011

Submitted to the Graduate Faculty of

School of Medicine in partial fulfillment

of the requirements for the degree of

Doctor of Philosophy

University of Pittsburgh

2018

UNIVERSITY OF PITTSBURGH

School of Medicine

This dissertation was presented

by

Long Kwan Metthew Lam

It was defended on

January 22, 2018

and approved by

Zandrea Ambrose, Associate Professor, Department of Medicine

Simon Barratt-Boyes, Professor, Department of Infectious Disease and Microbiology

Penelope A. Morel, Professor, Department of Immunology

Mark J. Shlomchik, Professor, Department of Immunology

Dissertation Advisor: William B. Klimstra, Associate Professor, Department of Immunology

Gamma-Interferon Attenuates Yellow Fever Virus Vaccine Strain 17D

Long Kwan Metthew Lam, PhD

University of Pittsburgh, 2018

The genus *Flavivirus* in the family *Flaviviridae* consists of many medically important vector-borne viruses, including West Nile, yellow fever (YFV), dengue, and Zika viruses. In the recent decade, these viruses have emerged beyond their historical geographical boundaries, causing outbreaks and posing a threat to public health systems. Despite their medical importance, licensed, effective drugs and/or vaccines against these viruses are lacking, with the exception of the YFV. The live attenuated vaccine for YFV, strain 17D, is among the most effective viral vaccines ever developed. While this vaccine is relatively avirulent and highly immunogenic, its attenuated phenotype was derived by blind passage of a virulent strain, leaving the mechanisms of attenuation unknown. Moreover, 17D has been engineered as a delivery vector for heterologous antigens. Importantly, the successful and safe use of 17D as a vaccine vector and the development of live attenuated vaccines (LAVs) to related flaviviruses requires an understanding of the molecular mechanisms leading to 17D attenuation.

Using subcutaneous infection of interferon signaling-deficient mouse models of wild type yellow fever virus (WT YFV) pathogenesis and 17D-mediated immunity, we have investigate the role of type II interferon (IFN-γ) in attenuation of 17D *in vivo*. We found that in the absence of type I IFN (IFN-α/β), IFN-γ restricted replication of 17D but not WT YFV by 2 days post-infection. In this context, IFN-γ responses protected 17D-infected animals from mortality, largely restricted the virus to lymphoid organs, and eliminated viscerotropic disease signs such as steatosis in the liver and inflammatory cell infiltration into the spleen. In contrast, WT YFV

caused a disseminated infection, gross liver pathology, and rapid death of the animals. We also uncovered a mechanism by which IFN-γ can restrict 17D in human vacinees. IFN-γ treatment of myeloid cells suppressed the replication of 17D significantly more than that of WT YFV *in vitro*, suggesting a direct differential effect on 17D virus replication. Overall, our results indicate that an important mechanism of 17D attenuation *in vivo* is enhanced sensitivity to IFN-γ-stimulated responses elicited early after infection.

TABLE OF CONTENTS

LIST OF TABLES

LIST OF FIGURES

PREFACE

I would like to express my sincere thanks to my mentors Dr. William Klimstra and the late Dr. Kate Ryman for giving me a valuable scientific training experience and an opportunity to learn about not only science, but also the dynamics of the society and human interactions. I would like to thank current and past members of the lab, especially Derek Trobaugh, Alan Watson, and Whitney Lane in helping me during the difficult times I had endured. I would like to also thank my dissertation committee for their guidance through my dissertation.

1.0 INTRODUCTION

1.1 FLAVIVIRUSES

1.1.1 Classification of flaviviruses

The genus *Flavivirus* belongs to the family *Flaviviridae* and consists of over 50 types of enveloped viruses with a positive-sense single-stranded RNA genome (1). Members of *Flavivirus* have a wide range of vertebrate hosts including rodents (2), birds (3), primates (4, 5), bats (6–8), and ungulates (9). The *Flavivirus* genus includes many important pathogenic viruses that have shaped our history and offered valuable tools to study biology. Many flaviviruses are transmitted between vertebrate hosts by specific arthropod vectors such as mosquitoes or ticks, which likely limits the geographical distribution of individual viruses. Ecology of the vector, such as feeding preferences for specific vertebrate hosts, and constraints of the vertebrate-arthropod transmission cycle limits the propensity of these viruses for mutation and altered virulence (10–12).

Historically, flaviviruses have been classified based on their vector competency, vertebrate host, antigenicity, disease inflicted on host, and nucleotide sequence. Flaviviruses can

be broadly classified into mosquito-borne, tick-borne, zoonotic without known vector, and insect-specific viruses with no known vertebrate host based on their host and vector specificities. In support of this, a comprehensive phylogenetic analysis of the nonstructural protein 5 (NS5, the virus replicase) sequences from 73 flaviviruses has been used to construct a tree that clusters the viruses according to vector competence (1). However, classification based on vector-competency is inadequate because mosquito-borne viruses can be isolated from ticks (13), and vice versa (14–16). A more functional approach to classification is cross-reactivity to neutralizing antibodies, which is able to predict relatedness of flaviviruses similar to genetic phylogeny (17). However, antibody escape mutants, lack of cross-reactivity, and low resolution of the assay may complicate the analysis (18).

Flaviviruses can also be separated into two groups by the disease they cause in the vertebrate host. Hemorrhagic flaviviruses include yellow fever virus (YFV) and dengue virus (DENV), which cause viscerotropic disease (tissue damage in visceral organs such as the liver and the spleen) and potentially hemorrhagic fever in primates. The encephalitic flaviviruses, including Japanese encephalitis virus (JEV), West Nile virus (WNV), and Murray Valley encephalitis virus (MVEV) cause encephalitic disease in humans. Interestingly, among these mosquito-borne flaviviruses, disease manifestations are also reflective of the virus' natural transmission cycle. For example, the hemorrhagic YFV and DENV have a forest cycle that involves non-human primates as vertebrate hosts and *Aedes* mosquitoes as a principle vector whereas the encephalitic JEV, WNV, and MVEV are transmitted between birds and *Culex* mosquitoes. While both YFV and DENV are transmitted in an urban cycle between humans and *Aedes aegypti*, it should be noted that DENV is adapted to humans and does not require a forest cycle for maintenance.

1.1.2 Virion Structure and genome organization

The flavivirus virion is a 50nm-diameter particle with icosahedral (T=p3) symmetry and composed of nucleocapsid encased in a lipid membrane studded with envelope (E) and membrane (M) proteins. The nucleocapsid consists of capsid (C) proteins and one copy of the RNA genome. The lipid envelope, derived from the ER of the host cell, is embedded with 180 copies of E and M protein (19, 20). In immature particles, E and precursor-membrane (PrM) proteins form heterodimers. As the virus particle matures in the secretory pathway, the PrM protein is cleaved and E proteins form homodimers, which lie approximately parallel to the virus membrane. It should be noted that expression of PrM and E proteins results in production of 31.5nm-diameter sub-viral particles with T=1 symmetry (21).

The flavivirus genome consists of a single positive-sense RNA molecule of ~11kb in length that has a type I cap at the 5' terminus that is immediately followed by a conserved stem-loop structure (22). Most flavivirus genomes lack a poly-A tail at the 3' genome terminus except several variants of tick-borne flaviviruses (23, 24). The 3' terminal dinucleotides of flavivirus genomes are conserved 5'-AG…CU-3'. The flavivirus genome encodes a single polyprotein ORF consisting of 3 structural proteins followed by 7 major non-structural (NS) proteins arranged in C-PrM-E-NS1-NS2A-NS2B-NS3-NS4A-NS4B-NS5 sequential order. The polyprotein is cleaved by host and viral proteases during of the viral replication cycle.

1.1.3 Virus replication cycle

The replication cycle of flaviviruses begins with attachment of viral particles to susceptible host cells. The entry receptor(s) for flaviviruses is/are currently unknown; however, integrins, C-type

lectins, and heparan sulfate have been implicated as attachment factors for various flaviviruses (25–27). After attachment, virus particles enter the cell through clathrin-mediated endocytosis and undergo membrane fusion as the pH of the endosome drops. Membrane fusion delivers the viral genome into the cytoplasm where the flavivirus polyprotein is translated by host ribosomes and then is processed by host and viral proteases in an ordered manner. The NS5 viral polymerase synthesizes negative-strand RNA, which is used as a template to synthesize positive-sense genome progeny. The capsid-bound viral genome buds into E and PrM-studded ER membranes to generate an immature virus particle, which goes through the secretory pathway. PrM proteins on immature particles are cleaved by host furin as they mature and are secreted outside the cells, which completes the replication cycle.

1.1.3.1 Attachment and Entry

Flaviviruses, as with most arboviruses, have a wide host range and are capable of infecting a wide range of cells from different species *in vitro*; thus the surface glycoprotein E uses multiple receptors for different cell types and species, receptors common to many cell types, or a combination of both. The glycoprotein E is responsible for receptor binding and entry into target cells. C-type lectins such as DC-SIGN (25, 26) and CLEC5A (28, 29), and phosatidylserine (PtdSer) receptors such as TIM/TAM (30, 31) and human Axl (32) have been implicated as mammalian entry factors for flaviviruses.

Upon binding to the receptor, flaviviruses are endocytosed into clathrin-coated pits, followed by membrane fusion in pre-lysosomal endosomes that release the nucleocapsid into the host cytoplasm. In the endosome, pH reduction triggers conformational changes in the dimeric E protein that re-configures them into monomers and then trimers. Changes in E protein conformation expose a fusion loop and provide energy for membrane fusion. In contrast to other

enveloped virus genera such as *Alphavirus* (33), the pH threshold of membrane fusion by flavivirus occurs at a relatively high pH of 6.6-6.8 (34, 35), suggesting fusion at the early endosome. Furthermore, membrane fusion does not require cholesterol or sphingomyelin but its efficiency is enhanced by cholesterol (35–37). In addition to using the conventional entry pathway involving direct binding of virion to the receptor, antibody-bound flaviviruses can enter susceptible host cells using the Fc receptor *in vitro* through antibody-mediated enhancement (ADE); however, *in vivo*, ADE does not appear to be a major pathway involved in flavivirus infection or pathogenesis with the exception of DENV (38, 39). After membrane fusion, the nucleocapsid is released to the cytoplasm and translation of the viral polyprotein is initiated.

1.1.3.2 Expression and functions of viral proteins

In this section, the function of flavivirus proteins will be discussed. The flavivirus genome mimics host messenger RNA in that, upon release of the nucleocapsid to cytoplasm, it is translated. The viral genome contains a single ORF encoding a polyprotein that is co- and post-translationally processed into more than 10 proteins. The three structural proteins are capsid (C), precursor membrane (PrM), and envelope (E), which are necessary for packaging viral genomes and forming infectious particles. The nonstructural (NS) proteins are ordered as follows: NS1, NS2A, NS2B, NS3, NS4A, 2K, NS4B, and NS5. During translation, nascent polypeptide is inserted into the ER and cleaved by signal peptidase at the junctions between C/PrM, PrM/E, E/NS1, and 2K/NS4b, whereas the viral protease NS2B3 complex cleaves NS2A/NS2B, NS2B/NS3, NS3/NS4A, NS4A/2K, and NS4B/NS5 junctions at a conserved basic motif. The enzyme that cleaves NS1/NS2A is unknown. Genome architecture and the topology of the viral polyprotein are presented in figure 1.

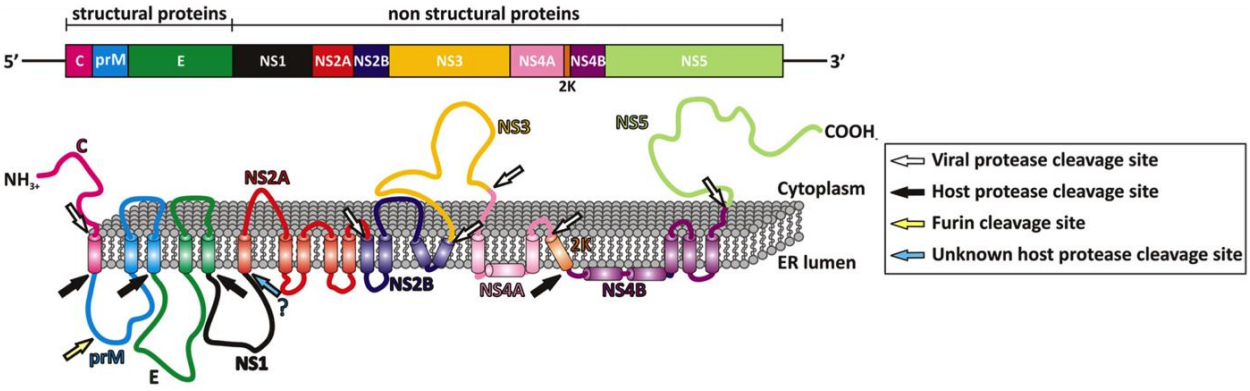

Figure 1: Topology of flavivirus polyprotein organization and processing.

Image adapted from (40).

Capsid

The capsid protein forms the viral nucleocapsid, which consists of multiple copies of capsid and one copy of viral genomic RNA. The capsid is a dimeric protein in solution that has a basic interface formed by the N- and C-termini and an internal hydrophobic domain (41, 42). The basic interface interacts with the 3'untranslated region (UTR) of the viral RNA and hence is responsible for packaging the genome whereas the hydrophobic interface interacts with the viral lipid membrane. Nascent, immature capsid peptide also contains a hydrophobic anchor sequence at the C-terminus that is necessary for peptide translocation of PrM into the ER. This anchor peptide is cleaved from capsid by NS2B3 at the late stage of the replication cycle to release capsid into the cytoplasm. The nucleotide sequence of capsid contains a conserved hairpin structure that directs ribosomes to the correct start codon. The capsid suppresses RNA interference in mosquito cells (43); however, its role in virulence in mammalian host remains unclear.

Precursor Membrane/Membrane

The M protein is translated as a precursor protein that functions as a chaperone to protect the E protein from undergoing conformational changes to the fusogenic form in the secretory pathway during virion egress. PrM is cleaved by a furin-like protease to M protein during migration through the secretory pathway. The C-terminus of M also mediates apoptosis *in vitro* (44).

Envelope

The E protein of flaviviruses is the major surface protein responsible for binding to target cells and fusing with endosomal membranes. Crystal structure and biochemical studies reveal that E protein is dimeric on the mature virion surface and contains three domains. Domain III has an immunoglobulin-like fold and protrudes from the virion surface, properties that corroborate its function as the receptor-binding domain (45–47). Domain II has an elongated structure that lies parallel to virus membrane and contains the fusion loop (nt 98-110) (48). Domain I is situated between domain II and III and has a β-barrel structure stabilized by disulfide bonds (48). In many flaviviruses, N-linked glycosylation in domain I masks the fusion peptide (49–51). Many neutralizing antibodies against flaviviruses are mapped to domain III; however, antibodies against other domains can be neutralizing, especially those that bind near or at the fusion peptide (52–54).

Multiple virulence determinants are located in the E protein. Mutations in domain III (E-303 and E-326) are associated with enhanced neurovirulence for YFV (55, 56). Residue 380 at domain III is relatively conserved among virulent flaviviruses. It forms the RGD motif that is implicated in binding to integrins (57). A synthetic peptide of residues 380-389 in DENV E protein blocked virus entry into mosquito cells (C6/36) but not mammalian baby hamster kidney (BHK) cells (58). Despite conservation of the RGD motif among many flaviviruses, mutagenesis

or blocking peptide fails to inhibit entry of other flaviviruses (57, 59). There are eight amino acid changes between Asibi and 17D substrains in the YFV E protein and the mutation at position 380 is implicated in virus attenuation. Detailed discussion of these amino acid changes and their implications for attenuation is presented in section 1.2. Nevertheless, these findings suggest E protein is an important virulence determinant of flaviviruses.

NS1

The first nonstructural protein, NS1, is a ~46kDa protein that is retained within, secreted from, and surface-associated with mammalian cells. Intracellular NS1 resides in vesicle packets that are thought to be site of virus replication and is necessary for synthesis of negative strand RNA in a virus species-specific manner (60). Trans-complementation of NS1-deficient YFV replicon with DENV NS1 did not rescue virus replication. Interestingly, a single mutation in NS4A permits YFV to use NS1 from both DENV and YFV, suggesting a genetic linkage of NS1 and NS4A (61). Two conserved N-linked glycosylation sites in NS1 have been shown to be important for RNA replication and subsequent virus production (62). Secretion of NS1 is regulated by the short peptide immediately after the signal peptide at residue 10-11 (63). Secreted NS1 activates complement with NS1 from DENV, YFV, and WNV binding C1s and C4, resulting in degradation of C4 and suppression of complement-mediated neutralization of virus (64). In addition, secreted NS1 from WNV also binds factor H, a regulatory factor for complement, and inhibits complement fixation (65). Association of NS1 with the endothelial cell surface and its ability to alter endothelial barrier integrity through modification of glycocalyx suggest that cell-associated NS1 is a virulence factor (66). In fact, flavivirus-infected humans and laboratory animals generate antibody against NS1, and some of these antibodies are protective (67–69).

NS2A

NS2A is a hydrophobic integral membrane protein that interacts with NS3 and is critical for packaging the nucleocapsid and forming the replicative complex (70). NS2A can be cleaved at the C-terminus, forming the NS2Aα protein with no known function. However, a basic residue at the cleavage site is necessary for packaging nucleocapsid in YFV particles (71). NS2A is also implicated in inhibition of interferon (IFN) responses (72, 73).

NS2B

NS2B is a cofactor for protease activity of the NS3. Ectopic expression of NS2B in *E. coli* enhanced penetration of impermeable antibiotics (74), and trimeric NS2B lysed red blood cells (75). These data suggest that NS2B can alter membrane permeability, but whether such a function occurs in more physiologically-relevant systems remains to be investigated. NS2B from DENV interacts with the innate DNA sensor cGAS, leading to its degradation and inhibition of apoptosis (76).

NS3

The NS3 is a 70kDa polyfunctional protein. The N-terminus of NS3 possesses serine protease activity that is activated by NS2B and is necessary for cleaving the viral polyprotein. Similar to other serine proteases, NS3 contains a catalytic triad and possesses strong substrate preference for consecutive basic residues (77). The protease complex NS2B3 also cleaves the host innate sensor STING to suppress interferon induction (78). The C-terminus of NS3 contains helicase and nucleoside triphosphatase (NTPase) activities important for replication. NS3 is also implicated in caspase recruitment and induction of apoptosis (79).

NS4A-2K-NS4B

NS4A and NS4B are small hydrophobic proteins (16 and 27kDa, respectively) connected by the short peptide 2K. NS4A is located in vesicle packets and convoluted membranes important for viral replication and polyprotein processing (80). NS4A also forms a stable complex with NS3 (81) and stimulates the helicase activity of NS3 (82). NS4B is an integral membrane protein that may play a role in viral replication as it co-localizes with dsRNA and NS3 (83). Both NS4A and NS4B can inhibit interferon signaling (72, 84) and induce autophagy (85–87). The connector peptide 2K is necessary for generating functional NS4B. Abolishing the 2K/NS4B cleavage site renders NS4B non-functional. Studies using lycorine, a flavivirus-specific inhibitor revealed that the 2K peptide may play an important role in virus replication (88).

NS5

NS5 is the largest protein encoded by the flavivirus ORF. NS5 can be detected in both cytoplasm and nucleus of infected cells. The N-terminus of NS5 has S-adenosyl methyltransferase (MTase) and GTP binding activity important for capping the viral genome (89). The C-terminus of NS5 contains the RNA-dependent RNA polymerase (RDRP), which replicates the viral RNA genome and contains the conserved Gly-Asp-Asp active site motif (90). This protein is also a virulence factor by targeting STAT2 for degradation via a ubiquitin-proteasome pathway (91, 92). Interestingly, NS5 from DENV can degrade the human STAT2 but not the murine homolog (91), suggesting host-specific subversion of antiviral mechanisms.

5' and 3' untranslated regions

The UTR of flaviviruses are important for regulating virus replication, virion packaging, and suppression of host IFN responses. The 5' end of the positive-sense RNA is capped,

allowing host translation machinery to recognize the RNA for translation. During replication, the virus genome circularizes due to complementary sequences in the UTR, which is described in more detail in the next section. The 3'UTR interacts with NS3 in the replicative complex (93).

Despite only possessing one putative transcriptional promoter, flaviviruses generate subgenomic RNA in host cells. The host exonuclease XRN1 participates in recycling nucleotides and controlling gene expression by degrading de-capped cellular mRNA (94). During replication, some copies of flavivirus genome are not capped and hence are susceptible to XRN1 degradation. However, two stem loop structures at the 3'UTR prevent complete degradation of the genome by stalling XRN1 (95, 96), forming a ~500nt fragment called subgenomic flavivirus RNA (sfRNA), which antagonizes IFN responses. Expression of sfRNA from JEV has been shown to suppress phosphorylation and nuclear translocation of IRF3. While sfRNA-deficient YFV and WNV replicate poorly in IFN-competent cells, they are able to replicate in cells deficient in IFN induction or response and when IFN is neutralized (97–99). DENV and ZIKV sfRNAs suppress IFN responses by antagonizing RIG-I and to some degree MDA5 (100). Studies with DENV reveal that sfRNA binds to and interferes with deubiquitination of TRIM25 and subsequent RIG-I activation, leading to suppression of IFN induction (101). In addition, dengue virus serotype 2 (DENV-2), but not YFV, Kunjin virus (KUNV), or DENV-3 modulate ISG induction through interaction with the stress granule proteins G3BP1, G3BP2, and CAPRIN1 (102), indicative of virus-specific functions of sfRNA.

1.1.3.3 Genome Synthesis

Upon translation and accumulation of nonstructural proteins, virus replication occurs. The negative strand is synthesized first, followed by the positive strand. RNA synthesis is performed by the replicative complex (RC) located in the invagination of ER membrane, composed of the

nonstructural proteins. NS2A, 2B, 4A, and 4B are involved in modification of ER membrane. Both NS3 and NS5 lack membrane-association regions (103). NS3 is likely anchored to the RC through interaction with NS4B via its helicase domain (104), whereas NS3-NS5 interaction aids retention of NS5 within the RC (105, 106). NS5 synthesizes and NS3 modifies the nascent strand. The current model for RNA synthesis by flaviviruses is that upon recognition of the positive strand by the RC, RDRP activity of NS5 synthesizes the negative strand, forming an RNase-resistant dsRNA replicative intermediate (RI). The RI is then re-used to synthesize the positive- or negative-strand RNA. During replication, the amount of positive strand is between 10- to 100-fold higher than negative strand (107). The mechanism controlling this ratio is unknown, but inhibition of genome circularization and sequestration of NS5 by sfRNA have been postulated as possible explanations (108).

Circularization of the flavivirus genome is important for efficient replication. The 5'UAR (upstream ATG region) and 5'CS (circularization sequence) base pair with the 3'UAR and 3'CS, respectively. These two pairs of complementary sequence elements are required for circularization and replication as mutations that abolish sequence complementarity in either one pair are lethal to virus replication (109). Circularization of the genome brings the conserved 5' stem loop, which binds to NS5, in close proximity to the 3' end, allowing genome synthesis to occur (110, 111).

RNA synthesis by flavivirus NS5 is initiated by *de novo* priming (110). A conserved histidine residue in the priming loop near the protein active site has been implicated in selecting ATP as the first nucleotide, as deletion of the priming loop led to incorporation of GTP instead (110). In the absence of an RNA template, NS5 only synthesizes the dinucleotide AG when Mg^{2+} is present, whereas NS5 coordinating with Mn^{2+} can synthesize other dinucleotides with a

preference for AG. These observations explain conservation of the end nucleotides 5'-AG…CU-3' for flaviviruses. After priming, the polymerase changes from the initiation conformation to the elongation conformation, allowing processive synthesis of nascent RNA. The MTase domain is important for this conformational change (89).

Following synthesis of the RNA, the 5' end of the positive strand is capped. Capping of flaviviruses follows the conventional capping mechanism similar to host mRNA, which begins with removal of a phosphate group from 5' triphosphate of the RNA by NTPase activity of NS3, followed by ligation of GMP by the guanylyl transferase in NS5. Finally, MTase methylates the guanosine cap at N7 position and the 2'OH of the first nucleotide (106, 111). No evidence for capping the negative strand exists.

1.1.3.4 Virion Assembly and Egress

Accumulation of viral genomes from replication eventually leads to packaging and egress of virions. Translation of the polyprotein results in ER-embedded PrM and E proteins. Capsid in the cytoplasm interacts with virus genome through its positively charged surface, forming nucleocapsid (42). No evidence for direct interaction of capsid with either PrM or E exists, and the mechanism by which nucleocapsid buds through the PrM and E coated membrane is unknown. NS2A may play a role in packing nucleocapsid in virions (112). Upon budding into the ER, immature virions are trafficked through the secretory pathways, where glycosylation of E and cleavage of PrM to M occur, resulting in mature infectious virions. It should be noted that cleavage of the chaperone protein PrM and protection of E protein by PrM is not uniform across a newly made virion, often resulting in mosaic virus particles that still retain some PrM proteins and/or contain copies of E proteins that adopt the acid-exposed conformation (113). These

differences in structure and composition of the virions have potentially important impacts on humoral immunity against flaviviruses (39).

1.1.4 Innate immunity against flaviviruses

The innate immune response is a relatively non-specific antimicrobial system that works with the adaptive immune response to restrain and resolve acute infection or protect vertebrate hosts from repeated infection. Flaviviruses are controlled by various innate pathogen sensors, inflammatory and cytokine responses, and immune cells. In particular, the interferon (IFN) system is important for resistance, control, and clearance of flaviviruses from infected vertebrate host. Defects in IFN induction and/or signaling can alter the outcomes of flavivirus infection. In addition to IFN and its downstream genes, NK cells are also important in controlling virus infection before the more specific and robust adaptive immunity is activated.

1.1.4.1 Interferon induction by flaviviruses

The RIG-I-like receptor (RLR) and Toll-like receptor (TLR) family pathogen recognition receptors (PRRs) are implicated in detection of pathogen-associated molecular patterns (PAMPs) associated with flaviviruses. In cell culture and animal studies, deficiency in PRRs leads to reduction in IFN and antiviral gene expression in a virus species-dependent manner. The RLR family members such as RIG-I and MDA5 detect dsRNA in the cytoplasm. Upon binding to the dsRNA substrate, ATP hydrolysis and oligomerization (114) of these sensors occur, allowing the sensors to interact with the adaptor protein MAVS on mitochondria or peroxisomes (115). The substrates of RIG-I are dsRNA bearing 5'-triphosphate or the absence of type I cap on dsRNA (116) whereas MDA5 detects long dsRNA (>300bp) (117–119). Activation of RLRs leads to

activation of TBK1 and initiates a signaling cascade that phosphorylates and activates transcription factor IRF3, which activates transcription of antiviral genes including type I IFNs (subtypes IFN-α4 and -β). Alternatively, PRR-mediated activation of IRF7, which is constitutively expressed in myeloid cells such as dendritic cells and macrophages, can also lead to rapid production of IFN-α/β (120). Upon secretion, IFN-α/β acts in an autocrine and paracrine manner to induce expression of various antiviral genes, PRRs, and transcription factors that lead to production of additional IFN.

Both RIG-I and MDA5 are implicated in sensing flaviviruses. WNV and DENV have been reported to replicate more efficiently in RIG-I-deficient mouse embryonic fibroblasts (MEFs). Correspondingly, these cells also had delayed IFN production and ISG upregulation (121–123). Similarly, MDA5-deficient MEFs have been shown to support greater WNV replication than WT MEFs; however, a delay in ISG induction is not observed. In addition, mice lacking either RIG-I or MDA5 are more susceptible to WNV infection (124). These results suggest that RIG-I and MDA5 are important for sensing WNV and DENV. In contrast, while JEV is more virulent in RIG-I-deficient mice and resulted in less IFN production, MDA5-deficient mice do not display enhanced susceptibility to the virus (117). RIG-I has also been shown to detect YFV in plasmacytoid dendritic cells (pDC). Interestingly, depending on the route of entry into pDC, RIG-I or TLR were differentially involved (125).

Members of the TLR family are transmembrane molecules expressed on the cell surface and in endosomal compartments in a cell type-dependent manner. The leucine rich repeats located in the ectodomain of TLRs mediate sensing of PAMPs. Binding of ligands to TLRs initiates a signaling cascade through the adaptor protein MyD88 for all TLRs except TLR3, which activates TRIF instead (126). Similar to RLRs, activation of TLRs results in activation of

transcription factors such as IRF3, IRF7, and NF-κB, leading to expression of antiviral molecules including IFNs.

Various TLRs are implicated in detection of flavivirus RNA. In human monocytes and fibroblasts, TLR3-mediated sensing of DENV are important for secretion of type I IFN and the proinflammatory cytokine IL-8 (127), whereas inhibition of TLR7 in human pDCs suppresses IFN induction upon DENV infection (128). Similarly, shRNA silencing of TLR-2, -7, -8, -9, and MyD88 suppresses IFN-β and cytokine production in human monocyte-derived dendritic cells (MoDCs) infected with YFV (129). In addition, pDCs secretes IFN-α/β upon ligation with YFV-infected cells in TLR7-dependent manner (125). In WNV infection, the role of TLR-3 and -7 remains controversial (130, 131). However, MyD88-deficiency renders mice more susceptible to WNV infection, suggesting a protective role for TLR signaling in WNV infection (132). On the contrary, MyD88-deficient mice do not display enhanced sensitivity to JEV (117).

Since RLR- and TLR-mediated sensing of viruses leads to robust antiviral responses, pathogenic flaviviruses have evolved to evade host recognition. While RNA fragments from WNV activate RIG-I and trigger the IFN response, WNV genomes and anti-genomes are poor activators for RIG-I (133), suggesting that potential secondary structures or genome modification may aid evasion of innate sensing. In addition, DENV also inhibits RIG-I activation by preventing its interaction with MAVS (134) and deubiquitination by TRIM25 (101), which is necessary for RIG-I activation. Overall, detection of flaviviruses by RLRs and TLRs is virus species- and cell type-dependent, and pathogenic flaviviruses deploy various means to suppress host virus sensing mechanisms.

1.1.4.2 Interferon antiviral activities against flaviviruses

IFNs are a group of broadly antiviral cytokines important for restricting pathogens and modulating other immune responses. Cells or animals lacking components of IFN induction or signaling are often defective in viral control and highly susceptible to infection with many different viruses including flaviviruses. There are three types of IFNs, and they have a similar overall signaling scheme (Fig. 2). Upon IFN ligation to its receptor, type I and III IFN utilize JAK1 and Tyk2 to phosphorylate STAT1 and STAT2, whereas type II IFN utilizes JAK1 and JAK2 to activate STAT1. These events lead to formation of STAT1/STAT2 heterodimers or STAT1 homodimers, which translocate to the nucleus and transcriptionally activate target genes. In addition, type I and type II IFN activate NF-κB and p38 MAPK, further regulating antiviral gene induction and fine-tuning the immune response (135).

Type I IFN (IFN-α/β) are broadly antiviral against flaviviruses *in vitro* and *in vivo*. IFN prophylaxis and treatment has been reported to suppress replication and delay death of mice infected with Modoc virus (a flavivirus) (136). This cytokine is also important in the pathogenesis of many flaviviruses, as animals lacking components of the IFN response, either pharmacologically (137, 138) or genetically (139–141), are more susceptible to flavivirus infection and disease than their immunocompetent counterparts. Many of the antiviral roles for IFN-α/β can be attributed to its direct antiviral effects due to induction of a large ensemble of antiviral gene products. While IFN-α/β serves as a major innate barrier for flaviviruses, it is also important for activation of T cells in WNV-infected mice (142).

Type II IFN (IFN-γ) also possesses moderate innate antiviral activities through induction of antiviral genes regulated by the gamma-activated sequence (GAS) promoter elements. Cells treated with IFN-γ are resistant to flavivirus infections *in vitro* (143–146); concomitantly,

prophylactic treatment of non-human primates with IFN-γ suppressed YFV load and disease (147). In addition, IFN-γ is a signature cytokine involved in differentiation of T cells to a TH1 phenotype. Details of IFN-γ induction and signaling of IFN-γ will be discussed in section 1.3.

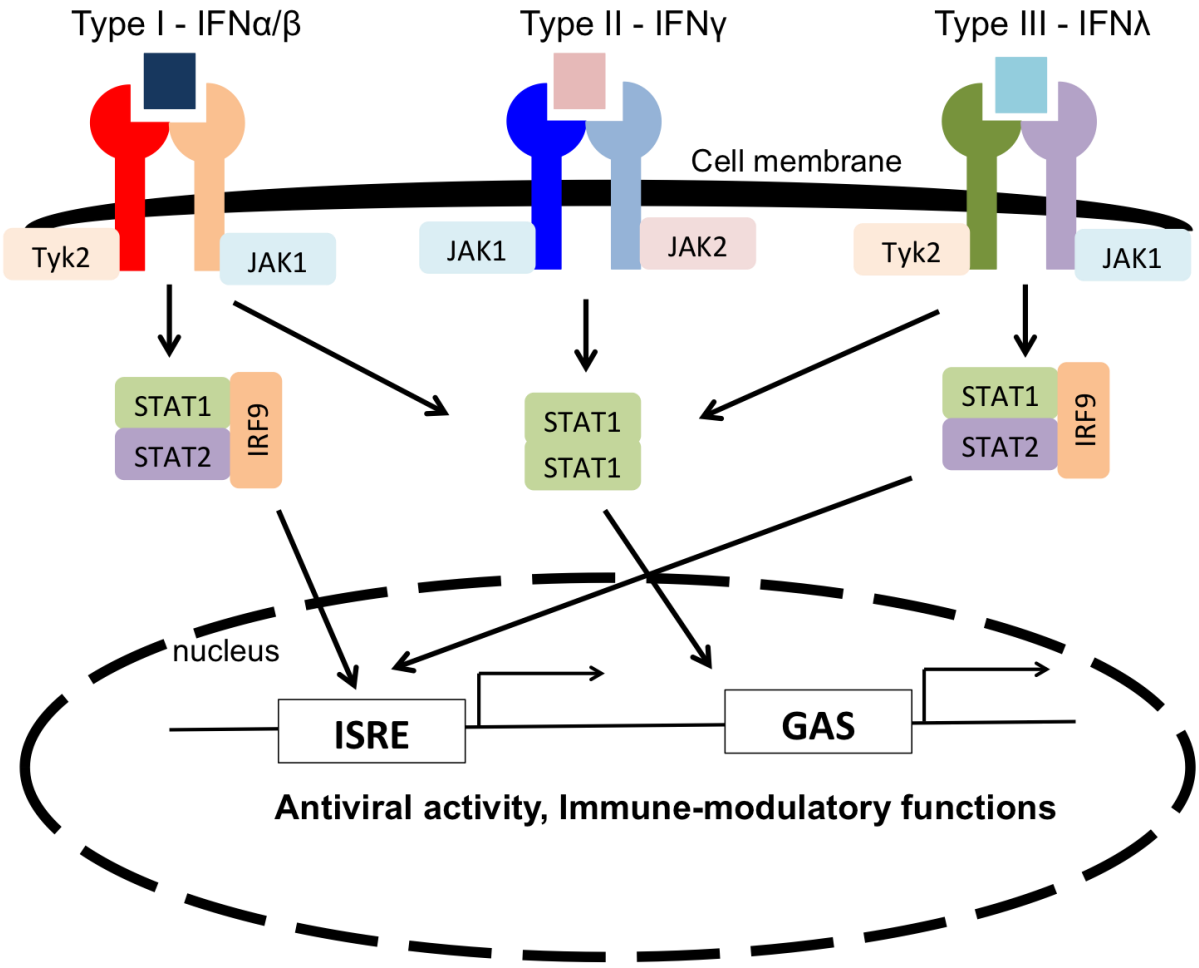

Figure 2: General interferon signaling pathways.

Similar to type I IFN, Type III IFN (IFN-λ) signals through STAT1 and STAT2, leading to a similar profile of antiviral gene induction. Despite activating similar transcription factors, direct antiviral activities of IFN-λ tend to be less robust than IFN-α/β (148, 149); however, IFN-λ has unique antiviral activities at the epithelial barrier. Neutralizing IFN-λ in placental organoids,

which produce IFN-λ constitutively, have been reported to enhance ZIKV replication (150). While IFN-λ does not inhibit WNV replication *in vitro*, mice lacking its receptor, IFNLR1, have enhanced vascular leakage and virus titer in the brain, suggesting IFN-λ is critical for restricting viral access through the blood-brain barrier (149). Similar barrier function is also observed in an encephalitic model for YFV (151).

1.1.4.3 Other innate immunity against flaviviruses

In addition to the IFN system, several other innate immune mechanisms play important roles in restricting flavivirus infection. The murine 2'-5' oligoadenylate synthetase 1b (OAS1b) is of particular importance for anti-flavivirus immunity. Mice have eight isoforms of OAS, which are involved in sensing dsRNA. Upon detection of dsRNA, OAS synthesizes 2'-5' oligoadenylate, which activates RNaseL to degrade cellular RNA, resulting in substrates for RIG-I and/or MDA5 activation (152). Genetic studies of mouse strains that are differentially resistant to flaviviruses but not other RNA and DNA viruses have revealed that a nonsense mutation leading to truncation of OAS1b is responsible for enhanced flavivirus susceptibility (153). One potential antiviral function of OAS1b is to inhibit viral replication as escape mutants insensitive to OAS1b frequently have mutations in the helicase domain of NS3 (154). However, the mechanism for OAS1b-mediated resistance remains elusive. In contrast to other OAS gene products, OAS1b does not have any apparent enzymatic activity. Overexpression of functional OAS1b or OAS1a only slightly restores anti-flavivirus activities. Thus, OAS1b is postulated to be a regulator for other OAS1 molecules and the truncated OAS1b is believed to work as a dominant negative inhibitor. It should be noted that humans have five OAS1 isoforms that are catalytically active and may be important for innate immune response against flaviviruses (155).

Natural killer (NK) cells are innate lymphoid cells that play crucial defense roles against many intracellular pathogens, including flaviviruses. NK cells can lyse virus-infected cells (156) and promote inflammation by producing cytokines such as IFN-α/β and -γ, TNFα, and RANTES (157, 158). Early activation of NK cells has been reported after YFV, DENV, and TBEV infection (159–162). NK cells can be activated by proinflammatory cytokines, ligation to cells lacking MHC-I, and antibody-bound cells (details discussed in section 1.3). To suppress NK cell activation and subsequent lysis of infected cells, surface MHC-I is upregulated in flavivirus-infected cells in a NF-κB-dependent and IFN-α/β-independent manner (163, 164). Expression of MVEV capsid and PrM enhanced surface MHC-I expression (165); however, DENV replicon expressing only nonstructural proteins also induced MHC-I expression (166), suggesting that flaviviruses may employ multiple mechanisms to enhance MHC-I expression and/or it is a virus-dependent process. Nevertheless, NK cell activation and differentiation are still observed *in vivo*. In addition to potential cytokine-mediated activation, direct ligation of domain III of E protein from WNV and DENV with the NK cell surface receptor NKp44 has been shown to trigger NK cell degranulation, lysis of infected cells, and induction of IFN-γ *in vitro* (167). In secondary infection, where anti-flavivirus antibody is present, antibody-mediated cellular cytotoxicity has been proposed to be a mechanism for NK cell-mediated control of DENV (156, 168).

1.2 YELLOW FEVER VIRUS

1.2.1 Transmission and Epidemiology

Transmission of YFV from its enzootic habitat to humans can be described in three main cycles – sylvatic, intermediate, and urban cycles. In the sylvatic cycle, YFV is circulated in the jungle between mosquitoes and non-human primates. In South America, the sylvatic cycle is primarily maintained by mosquitoes in the genus *Haemagogus* and *Sabethes*, whereas in Africa, the sylvatic cycle is primarily maintained by *Aedes africanus*. YFV replicates and seeds serum viremia in the non-human primate (NHP) host, allowing the subsequent blood-feeding mosquitoes to pick up the virus (169, 170).

In the intermediate cycle, YFV transmission to humans occurs when various tree-hole dwelling *Aedes* mosquitoes indiscriminately feed on humans rather than NHPs. The intermediate cycle primarily occurs in Africa where human activities and settlement tends to be proximal to jungles in contrast with South America. Human activities in forests such as logging and tourism, encroachment of human habitats into jungles (169), and environmental factors boosting mosquito populations such as rain or flood (171, 172) can enhance the risk of YFV spillover to humans. Human infections in the intermediate cycle can lead to outbreaks in urban areas when *Ae. aegypti*, an urban-dwelling mosquito that bites humans aggressively (173), feeds on YFV-infected individuals. This can occur when infected humans travel to urban areas to seek hospitalization. In this urban cycle, *Ae. aegypti* propagates YFV to a human host and subsequently to other *Ae. aegypti*, potentially leading to large-scale outbreaks.

Historically, the geographical range of YFV spanned North and South America, Europe, and sub-Saharan Africa, with outbreaks occurring in these regions during the 17th-19th centuries.

Due to active vaccination and mosquito abatement programs in the 19th century, YFV is currently only found in South America and sub-Saharan Africa; however, in recent decades, YFV has been re-emerging (169, 174–178). One prominent example is an outbreak in Uganda in 2011, which led to at least 58 deaths. This is the largest recorded YF outbreak in Uganda, and the last documented outbreak was in 1972 (175). The upsurge of YF cases has led the World Health Organization (WHO) to expand the definition of geographical regions that are considered to be at risk for YFV (178). The reason for YFV re-emergence is unknown. However, human encroachment to the sylvatic regions (175, 177) and lack of vaccination (179) are the likely contributing factors. In addition, an increase in traveler-associated cases has raised concern for potential expansion of YFV beyond its current boundary (180). Interestingly, local transmission of YFV has never been documented in Asia. This phenomenon may be explained by factors of vector competency and/or pre-existing cross-protective immunity from endemic circulation of DENV and JEV (181).

1.2.2 Pathogenesis and pathophysiology in human infection

Most YFV infections in humans are abortive or subclinical (182, 183); however, in symptomatic cases, the disease ranges from mild disease to fulminant pan-systemic disease. Disease severity and pathogenesis are influenced by the virus strain, host development and genetics, and environmental factors.

After a three to six day of incubation period, patients generally develop abrupt fever and chills. Three phases of disease have been described in human YF. In the initial phase, known as the “period of infection,” patients experience general malaise, headache, and nausea. Viremia peaks 2-3 days after the onset of illness. More severe signs including liver tenderness,

leukopenia, hyperemia of skin, and Faget's sign (fever with low pulse) are also commonly reported. The "period of infection" is followed by the "period of remission," where patients recover and symptoms disappear, lasting for up to 48hr. Most patients recover from YF at this point; however, 1 in 7 patients will progress to the severe disease phase known as the "period of intoxication" (169, 182, 184).

In the "period of intoxication," which occurs in three to six days after the onset of illness, patients experience moderate to severe hemorrhagic fever and multi-organ failure. Typical signs include high fever, black vomit, jaundice, enlarged liver, and renal dysfunction. Serum antibodies appears while viremia declines at this stage. In addition, both serum aspartate aminotransferase (AST) and alanine aminotransferase (ALT) levels are elevated, with AST surpassing ALT, indicative of muscle and liver damage. Serum transaminase and bilirubin levels directly correlate to disease severity. Proteinuria (excess protein in urine) and metabolic acidosis can be detected from patients' urine. Perivascular hemorrhage and edema in the brain indicates involvement of the central nervous system (CNS). In rare cases, neuroinvasion of virus and immune infiltration is possible. Jaundiced patients have an approximately 20% mortality rate. Survivors of YF have neutralizing antibodies against YFV and are considered to be protected from future infections.

1.2.3 Live attenuated vaccines for yellow fever

1.2.3.1 History of yellow fever vaccines

Historically, there have been two live attenuated vaccines used for YF, known as 17D and the French neurotropic vaccine (FNV). Both were developed independently during the late 1920s when researchers from the west were investigating YF outbreaks in West Africa. In the summer

of 1927, while studying YF in Ghana, Adrian Stokes and colleagues inoculated the blood from a 28-year-old patient, named Asibi, experiencing mild febrile illness, into rhesus macaques. Some of the infected animals showed signs of illness and histology similar to human yellow fever. Furthermore, blood from the sick monkeys was infectious and the infectious agent could be propagated in mosquitoes and/or monkeys. Importantly, Stokes also discovered that the infectious agent was filterable, suggesting bacteria were not involved. The virus, which was maintained by passaging in rhesus monkeys, was named Asibi (185). Tragically, Stokes contracted YF and passed away soon after the discovery. At the same time in Senegal, Sellards, Mathis, and Laigret isolated another YFV strain using a similar approach and named it Mayali, now known as French viscerotropic virus (FVV). In addition, the Sellards team found that the virus survived freezing in tissues (186), allowing storage and transport of the virus when monkeys were not available.

Vaccine development started when the Asibi virus eventually arrived at the Rockefeller Institute. Interest in vaccine development stemmed from the need to protect researchers and field workers from contracting yellow fever, which had led to at least 32 laboratory-acquired cases and 5 deaths between 1927-1931 (187). When Max Theiler and his colleagues attempted to culture the Asibi virus in small animal models via various routes of infection, only intracerebral inoculation led to disease and death of infected mice. After passage in mouse brain, the resulting virus lost viscerotropic virulence in rhesus monkeys but became more neurovirulent. In contrast, intrahepatic inoculation of rhesus macaques restored viscerotropism. The ability to alter virus virulence and tropism founded the basis for developing a vaccine for YFV. To attenuate YFV, the researchers serially passaged the Asibi virus 18 times in mouse embryos and 50 times in chicken embryos. To eliminate concern about enhanced neurovirulence, the virus was further

passaged 108 times in chicken embryos with neurologic tissues removed (188). Eventually, by passage 176, the resulting virus had lost viscerotropism and neurotropism in macaques, and infected macaques developed immunity against Asibi infection. This resultant attenuated virus strain was designated 17D and became parental material of the present vaccine for YFV. Since its derivation in 1937, new lots of the 17D vaccine have been generated by continued passaging of 17D in chicken embryos. Subsequent clinical trials demonstrated the safety of the vaccine for human use, and 17D was further passaged to generate sub-cultures for vaccine manufacturing. Today, two vaccine substrains exist; the sub-strain 17DD, maintained in Brazil and the 17D-213 line that is maintained by the WHO. The substrain 17D-204, which is commonly used in laboratory research, is the parent strain of 17D-213.

The second independent live-attenuated vaccine, the French neurotropic virus (FNV), was developed at the Pasteur Institute. FVV was attenuated by serially passaging through intracerebral (i.c.) inoculation of mice. Similar to Theiler's observation, the resultant virus lost the ability to cause viscerotropic disease in macaques but acquired enhanced neurovirulence in monkeys and mice at passage 128. Subsequently, the virus was named FNV for its neurotropism. At passage 237, the virulence of FNV remained stable and could induce protective immunity in humans upon skin scarification with viral inoculum. It was thus used as a vaccine in French-speaking colonies in Africa between 1939-1980. However, because FNV was associated with high rates of encephalitis, the WHO prohibited its usage in children less than 14 years of age. With the availability of 17D, the FNV lost popularity and was discontinued in 1980 (189).

While 17D is relatively safe and effective, achieving its widespread application was not without complications. In 1943, vaccination with the sub-strain 17DD, which was passaged more than 300 times, failed to elicit immunity due to the loss of infectivity in humans. Protective

immunity was restored by using vaccine stocks at lower passage. Moreover, hepatitis in vaccinees occurred because human serum was used as a vaccine stabilizer. This was resolved by replacing human serum with egg protein. In Brazil, cases of viral encephalitis in children were reported and led to the suspicion of residual neurovirulence in the vaccine. Due to such issues with the 17D vaccine, in 1945, the WHO generated guidelines and standards for YF vaccine manufacturing that employs a seed lot system to control passage level and a monkey neurovirulence test, which stated that i.c. infection with the vaccine stock in monkeys should lead to no more than one case of lesion in the brain and no serum viremia higher than 10^4 PFU/mL (190).

1.2.3.2 Innate Immunity to Yellow Fever Vaccination

17D vaccination triggers robust innate and adaptive immunity. In the first few days after 17D vaccination, local reactions such as redness and swelling often occur at the injection site, and low levels of circulating viral RNA and infectious particles are detectable in the blood. Elevated serum cytokines, including IFN-α, IFN-γ, IP-10, and MCP-1 can be detected early after vaccination (191). Early cytokine induction by 17D is likely due to activation of NK cells and DCs, as *ex vivo* stimulation of these cells led to activation and production of proinflammatory cytokines. However, the role of these cells and cytokines in controlling 17D remain unclear *in vivo*. Peripheral NK cells rapidly mature and differentiate in vaccinees as indicated by expression of CD57 and enhanced responsiveness to IL-12 and IL-18 (159). Elevated levels of TLR-3 and -9 have also been detected, suggestive of enhanced viral sensing capability. Differentiation of NK cells is independent of expression of NK cell inhibitory receptors, but the NK cell response is correlated to serum type I and/or type III IFN concentration. Interestingly, 17D infection in mice lacking the receptors for both type I and III IFN led to elevated numbers of NK cells in the

spleen and liver (151), whether this phenotype is linked to a failure in NK cell activation remains to be investigated. In vaccinated mice, NK cells in lymphoid tissues rapidly produced IFN-γ (160). Stimulation of monocyte-derived dendritic cells (moDC) from human vaccinees leads to production of IL-6, MCP-1, IL-10, IP-10, and IL-12 (p40 and p70) and upregulation of activation markers CD80 and CD86 (129). Similarly, *in vitro* infection of human DCs with 17D leads to upregulation of activation markers such as MHC-II, CD80, and CD83 and results in enhanced capability to present antigens to T cells (192). In mice, 17D-mediated DC activation, cytokine secretion, and enhanced antigen presentation are dependent on TLR and MyD88 signaling (129). Investigation of the transcriptome of PBMCs from human vaccinees has demonstrated the importance of innate immunity. Signature genes for the IFN response including STAT1, IRF7, OAS1, IFIT1, ISG15, and IP-10 are strongly upregulated and likely shape downstream responses for activating adaptive immunity (193).

1.2.3.3 Adaptive Immunity to Yellow Fever Vaccination

The goal of yellow fever vaccination is to induce of long-term protective immunity. The primary immune component involved in protection in humans is believed to be neutralizing antibody. Vaccination triggers a robust humoral response in humans, and >90% of vaccinees seroconvert within two weeks. Neutralizing IgM can be detected as early as six days post-vaccination, and the number of plasmablasts in circulation also increases and peaks at 14 days post vaccination (194). Persistent levels of serum IgM lasting for at least four years have been documented (195). Convalescent sera from human patients or vaccinees protect mice and monkeys from lethal YFV infection. Thus, serum antibody has been used as a correlate for protection. Detection of circulatory IgG, which can last more than 35 years (196–198), and increases in antibody titer upon booster doses (199), suggest the presence of a long-lived

memory response. In fact, vaccinees receiving hematopoietic stem cell transplantations for leukemia treatment have been reported to remain seropositive for YFV for at least one year after transplantation (200, 201), indicating that memory cells persist and remain functional in non-hematopoietic compartment. The mechanisms leading to a long-lived adaptive immune response are currently unknown. Antibody response to vaccination is correlated to expression of TNFRSF17, a receptor for B cell growth factor, in PBMCs, while detection of viral RNA up to 6 months post-vaccination suggests viral antigens may persist in vaccinees, potentially contributing to long-term protection (202).

In addition to neutralizing antibody, 17D vaccination elicits robust, polyfunctional, and long-term T cells responses. Activation of $CD8^+$ T cells can be observed as early as three days post-vaccination (193). Peak $CD4^+$ T cell responses occur between 7-14 days, whereas the $CD8^+$ responses peak between 14-28 days (194, 203, 204). Activation of $CD8^+$ cells appears to be antigen-driven (204). Around 5% of virus-specific $CD8^+$ T cells differentiate into either central memory (T_{CM}) or effector memory (T_{EM} or T_{EMRA}) T cells that persist for years (198). At the peak response, 17D-specific $CD8^+$ T cells express granzyme B and cytokines including IFN-γ and TNFα (203, 205), suggestive of cytolytic, polyfunctional T cells. For $CD4^+$ T cells, both TH1 and TH2 T cells are present, as are their signature cytokines (IL-2, IFN-γ, TNFα, and IL-12 for TH1 and IL-4, IL-5, IL-10, and IL-13 for TH2) in the serum of vaccinees (194, 206–209). However, one study suggested the response is polarized towards a TH1 phenotype as indicated by the typical $CXCR3^+$ IFN-γ^+ phenotype of $CD4^+$ T cells (208). After the peak response, YFV-specific $CD4^+$ T cells gradually gain expression of CCR7, indicative of a shift to T_{CM} phenotype. Since human experimentation is not feasible, the role of T cells in humans is unclear, but $CD4^+$ T

cells and antibodies protect mice from viscerotropic infection by WT virus (210) whereas $CD8^+$ T cells and antibodies protect mice from i.c. challenge (211).

1.2.4 Attenuation of Yellow Fever Vaccine strains

Despite a long history of 17D vaccination and numerous potential applications of 17D as a vector for other vaccines, very little is known about its attenuation mechanisms. Between 17D substrains and their parent Asibi strain, there are an average of 48 nucleic acid changes leading to 20 amino acid changes and 4 mutations in the 3'UTR (summarized in Table 1). The roles of these mutations in attenuation or pathogenesis of 17D have remained largely uncharacterized; however, two conserved mutations, M-L36F and NS4B-I95M, are consistently different between WT YFV strains (Asibi and FVV) and their corresponding attenuated strains (17D substrains and FNV) (212). For M-L36F, substitution of the analogous amino acid in JEV leads to a mutant virus defective in virion maturation. This residue is located at the perimembrane helix that interacts with the E protein. Of note, WT strains of JEV, DENV, WNV, and YFV have a nonaromatic aliphatic residue at M36 and alanine substitution does not alter virion production (213). It is possible that the aromatic property of phenylalanine or its bulky side chain can interfere with E protein interaction, resulting in altered kinetics of virus maturation and/or sensitivity to the antiviral response. NS4B is important for formation of the virus replication machinery and resistance to host immunity. I95M is located at the end of the helix α_2 where IFN antagonism and interaction with NS1 occurs (214). Attenuation of Asibi can also be achieved by serial passage of Asibi in HeLa cells six times. This strain, HeLa-p6, is attenuated in mice and has three amino acid changes, I95M, V98I, and E155K in NS4B (215), suggesting I95M is likely involved in attenuation *in vivo*. Interestingly, the V98I mutation was also observed in hamster-

adapted Asibi, which gained virulence in hamsters (216). While V98I is not likely to be involved in attenuation, development of mutations in NS4B during passaging or adaptation suggests mutations in NS4B are important for viral fitness in different hosts. It should be mentioned that the mutation NS5-P901L, which is observed in 17D substrains and HeLa-p6, might also contribute to attenuation (212, 215); however, little is currently known about this residue at this point.

There are eight amino acid differences in the E protein. E-M299I, E-S305F, E-T380R, and E-A407V are located in domain III, the putative receptor-binding domain. A positive-charge mutation, E-T380R is implicated in enhanced binding to glycosaminoglycans (GAGs). This mutation leads to enhanced virus clearance from circulation and hence attenuation *in vivo* (27). The role of other mutations has not been well characterized individually; however, one recent study suggested that 17D can enter susceptible mammalian cells through a clathrin-independent pathway whereas entry of Asibi requires clathrin-coated pits. The usage of this alternative entry pathway is mediated by mutations in the E protein and the mutation at position 380 alone is insufficient to generate this phenotype. Moreover, this clathrin-independent pathway triggers more robust innate immune responses, which may contribute to attenuation (217). E-G52R is located at the hinge region between domains I and II, which participates in fusion. Mutations in the hinge region can have inhibitory effects on virus entry. Cell culture-adapted JEV bearing a mutation at position 52 has reduced peripheral virulence (218) and possesses different antibody-binding activity than its parent strain (219). Substitution of the analogous residue in DENV-2 have no effects on virus growth or fusion activity *in vitro* (220). E-A170V, E-T173I, and E-K200T are located at the dimerization interface between M and E proteins. Reversion of position 173 to the WT residue leads to enhanced neurovirulence. In addition, reversion of both E-G52R

and E-T173I have been observed in neuroadaptated 17D, suggesting their potential role of neurovirulence *in vivo* (55).

Table 1: Sequence Comparison between YFV Asibi and its derivative strains.

Rows in grey are the 20 conserved amino acid differences between Asibi and substrains of 17D. Empty cells indicate that the amino acid or nucleotide is identical to Asibi.

Gene	Codon	WT	Attenuated strains				Adapted WT
		Asibi	**17D-204**	**17D-213**	**17DD**	**HeLa-p6**	**Hamster-p7**
M	36	L	F	F	F		
E	27	Q				H	H
E	28	D				G	
E	52	G	R	R	R		
E	155	D				A	A
E	170	A	V	V	V		
E	173	T	I	I	I		
E	200	K	T	T	T		
E	288	M				K	
E	299	M	I	I	I		
E	323	K					R
E	331	K				R	R
E	305	S	F	F	F		
E	380	T	R	R	R		
E	390	H				P	
E	407	A	V	V	V		
NS1	307	I	V	V	V		
NS2A	48	T				A	A
NS2A	118	M	V	V	V		
NS2A	167	T	A	A	A		
NS2A	172	T	A	A	A		
NS2A	183	S	F	F	F		
NS2B	109	I	L	L	L		
NS3	485	D	N	N	N		
NS4A	146	V	A	A	A		
NS4B	95	I	M	M	M	M	
NS4B	98	V				I	I
NS4B	144	E				K	
NS5	836	E	K	K	K		

NS5	901	P	L	L	L	L	
3′UTR	-	T	C	C	C		
3′UTR	-	T	C	C	C		
3′UTR	-	G	A	A	A		
3′UTR	-	A	C	C	C		

1.2.5 Severe adverse events associated with 17D vaccination

Yellow fever vaccination is associated with mild adverse events such as myalgia, headache, and local reactions at the site of injection and severe adverse events (SAEs) including anaphylaxis and hypersensitivity and rare but potentially lethal neurotropic (YEL-AND) and viscerotropic (YEL-AVD) manifestations. Anaphylaxis and hypersensitivity due to 17D infection are not well studied. Some cases are linked to patient histories of allergy to known allergens in the vaccine; however, the absence of gelatin or egg allergy in some patients suggests the antigens and/or other ingredients may serve as allergens (221). Similar negative consequences have also been reported for other vaccines. YEL-AND and YEL-AVD are unique to YF vaccination. Currently, documented or suspected cases of YEL-AND and YEL-AVD number at least 200 and 70, respectively. Most cases have occurred after primary vaccination, and at least four cases have occurred after a booster dose (1 for YEL-AVD; 3 for YEL-AND) (184, 212). YEL-AND includes several typically self-limiting neurotropic syndromes such as Guillain-Barré syndrome, meningitis, encephalitis, and disseminated myeloencephalitis, followed by complete recovery. However, residual ataxia has been reported for 11 months in one case (222) and at least one death occurred in an HIV-positive patient with a low CD4 count (223). YEL-AND is more common among infants, especially before 1950, when infants younger than 4 months old were commonly vaccinated. Post-vaccination encephalitis has been associated with regain of neurovirulence through manufacturing, leading to the implementation of the seed-lot system and

monkey neurovirulence test, described above, to ensure efficacy and safety. Today, despite stricter safety standards, YEL-AND still occurs, suggesting additional, unknown underlying causes exist. Age-dependence of blood-brain barrier integrity and immune maturity has been hypothesized for increased risk for neurologic disease in infants (224). The incidence of YEL-AND is higher in males. The overall fatality rate for YEL-AND is 5% (184).

In YEL-AVD, patients experience a syndrome resembling WT virus infection – pansystemic disease with high virus titer in visceral organs and cytokine storms, with 60% lethality (169). Patients who survive YEL-AVD tend to have higher than expected antibody titers (≥1:10,240), which are likely due to overwhelming infection and high antigen levels (225–228). Advanced age and history of thymic disorder are considered potential risk factors (229), but no single factor has been identified as the cause of these SAEs, although host genetics and virus mutations are hypothesized to contribute. In one case, a patient, who had enhanced and prolonged serum viremia and T cell response, was found to possess single nucleotide polymorphisms (SNPs) in the CCR5 and RANTES genes (230). While virus isolated in another YEL-AVD case had amino acid changes compared to the parent virus from the vaccine stock (231), virus mutations are not always found in YEL-AVD patients (232). Some YEL-AVD cases have occurred concurrently with additional traveler vaccinations (228) and immune interference has been documented (233), raising the possibility that multiple vaccinations with 17D may increase the risk for SAEs. Together, the data on 17D-associated SAEs highlight not only the very limited understanding we have of this vaccine and its mechanisms of attenuation and immune response elicitation, but also the critical need to address these gaps in knowledge. Before 17D can be used extensively for other applications, such as heterologous vaccine development, the molecular mechanisms conferring its attenuation phenotypes must be

delineated because these vaccine candidates may retain the ability to cause SAEs. This knowledge will facilitate further studies into the mechanisms underlying SAEs and what can be done to improve the safety profile of 17D-based therapeutics in the future.

1.3 GAMMA-INTERFERON AND ITS ANTI-FLAVIVIRUS ACTIVITIES

Type II interferon (IFN-γ) is an important cytokine in both innate and adaptive immunity against many pathogens. IFN-γ is mainly produced by NK, NKT, T, and innate lymphoid cells (234–236). Macrophages (237), dendritic cells (238, 239), neutrophils (240), and B cells (241) have been implicated to produce IFN-γ in certain experimental systems. The immune-modulatory functions of IFN-γ are important for suppressing intracellular pathogens in responsive cells. In addition to inducing antiviral states, similar to other IFNs, IFN-γ strongly induces nitric oxide, GTPases that modulate intracellular membranes, and proteins involved in antigen presentation (145, 242, 243). In fact, deficiency in IFN-γ induction or response enhances susceptibility to intracellular pathogens ranging from bacteria, parasites, and viruses, highlighting its broad role in antimicrobial immunity (244–247).

1.3.1 Induction and transcription regulation of IFN-γ

1.3.1.1 Transcription regulation of IFN-γ

The *Ifng* gene is composed of four exons spanning 5.5kb and a 600bp upstream promoter element located on chromosome 12 in humans and chromosome 10 in mice. Gene sequences and regulatory elements at this locus are highly conserved between humans and mice. The *Ifng*

promoter contains binding sites for various transactivation factors such as STAT4, NF-κB, and T-bet and repressors such as STAT6, SMAD3, and GATA3 (248). Within the intronic regions of *Ifng*, hotspots of DNA methylation and histone modification sites also regulate its expression. Downstream of *Ifng* is the non-coding RNA *Tmevpg1* that can enhance *Ifng* transcription (249). In addition, *Ifng* is flanked by multiple distal conserved noncoding sequences (IfngCNS) containing CpG sites and hot spots for histone modification located at least kilobases away from *Ifng* (248, 250). These IfngCNS are important for fine-tuning transcriptional regulation of *Ifng* in T cells.

Naïve CD4 T cells are capable of differentiating into various lineages of helper T cells to exert specific immune functions, and IFN-γ is a signature cytokine of differentiation into the TH1 phenotype. In naïve CD4 T cells, the *Ifng* promoter site is unmethylated; however, methylation at CpG sites of intronic regulatory elements and the absence of histone modifications that favors transcription (H3-K4^{Me} and ^{Ac}H4) at the promoter, and intronic regulatory elements suppress *Ifng* transcription. TH1 signals such as IL-12 trigger epigenetic changes to the *Ifng* locus, leading to demethylation of the intronic regulatory elements and acetylation of histones H3/H4 around the *Ifng* loci, including IfngCNS (250). Chromatin remodeling enhances DNase sensitivity of this locus, indicating increased accessibility of the gene and active transcription. In contrast, TH2 stimuli such as IL-4 lead to hypermethylation of the *Ifng* promoter, suppressing expression of *Ifng* and differentiation towards the TH1 phenotype (250, 251); however, ectopic overexpression of T-bet in terminally differentiated TH2 overrides the repression and results in IFN-γ expression (252).

The NF-κB family transcription factors are activated by multiple pathways and are important in IFN-γ expression in T and NK cells. The NF-κB family proteins such as RelA

(p65), RelB, c-Rel, p50 (NF-κB1), and p52 (NF-κB2) have been shown to play important roles in T cell differentiation. Active NF-κB complexes are composed of heterodimers of RelA/p50 or RelB/p52. Both RelA and RelB contain a transactivation domain and a DNA-binding domain, whereas p50 and p52, which contain only the latter, are implicated in gene repression; however, Bcl-3, which has a transactivation domain, can associate with p50 dimers, resulting in gene induction (253). NF-κB in cytoplasm is normally sequestered by the inhibitor IκB. Upon stimulation, IKK phosphorylates IκB, leading to its degradation and release of the active NF-κB complex, which enters the nucleus and activates transcription of many genes, including proinflammatory cytokines (254). Expression of degradation-resistant IκB in naïve T cells suppresses TH1 polarization and IFN-γ expression (255). In addition, RelB-deficient T cells fail to express STAT4, T-bet, and IFN-γ upon IL-12 treatment (256, 257). On the contrary, while p50- or Bcl-3-deficiency suppresses TH2 differentiation upon IL-4 treatment, enhanced proliferation and IFN-γ secretion is detected in p50-deficient mice (257). Interestingly, deficiency in c-Rel does not affect T cell polarization, but c-Rel knockout mice are deficient in IFN-γ secretion by NK cells, indicating the influence of lymphocyte differentiation and IFN-γ production by NF-κB family members is cell type-dependent (253, 257). The long non-coding RNA located downstream of *Ifng*, *Tmevpg1*, also regulates *Ifng* expression (249). *Tmevpg1* opens up the chromatin by recruiting WDR5, a subunit in H3K4 methyltransferase to the *Ifng* loci (258). *Tmevpg1* overexpression is insufficient for inducing IFN-γ and T-bet is required to stimulate IFN-γ transcription in CD4 T cells; concomitantly, expression of *Tmevpg1* is controlled by STAT4 and T-bet (259).

1.3.1.2 Regulation of IFN-γ in NK cells

Constitutive expression of *Ifng* positions NK cells to produce IFN-γ rapidly upon activation (235). NK cells can be activated by two major pathways – surface receptors and cytokines. NK cells express multiple surface receptors that regulate their activities. Activation receptors recognize the presence of stress signals such as MICA, specific C-type lectins, and antibodies on the target cells (234). These receptors are associated with ITAM-containing proteins, which upon activation, lead to phosphorylation of src family phosphotyrosine kinases (PTKs), Syk family kinases, and eventual activation of MAPK pathways (234). Activation of MAPK kinase and subsequent calcium ion influx are critical for IFN-γ secretion for both murine and human NK cells, despite possessing different activating receptors. On the contrary, inhibitory receptors, which contain ITIMs, recognize MHC-I and deactivate NK cells through activating SHP family phosphatases that dephosphorylate kinases downstream of src (260). Thus, the balance of activation and inhibitory signals is an important fulcrum for IFN-γ production versus inhibition through this pathway.

NK cells can also be activated by cytokines. IL-12p70, an active heterodimeric cytokine composed of p35 and p40 chains, is a prominent IFN-γ inducer that signals through STAT4. While the source for IL-12 is debatable and is likely immune context-dependent, macrophages (261–263), dendritic cells (264, 265), and PMNs (266, 267) have been implicated as IL-12 secretors. IL-12 also indirectly enhances IFN-γ expression through induction of CD28. Ligation of CD28 with CD80/86 enhances NK cell cytotoxicity and IFN-γ production (268, 269). IL-12 induces T-bet expression, which is the signature transcription factor for TH1 polarization. In murine NK cells, while T-bet deficiency does not influence the capability to produce IFN-γ, T-bet is needed for sustained IFN-γ production; correspondingly, T-bet binds to *Ifng* upstream of

the promoter site (252). IL-2 primarily signals through STAT3 and STAT5, but it also activates STAT4 and MAPK in NK cells and leads to IFN-γ production (270); it also enhances IFN-γ production independent of STAT4. Other proinflammatory cytokines cannot induce IFN-γ secretion alone but augment *Ifng* transcription in IL-12- and IL-2-responding cells. Type I IFN primarily signals through STAT1 and STAT2 but can also activate STAT4 to enhance *Ifng* induction (271). IL-1 (272) and IL-18 (273), which activate NF-κB, have also been shown to augment *Ifng* transcription. IL-15 may work in synergy with IL-18 to stimulate IFN-γ expression; moreover, IL-15 is a proliferation and maintenance signal for mature NK cells. Deficiency in IL-15 or its receptor led to loss of NK cells in mice (274, 275). On the other hand, IL-10 and TGFβ negatively regulate induction of IFN-γ. IL-10 has been shown to both stimulate and inhibit IFN-γ production by NK cells through distinct mechanisms. While IL-10 augments IFN-γ production by activated NK cells (276), it also inhibits IL-12 production by myeloid cells, indirectly suppressing IFN-γ induction (277). TGFβ is an important negative regulator for IFN-γ. TGFβ signals through SMAD3 complexes, which occupy the *Ifng* promoter, subsequently suppressing transcription (278, 279). It also inhibits expression of STAT4, IL-12Rβ2, and T-bet, which are important for IFN-γ expression, but such inhibition can be countered by IL-12, IL-15, and IL-18.

1.3.1.3 Regulation of IFN-γ in T cells

Production of IFN-γ by T cells is contingent upon T cell maturation and differentiation. Thus, *Ifng* gene expression is tightly regulated in T cells. Activation signals from the TCR and ligation of CD28 to the co-stimulatory molecules CD80 or CD86 on antigen-presenting cells drive maturation of naïve T cells. While naïve $CD8^+$ T cells have a strong tendency to mature into cytolytic lymphocytes that secrete IFN-γ, differentiation of $CD4^+$ T cells requires additional

cytokine signals. Similar to NK cells, IL-12 also promotes TH1 development and *Ifng* expression in T cells; however, STAT4-deficient cells are capable of producing a low level of IFN-γ in response to TCR ligation, suggesting IL-12/STAT4 signaling is needed for amplification but not initiation of IFN-γ transcription in $CD4^+$ T cells. Sustained TH1 response and IFN-γ production requires STAT4 and T-bet (280).

Activation signals and costimulation combined with IL-12 drive expression of T-bet and subsequent *Hlx* and *Runx3* transcription. HLX is a homeobox transcription factor that increases chromatin accessibility for *Ifng* (281). Sustained HLX expression in mature TH1 suggest its role in genetic imprinting and/or maintenance of the TH1 phenotype (282). T-bet and RUNX3 bind to and activate the *Ifng* promoter while silencing IL-4 expression, further polarizing immune response towards the type I phenotype (283). Secretion of IFN-γ by memory T cells (T_{MEM}) is more rapid and has a lower threshold than naïve T cells. T_{MEM}, especially $CD8^+$ T_{MEM}, are capable of producing IFN-γ within hours of stimulation by cytokine or antigen in the absence of costimulation (284). This can be attributed to the higher levels of IL-12β2 and IL-18 receptors in memory cells.

1.3.2 Signaling of IFN-γ

Upon ligation of IFN-γ to the receptor complex IFNGR1/IFNGR2, JAK1 and JAK2 trans-phosphorylate each other and the receptor, creating docking sites for STAT1 and leading to STAT1 phosphorylation at Y701 (pSTAT1). Active pSTAT1 dimerizes and translocates to the nucleus. Active pSTAT1 dimers induce expression of target genes regulated by the gamma-activated sequence (GAS) element. In the nucleus, acetylation of pSTAT1 by CBP acetyltransferase lead to recruitment of phosphatases and inactivation of STAT1, which is

shuttled back to cytoplasm for re-activation (285). Maximum transactivation by STAT1 also requires activation of PI3K by the JAK kinases phosphorylating and activating PKC, which in turn phosphorylates STAT1 at S727 (286–288).

In addition to STAT1, IFN-γ also activates other signaling pathways, including STAT3, MAPK, and mTOR pathways in a cell type- and stimulus-dependent manner. IFN-γ treatment results in transient activation and phosphorylation of STAT3 at Y705 in a GSK3β- and src kinase- dependent manner, resulting in transcription of survival genes (289). MAPK is a signaling pathway that involves cascades of kinases and results in activation of many genes. IFN-γ activates the MAPKs JNK-1, p38, and ERK1/2, which play distinct functions in macrophages. JNK-1 activates genes associated with antigen presentation (CIITA, MHC-II) whereas p38 activates primarily transcription of chemokines (CCL5 and IP-10) and proinflammatory molecules (nitric oxide and TNFα). While Erk1/2 is also phosphorylated in IFN-γ-treated cells, modest effects are observed on inflammation and antigen presentation (290). Downstream of PI3K, Akt and mTOR are activated, which regulate mRNA translation. In macrophages, suppression of mTORC1 and translation upon IFN-γ treatment inhibits non-opsonized phagocytosis (291) and promotes autophagy (292). In fibroblasts and monocytes, mTORC2 is activated and necessary for induction of antiviral responses (293). Activation of additional signaling molecules such as STAT5 and CrkL/C3G has been reported also (294); however, their effects on immune modulation remain unclear.

Termination of IFN-γ signaling is important as sustained interferon signaling results in chronic inflammation that could be pathological. IFN-γ responses can be halted by inactivation of downstream signaling molecules and by abolishing IFN-γ-receptor interaction. The suppressor of cytokine signaling (SOCS) molecules SOCS-1 and SOCS-3 (295, 296), which are downstream

of STAT1, inactivate JAK1/2 and provide negative feedback to inhibit signaling. Mice lacking SOCS-1 rapidly succumb to autoimmunity and inflammation (297). Conversely, overexpression of SOCS proteins can reverse IFN-γ-mediated chronic inflammation (298). The SOCS family molecules inhibit JAK-STAT signaling by binding and sequestering JAKs (299–302) and/or targeting them for proteasome degradation (303). Tyrosine phosphatases such as TC-PTP and the SHP family phosphatases inactivate IFN-γ signaling by dephosphorylating the receptor, JAK, and STAT1. Receptor endocytosis has also been hypothesized to influence IFN-γ signaling. Upon ligation to the receptor, IFN-γ/IFNGR complexes are aggregated on lipid rafts and endocytosed in clathrin-coated pits, leading to degradation of IFN-γ by fusion with lysosomes. Alternatively, IFNGR has been reported to localize in cav-1-containing caveolae (304). While IFNGR is not endocytosed by caveolae, cav-1 acts like a SOCS protein by interacting with and inhibiting JAK2, and deficiency of cav-1 results in hyperactivation of JAK-STAT signaling and pathology *in vivo*.

1.3.3 Control of flaviviruses by IFN-γ

Because IFN-γ signals through STAT1, establishment of innate antiviral state through induction of ISGs is likely one mechanism for IFN-γ control of flaviviruses. Treatment of various cell types with IFN-γ inhibits replication of JEV, TBEV, WNV, and DENV *in vitro* (143–146). In mice lacking IFN-γ response, defects in viral control as early as one day has been reported (146). IFN-γ-activated macrophages possess enhanced phagocytic activity and capacity to eliminate pathogens (305). One effector downstream to IFN-γ is induced nitric oxide synthase (iNOS), which generates nitric oxide, a potent radical that can modify macromolecules (306). Inhibition

of JEV by IFN-γ treated macrophages is dependent on nitric oxide induction, as pharmacological inhibition of iNOS abolished the effects of IFN-γ (145).

IFN-γ also influences the pathogenesis of various flaviviruses differently. IFN-γ-deficiency resulted in increased viral load in the spleen and the CNS of mice infected with WNV (146) and DENV (246), whereas in MVEV (140) and JEV (307) infection, only the CNS viral load was increased. Prophylactic treatment of NHPs with IFN-γ suppressed WT YFV replication and delayed death (147). In addition, the sources of IFN-γ are also dependent on the virus and/or the model. IFN-γ, which regulates T cell differentiation and class switching, is also important in formation of memory response as 17D vaccinated IFN-γ-deficient mice exhibited poor virus control upon intracerebral challenge (308).

1.4 MAMMALIAN MODELS FOR YELLOW FEVER VIRUS

Animal models are valuable for understanding host-pathogen interactions. Historically, YFV has been studied in multiple mammalian models that recapitulate various aspect of YFV biology, each with its own benefits and drawbacks. A good animal model should recapitulate important aspects of human-pathogen interactions despite potential genetic and physiological discrepancies. Technical aspects including cost-effectiveness and availability of reagents are also critical. To model YFV, considerations such as route and dose of infection, disease course and pathology, and immune response should be made. One major challenge for developing a small animal model for YFV is resistance to disease by non-primates. One possible explanation is that, because YFV is transmitted between primates and mosquitoes in nature, the virus may have

evolved to overcome the primate immune system but not necessarily the murine immune system. In this section, common animal models for studying YFV will be briefly discussed.

1.4.1 Non-human primate

Genetic and physiological similarities between human and non-human primates (NHPs) make NHPs valuable for studying YFV biology. In NHPs, subcutaneous (s.c.) infection with virulent wild-type YFV leads to viscerotropic disease similar to human YF, and vaccination with 17D leads to protection from wild-type virus challenge. The NHPs are valuable tools for studying immunity, pharmaceuticals efficacy, vaccinology, pathogenesis, and ecology with respect to YFV; however, the cost, availability of molecular tools, and genetic variations among individual NHPs hinder their extensive use as a model (185, 309). Furthermore, different species of NHPs, particularly old world versus new world monkeys, respond differently to YFV infection. Specifically, with the exception of rhesus and cynomologous macaques, old world NHPs such as baboons experience milder disease than new world NHPs such as marmosets, which are highly susceptible to YFV infection (310). This is largely consistent with the fact that YFV originated in the old world and spread to other continents through slave trade; hence, old world NHPs likely co-evolved with YFV and are more resistant to it.

In rhesus macaques, infection with WT YFV usually leads to a more rapid and severe disease than in humans. Upon s.c. infection, serum viremia is detectable at 3dpi and continues to increase until the host succumbs to disease, which often occurs within a week. In deceased monkeys, cytokine storm, lymphopenia, and necrosis in visceral organs like spleen, liver, and kidney are observed. Decline in liver and kidney functions are detected within 24hr before death. Interestingly, YFV antigen is only detectable in liver but not spleen or kidney, suggesting soluble

mediators rather than viral replication may contribute to YFV pathogenesis in this model (224, 309). In addition, expression of zinc-binding proteins is disrupted in WT infection but not 17D vaccination in circulatory monocytes, which may explain the differential pathogenesis between virus strains.

1.4.2 Golden Syrian Hamster

The Golden Syrian hamster (*Mesocricetus auratus*) is a susceptible host for YFV. Intraperitoneal (i.p.) infection with WT strains of YFV results in viremia without obvious signs of disease in hamster; however, hamster-adapted WT virus strains of Asibi (216) and Jimenez (311, 312) lead to viscerotropic disease similar to human YF in this model. When compared to the parent Asibi strain, the hamster-adapted Asibi strain has 11 nucleotide changes, leading to seven amino acid changes. No nucleotide change occurs in the UTRs. Among these amino acid differences, five occur in the E protein, one in NS2A, and one in NS4A. While the contribution of these mutations to pathogenesis remains to be studied, it is likely that changes in E protein aid receptor binding or entry processes because most of these mutations are located at the exposed surface of domain III of E protein, which binds the receptor (216). The need to adapt the virus in hamster and the lack of immunological reagents renders direct comparison of 17D to Asibi difficult in the hamster model; however, this system has been useful in evaluating drug candidates against YFV. Two antiviral compounds, Flavipiravir (an RDRP inhibitor, also known as T-705) (313) and BCX-4430 (a nucleoside analog) (314), have been shown to have potent antiviral activities against YFV in hamsters. It remains to be investigated if such results can translate to humans clinically. Prophylactic treatment with IFN delivered by an adenovirus vector also protects hamsters from YFV infection (315).

1.4.3 House mouse

The house mouse (*Mus musculus*) from various backgrounds such as 129, BALB/c, Swiss, and C57BL/6 has been used for studying YFV. Immunocompetent adult mice are highly resistant to peripheral infection with both WT and 17D viruses but are susceptible to i.c. infection that leads to encephalitic disease. However, this model does not readily distinguish 17D and WT strains. One way to circumvent the need for i.c. infection is neuroadaptation of YFV. Serial passaging of 17D in mouse brain suspension led to enhanced neuroinvasiveness and neurovirulence and adult mice were susceptible to i.p. infection of the neuroadapted 17D (55). In contrast to adult mice, suckling mice are susceptible to peripheral infection with YFV through the i.p. route. While 17D and WT strains can be differentiated based on relative virulence, infection still results in lethal encephalitic disease and susceptibility to both viruses is age-dependent.

Mice lacking various innate immune components have proven to be extremely valuable in studying YFV. From an evolutionary perspective, YFV circulates between mosquitoes and NHPs but not rodents; thus, it is rational to reason that YFV has adapted to overcome antiviral mechanisms in primates more efficiently than in rodents. This is corroborated with reports that multiple flaviviruses antagonize human IFN response proteins more efficiently than the murine homologs (78, 91, 92). Intraperitoneal infection with WT YFV strain Asibi in rhesus macaques is uniformly lethal whereas nude-athymic mice are protected (316), suggesting that murine innate immunity exerts a strong blockade against YFV infection (317). Mice that lack the type I IFN receptor ($IFNAR^{-/-}$) are highly susceptible to WT YFV infection and s.c. infection leads to viscerotropic disease similar to human YF, including midzonal necrosis in liver, elevated cytokines, splenomegaly, and death (139). In contrast, while 17D vaccination in $IFNAR^{-/-}$ mice leads to serum viremia and viral replication in various tissues, 17D is avirulent and confers

protection to WT virus challenge afterwards, similar to human vaccination. Despite the lack of type I IFN responses, IFNAR$^{-/-}$ mice vaccinated with 17D have robust, functional, and long-term protective immunity (210). Neutralizing antibody is the main protective factor against WT virus infection, and different lineages of T cells likely have different protective roles. In the peripheral challenge model, which leads to viscerotropic disease in IFNAR$^{-/-}$ mice, CD4^{+} T cells and antibodies are important for protection, and some immune CD4^{+} T cells are cytolytic (210). However, in an intracerebral challenge model in immunocompetent mice, CD8^{+} T cells and antibodies are needed instead (211). While the latter model uses a non-physiological route of infection, these data overall suggest that 17D elicits a diverse T cell response that plays distinct roles in protection in different anatomical regions.

Interestingly, mice that lack both type I and type II IFN (IFNAGR$^{-/-}$) are susceptible to 17D infection and disease (139, 318). Intraperitoneal and s.c. infections with 17D are uniformly lethal in IFNAGR$^{-/-}$ mice. High 17D viral titer can be detected in both visceral and neuronal tissues at late stages of infection. These reports indicate that type II IFN is an attenuation factor for 17D, and IFNAGR$^{-/-}$ mice can serve as a potential model for severe adverse events associated with 17D vaccination.

1.5 HYPOTHESIS

Despite the long history of 17D vaccination and current efforts to utilize 17D as a vector for other vaccines or as a template for generation of LAVs for other flaviviruses, our understanding of 17D attenuation and YFV pathogenesis is limited. One major obstacle for understanding attenuation of YFV vaccine strain 17D is the lack of a small animal model that recapitulates

important aspects of YFV biology, i.e., differential virulence of WT strains and 17D upon s.c. infection where WT virus infection causes viscerotropic disease, and 17D vaccination confers immunity. Most previous mouse studies on YFV were performed by i.c. infection, which led to neurologic disease. These studies have highlighted the importance of envelope glycoprotein and NS1 glycosylation as virulence determinants. However, the lack of differential virulence between 17D and Asibi in i.c. infection models suggests the need for a more stringent animal model to study human-YFV interactions.

The mechanisms of 17D attenuation remain elusive. As described above, regarding viral attenuation factors, Lee et al. reported that enhanced glycosaminoglycan binding of 17D due to genetic changes in E-380 led to enhanced viral clearance from serum and attenuation; however, reversion of this mutation alone was insufficient to restore virulence to WT level, suggesting multiple mutations are involved in attenuation (27). In addition, one report suggested that 17D enters susceptible human cells through a clathrin-independent pathway whereas Asibi uses clathrin-coated pits (217). This phenomenon is due to genetic changes in the E protein but E-380 alone cannot confer the phenotype. On the host side, we and others have reported that mice that lack both type I and II IFN systems are highly susceptible to 17D infection while mice that lack only the type I IFN receptor are resistant to peripheral infection, indicating that type II IFN is an attenuation factor *in vivo* (139, 210, 318). A recent study also suggested the potential neuroprotective role of type III IFN in 17D infection (151); however this study used the intravenous route of infection with a non-physiological high dose (10^7 PFU) of virus, which renders relevance of the data to human vaccinees questionable.

Previous studies from our lab have developed a mouse model that recapitulates the important aspects of YFV infection in humans (139, 210). In this model, mice lacking the type I

IFN receptor ($IFNAR^{-/-}$) are resistant to 17D infection and disease but susceptible to WT YFV infection and disease through the s.c. route. WT virus infection leads to viscerotropic disease signs, including mid-zonal necrosis of liver and loss of lymphoid follicles in the spleen, whereas 17D vaccination in $IFNAR^{-/-}$ mice confers protective immunity against WT virus challenge for more than 18 months post-vaccination. Upon challenge, vaccinated $IFNAR^{-/-}$ mice has no sign of disease and the virus titer is almost undetectable. In addition, we and others have reported that additional deletion of the type II IFN receptor renders the animal susceptible to 17D disease, indicating IFN-γ is an important attenuation factor for 17D (139, 318). Based on these results, I propose the following hypotheses for my studies:

1. IFN-γ restricts 17D viral replication and dissemination *in vivo*.

2. IFN-γ is directly antiviral to 17D but not wild-type YFV.

The results of this study will advance our understanding of one mechanism of attenuation of YFV vaccine strain 17D and will provide insights on generating live attenuated flaviviruses as vaccine candidates.

2.0 PATHOGENESIS OF 17D IN THE ABSENCE OF GAMMA-INTERFERON SIGNALING

2.1 PREFACE

Most of the work described in this chapter are adapted from a published study (LK Metthew Lam, Alan M. Watson, Kate D. Ryman, William B. Klimstra, 2018, *NPJ Vaccines* **3**, article number 5).

2.2 INTRODUCTION

YFV is the prototypical member of the *Flavivirus* genus of the *Flaviviridae* family, which includes many important arthropod-borne pathogens such as dengue, Zika, West Nile, and Japanese encephalitis viruses. YFV is estimated to cause 200,000 cases of disease and 30,000 mortalities annually (184). Historically, YFV has caused devastating outbreaks in North America, South America, Africa, and Europe but is currently endemic to sub-Saharan Africa and South America. However, a recent YF outbreak in Angola led to at least 300 deaths (319) and 10 symptomatic traveler-associated cases in China (180). In addition, outbreaks that occurred in Espírito Santo in 2017, which is not considered at risk for YFV historically, and Uganda in 2011, which has not experience YFV outbreak since 1972, suggest that YFV remains a problem in the

modern world and threatens to expand geographically (320, 321). Mosquito abatement programs and vaccination with the live-attenuated YFV vaccine strain 17D remain the primary strategies for controlling YF outbreaks (169, 322).

The YFV vaccine strain, 17D, is arguably one of the most effective vaccines ever developed. A single dose of 17D results in seroconversion in >90% of vaccinees within a week and can offer essentially life-long immunity against YFV infections (196, 323). While the safety record of 17D is exemplary, potentially lethal severe adverse events occur with low frequency and these can involve both viscerotropic and neurotropic manifestations of virus disease (221, 227, 230, 324, 325). Regardless, due to the overall safety and effectiveness of 17D, multiple candidate vaccine vectors have been created using its genetic backbone, and these are currently being tested as a delivery system for antigens of other flaviviruses or other pathogens (326–329).

Despite being safe and effective, the mechanisms for attenuation and immunogenicity of 17D remain elusive. The 17D vaccine strain was derived by Max Theiler in 1930s through serial passaging of wild-type YFV strain Asibi in tissue culture, resulting in loss of viscerotropism and neurovirulence in non-human primates (330). Multiple substrains of 17D, including 17D-204, 17D-213, and 17DD have been generated and used for vaccination (331), with similar efficacy (207, 332). An average of 48 nucleotide and 20 amino acid changes distinguish 17D substrains from the parent Asibi strain (333, 334). The attenuation of 17D is attributed to genetic differences in both structural and non-structural proteins, but the role of specific mutations in the attenuation phenotype is not well characterized. Lee et al. suggested that a positive-charge mutation in the 17D E protein that leads to enhanced glycosaminoglycan binding, contributes to attenuation, but attenuation likely involves multiple 17D loci (27). It was recently demonstrated that E protein mutations allow 17D to enter susceptible cells through clathrin-independent

pathways, leading to an enhanced antiviral response *in vitro* (217). We recently reported that both neutralizing antibody and $CD4^+$ T cells are important in 17D-mediated protection from lethal wild-type YFV infection in a viscerotropic disease model (210). However, questions remain regarding the specific virus-host interactions that are modified by the 17D attenuating mutations and the mechanisms through which 17D induces highly protective immune responses. Understanding of the mechanisms of 17D attenuation will promote informed design of live attenuated versions of other flaviviruses and vaccines derived from other virus types.

To assess the specific host interactions affected by 17D attenuating mutations, we have used a pathophysiologically relevant mouse model to study host-pathogen interactions of YFV. Many WT flaviviruses, including YFV, replicate extremely poorly in mice with a functioning type I IFN system, precluding study of the roles of other host factors in their pathogenesis. Flaviviruses are more effective at antagonism of human type I IFN signaling than the analogous mouse responses (78, 91). Indeed, mice deficient in the type I interferon (IFN-α/β) receptor (AB6) are susceptible to viscerotropic disease and lethality after s.c. infection with wild-type YFV strains Asibi and Angola71 (139). Interestingly, s.c. infection of 17D in AB6 mice, which mimics vaccination, does not cause discernable disease and results in life-long immunity against challenge with a WT virus strain Angola71 (210). However, mice lacking both type I and type II IFN receptors (AGB6) are susceptible to lethal infection by 17D by either subcutaneous or intraperitoneal routes (27, 139, 318). The fact that the additional deficiency of the type II IFN (IFN-γ) receptor renders 17D infection lethal in AB6 mice suggests that the type II IFN system plays a critical role in attenuation of 17D *in vivo*.

To begin to understand the effects of IFN-γ on 17D, we have compared infection of AB6 and AGB6 mice. IFN-γ restricted 17D virus replication and dissemination early during infection

and enhanced clearance later after infection. Antiviral gene induction and cytokine production was also influenced by the presence or absence of type II IFN signaling. Finally, 17D infection resulted in liver stress and histological abnormalities in the spleen and brain of AGB6 but not AB6 mice, demonstrating that both viscerotropic and neurotropic diseases occurred in the absence of IFN-γ signaling and revealing a possible application for the AB6 model in understanding vaccine-associated viscerotropic and neurotropic adverse events.

2.3 RESULTS

2.3.1 IFN-γ attenuates 17D but not virulent YFV *in vivo*

To investigate the role of IFN-γ in 17D attenuation, we compared pathogenesis of 17D in AB6 and AGB6 mice. Groups of 6-week-old mice were infected subcutaneously with 10^4 PFU of YFV strains 17D-204 or Angola71 in both of the hind limb footpads. The virulent WT strain Angola71 was used as control. Similar to our previous reports (139, 210), Angola71-infected mice experienced severe weight loss and disease, requiring euthanasia (AST 7.5 +/- 0.6dpi), whereas 17D-204 was uniformly non-lethal in AB6 mice. In contrast, 17D-204-infected AGB6 mice experienced severe weight loss and eventually succumbed to disease (AST 10.75 +/- 0.5dpi) (Fig. 3A-B). Both 17D-204-infected AB6 and AGB6 mice exhibited footpad swelling, which peaked between 7-8dpi (Fig. 3C). In addition to footpad swelling, 17D-204-infected AGB6 mice displayed signs of brain infection and neurologic disease including hind limb paralysis, paresis, and/or seizures at late stages of infection, before euthanasia (Fig. 3D).

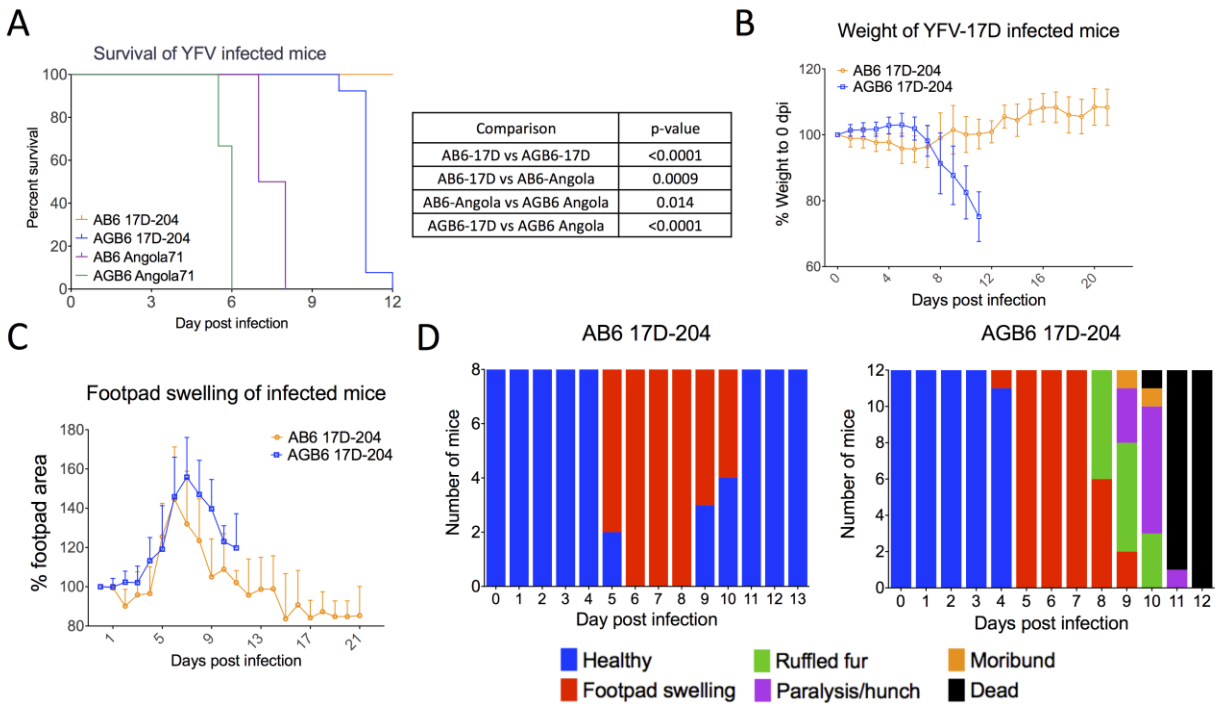

Figure 3: IFN-γ attenuates YFV-17D in vivo.

Groups of 6-week-old AB6 or AGB6 mice were infected s.c. with 10^4 PFU YFV 17D-204 or Angola71. (A) Survival, (B) weight loss, (C) footpad swelling, and (D) symptoms of diseases were measured daily. Data in (A) are analyzed with log-rank test. Data in (B) and (C) are presented as mean ± SD. (17D-204 infections, n >6; Angola71 infections, n = 4.)

2.3.2 IFN-γ restricts 17D replication and replication *in vivo*

Because IFN-γ influenced survival of mice after 17D-204 infection, we hypothesized that virus replication is reduced and restricted in its presence. Thus, we compared 17D virus replication kinetics in different tissues of the AB6 and AGB6 mice. In parallel, tissues from 17D-204-infected wild-type (C57BL/6) mice were harvested, but no infectious virus was recovered from any sampled tissue (Fig 4A-F).

The regional lymph node draining the site of infection (DLN) is one of the earliest sites for flavivirus replication and important for seeding viremia and dissemination (139). At 1dpi, 17D-204 virus was recovered from the DLN in both AB6 and AGB6 mice. In the absence of the IFN-γ response, 17D-204 virions were more abundant as early as at 1dpi (Fig. 4A). Serum viremia was first observed at 2dpi; however, no significant difference was observed in AB6 *versus* AGB6 at this time point. 17D-204 virions were detectable in bone marrow aspirate and spleen at 2dpi only in the absence of IFN-γ response. However, by 4dpi, high virus titers were observed in the spleen, bone aspirate, non-draining lymph nodes (mesenteric LN), and adrenal glands in both types of mice (Fig. 4C-G), although, higher virus titers were observed in AGB6 mice in most of these tissues. Interestingly, infectious virus particles were recovered from kidney, liver, and brain in AGB6 mice but not with AB6 mice (Fig. 4F, H-I). In the presence of IFN-γ responses, virus clearance was observed from most organs by 8dpi, but virions were still detected in all sampled organs in AGB6 mice at this time. Despite lacking both type I and type II IFN, virus clearance was observed in most the non-CNS tissues of AGB6 mice by 12dpi, before they succumbed to disease. In contrast, virus replication in the brain increased through 12 dpi (up to 10^6 PFU/g) in the AGB6 mice (Fig. 4F), through the times when neurological signs were observed (Fig. 3D). Overall, in the presence of IFN-γ, 17D-204 replication was controlled as early as 1dpi. Some dissemination of virus still occurred in AB6 mice, but the peak viral load was significantly lower than that of AGB6 mice. Virus tropism was also restricted by IFN-γ, most notably absent from liver and brain, and virus clearance was observed in most tissues by 8dpi. In the absence of IFN-γ responses, virus clearance occurred later and replication in the CNS tissues was poorly controlled.

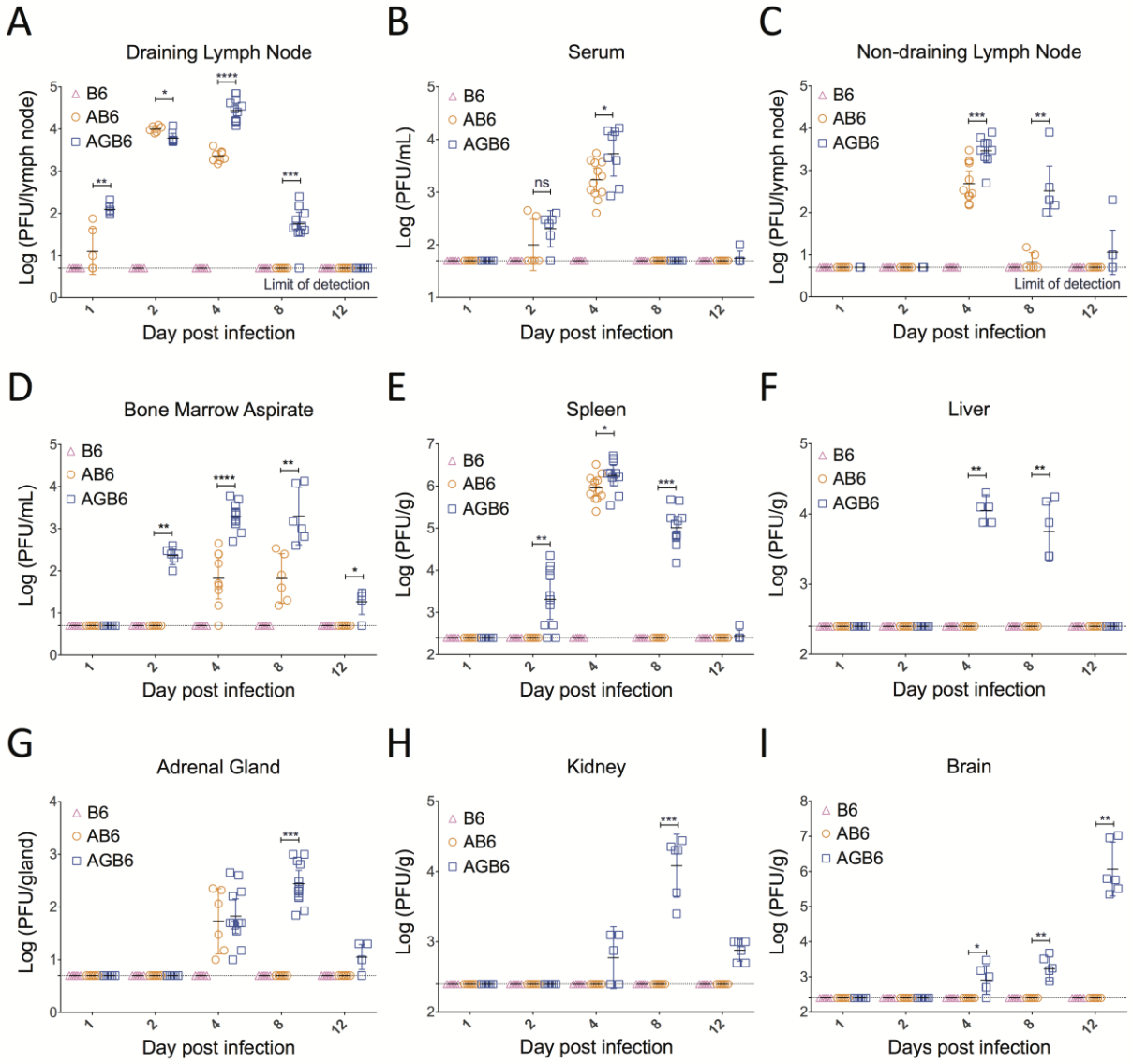

Figure 4: IFN-γ restricts 17D-204 replication and dissemination in vivo.

Tissues from 17D-204-infected mice were harvested at various days post-infection (B6 = C56BL/6). Tissues were homogenized, and virus titers were determined by standard plaque assay on Huh7 cells. (A) Draining (popliteal) lymph node, (B) serum, (C) non-DLN (mesenteric), (D) 1mL bone marrow aspirate, (E) spleen, (F) liver, (G) adrenal gland, (H) kidney, and (I) brain titers were measured. Data are presented as geometric mean ± 95% CI. (* $p < 0.05$; ** $p < 0.01$; *** $p < 0.005$; **** $p < 0.001$; multiple t-test, corrected by Holm-Sidak method.)

2.3.3 IFN-γ protects mice from 17D-induced viscerotropic and neurotropic diseases

Because 17D is known to cause viscerotropic and neurotropic infection in vaccine-associated SAE cases, we sought to determine if tissue pathology could be detected after 17D infection in the absence of an IFN-γ response. We investigated tissue pathology at 4dpi, which is the peak of viral replication in most visceral organs in both AB6 and AGB6 mice and 11dpi, when AGB6 animals displayed neurologic signs before succumbing to disease. At 4dpi, hematoxylin and eosin (H&E) stained spleen sections (Fig. 5A) of 17D-204-infected AB6 and AGB6 mice were indistinguishable from mock-infected animals. In contrast, spleens of Angola71-infected mice displayed loss of splenic architecture and increase in inflammatory infiltrates, similar to our previous findings (139). Despite the lack of titerable virus in the spleen at 11dpi (Fig. 4C), spleens of 17D-204-infected AGB6 had increased numbers of inflammatory infiltrates and exhibited a loss of splenic architecture (Fig. 5A). Immunostaining of spleen sections from infected AB6 and AGB6 mice demonstrated the presence of YFV antigens in F4/80$^+$ cells (red pulp macrophages) and cells in the outer marginal zone (Fig. 5B) at 4dpi at similar levels. H&E-stained liver sections revealed microsteatosis occurring only in the liver of 17D-204-infected AGB6 mice at 4dpi (Fig. 6A), a time at which virions were detectable in the liver (Fig. 4E), and thus, indicative of a viscerotropic phase of 17D infection in the absence of IFN-γ responses. Moreover, YFV antigen could be detected in some F4/80$^+$ cells in the liver of infected AGB6 mice, suggesting that Kupffer cells were infected in these animals (Fig. 6B). Corresponding to the time of neurological signs in 17D-204-infected AGB6 mice (11dpi, Fig. 3D), we observed an increase in immune infiltration to the cerebral cortex (Fig. 7A) and virus-infected cells in the cerebral cortex and cerebellum of the brain (Fig. 7B), indicative of neurotropic disease. No such phenomena were detectable in 17D-204 infected AB6 animals. Overall, the histology data

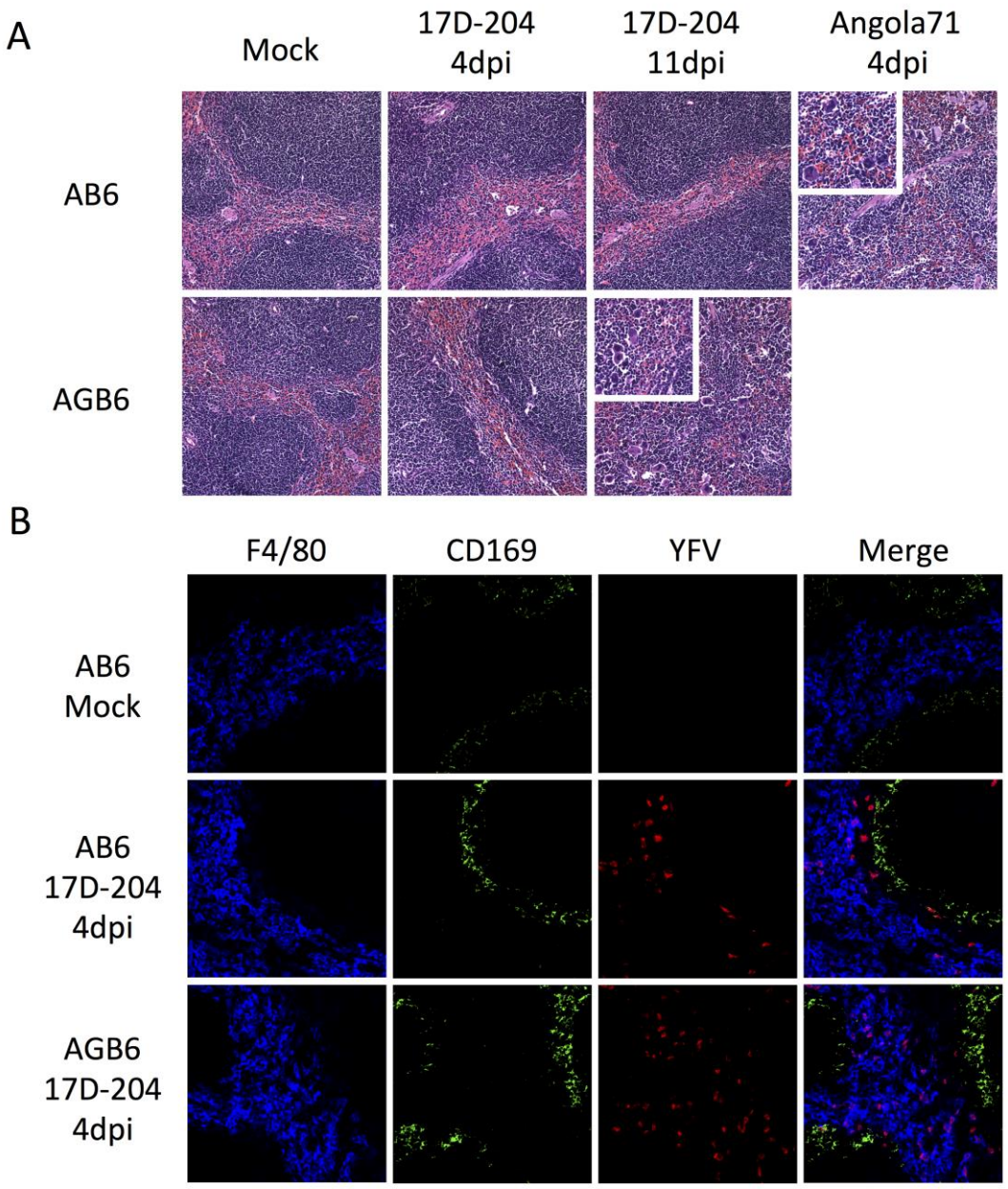

Figure 5: 17D infection led to splenic damage in the absence of IFN-γ.

(A) H&E sections from spleen of 17D-204-infected animals were indistinguishable at 4dpi, whereas Angola71-infected animals display loss of white pulp and red pulp architecture and increase in infiltrating macrophages and neutrophils (inset) at 4dpi. At 11dpi, 17D-204 infected AGB6 has increased immune infiltration and disruption of lymphoid follicles but not AB6 mice. (B) YFV antigen can be detected in the spleen at 4dpi in both AB6 and AGB6 mice in the red pulp and outer marginal zone area. n≥3, original magnification = 40x.

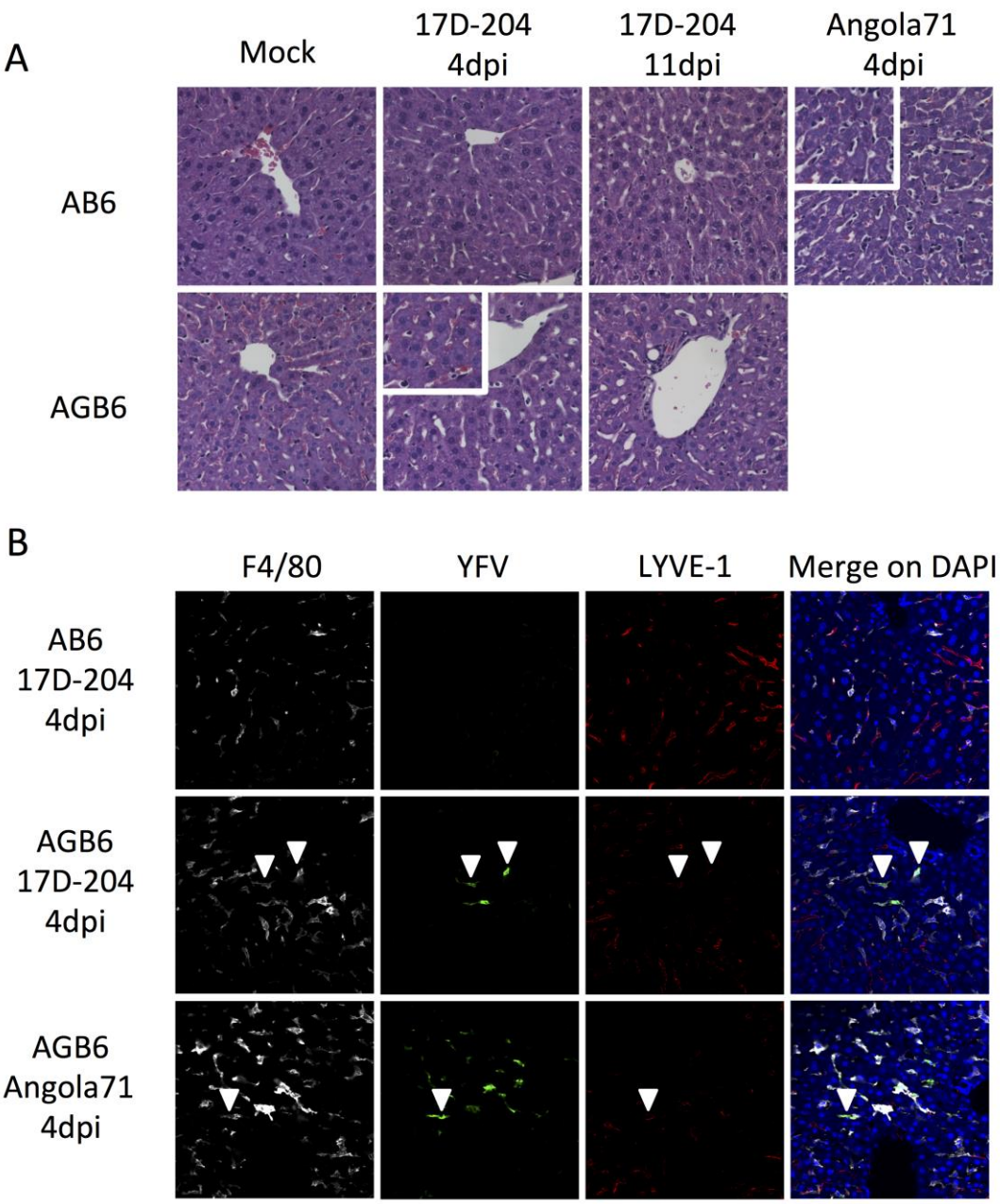

Figure 6: 17D infects liver and induces liver stress in the absence of IFN-γ.

(A) H&E sections of 17D-204-infected AB6 mice do not display major histological changes but infected AGB6 mice and Angola71-infected animals had microsteatosis (inset) at 4dpi. In AGB6 mice, microsteatosis only occur transiently at 4dpi and resolved by 11dpi. (B) Antibody-stained frozen sections revealed that YFV antigen could only be detected in infected AGB6 mice at 4dpi but not AB6 mice, parallel to titer data in Fig. 2. Arrowhead indicates YFV-infected F4/80^{+} cells. n≥3, original magnification = 40x.

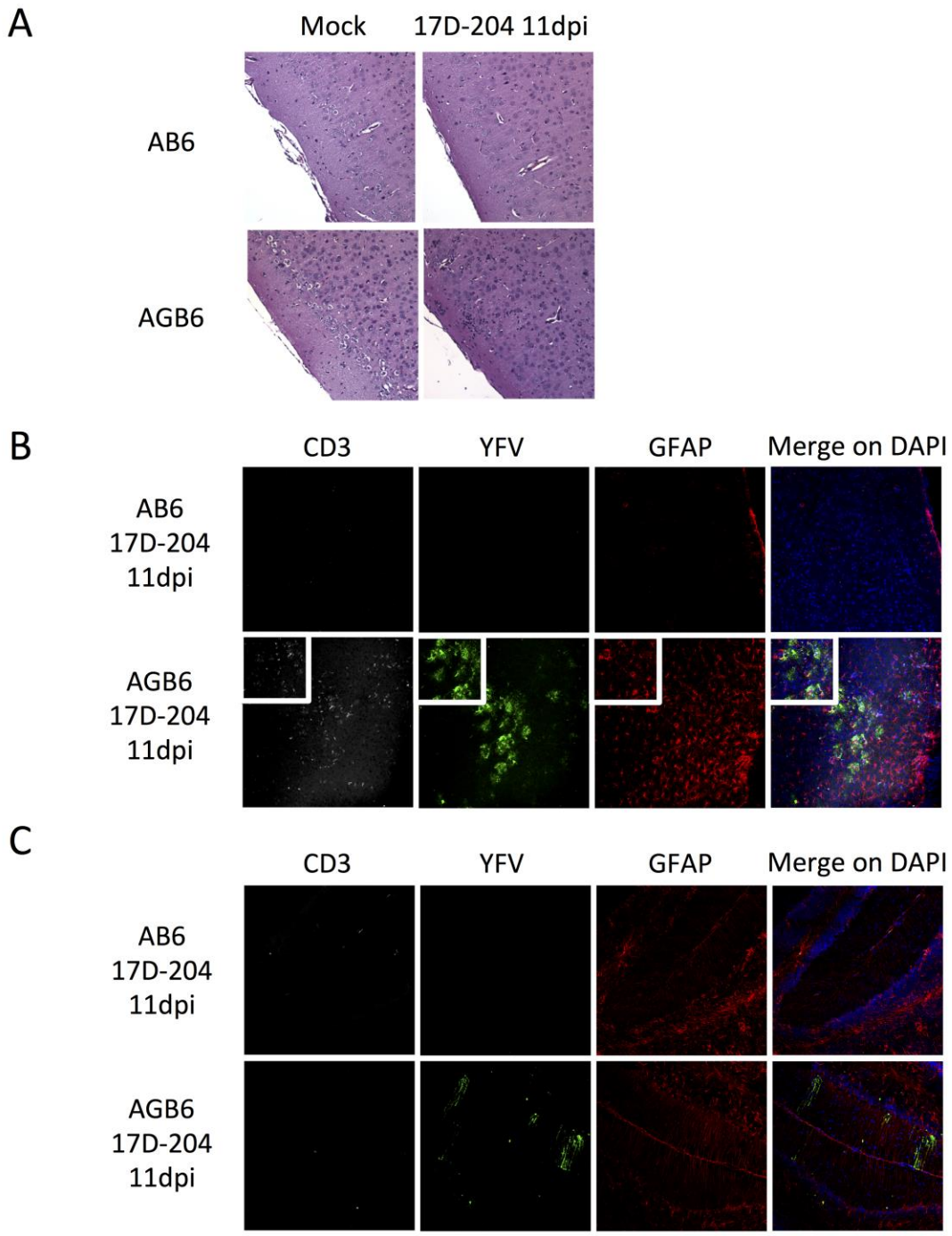

Figure 7: Inflammation and viral antigens in brains of 17D-infected AGB6 mice.

In (A) H&E stained brain sections, 17D-204-infected AGB6 mice but not AB6 or mock-infected animals had increased cellular infiltration into the cerebral cortex at 11dpi. Concomitantly, YFV antigens can be detected in (B) cerebrum and (C) cerebellum. n≥3, original magnification: (A-C) 20x, inset in (B) 40x.

demonstrate that IFN-γ restricts 17D-204 dissemination and protects mice from viscerotropic and neurotropic diseases.

2.3.4 Cytokine induction is impaired in the absence of IFN-γ

IFN-γ is central to activation of T cells and macrophages, and induces production of other proinflammatory cytokines. Therefore, we hypothesized that the absence of IFN-γ would impact cytokine production during 17D infection. To this end, serum cytokine levels in infected mice were measured at various times post-infection using the Cytokine 20-plex Mouse Panel (Fig. 8). In AB6 mice, serum levels of IFN-γ, IL-12p40, MIG, MCP-1, and IP-10 were elevated transiently *versus* uninfected controls on day 4pi, corresponding to the peak spleen virus titer (Fig. 4D). While AGB6 mice also exhibited a slight increase in serum IL-12 and MCP-1 levels on day 4pi, serum IFN-γ levels were highly elevated in comparison with control or AB6 mice on this day and at days 8 and 12pi. Wild-type YFV-infected AB6 mice produced higher levels of serum cytokines (IFN-γ, MIG, MCP-1, IL-4, IL-5, IP-10, and TNFα) more rapidly than in 17D-infected AB6 or AGB6 mice (Fig. 8), possibly associated with the severe viscerotropic disease and rapid death of the WT virus-infected animals (139). The cytokines that were more significantly upregulated in 17D-204-infected AB6 but not AGB6 mice, i.e. IL-12, MCP-1, MIG, and IP-10, are all IFN-γ-inducible, suggestive of a central role for IFN-γ in protecting AB6 mice from 17D-204 infection is through cytokine induction. Similar to our observations, in adult male vaccinees receiving YFV vaccine substrain 17DD, serum levels for IFN-γ, MCP-1, MIG, IP-10, and IFN-γ were reported to be elevated (191).

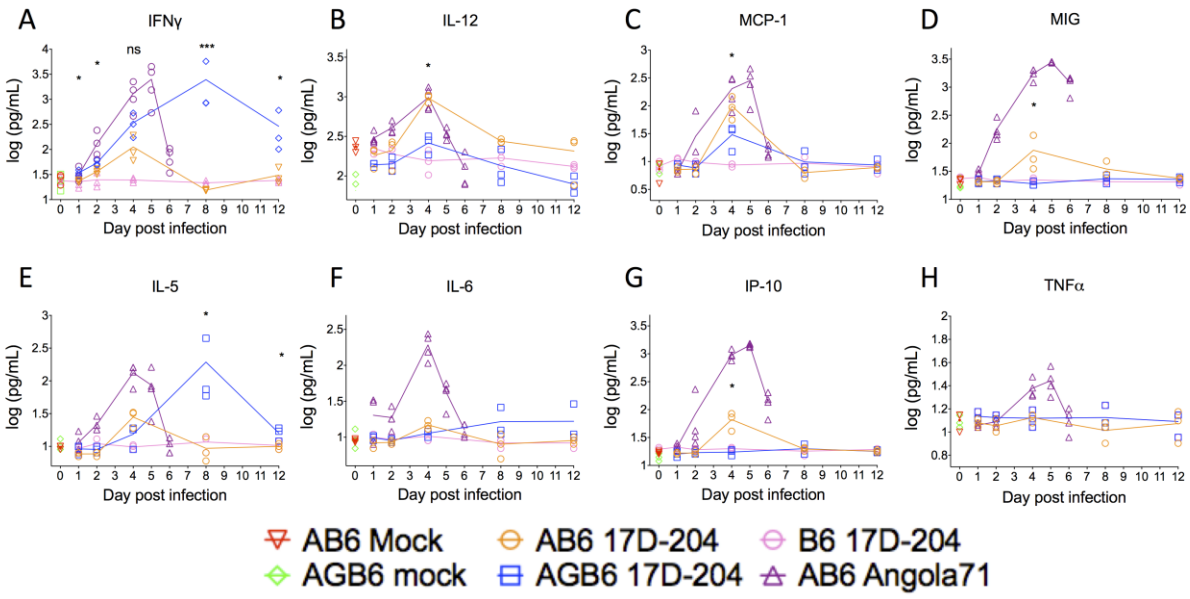

Figure 8: Cytokine response of 17D-infected animal.

Groups of 6-week-old B6, AB6, or AGB6 mice were infected s.c. with 10^4 PFU of YFV 17D-204 or Angola71. Sera were harvested at the indicated time points post-infection by the bleeding at submandibular vein. Serum cytokines (A) IFN-γ, (B) IL-12, (C) MCP-1, (D) MIG, (E), IL-5 (F), IL-6, (G) IP-10, and (H) TNFα were quantified using Cytokine 20-Plex panel bead-based assay. Data are presented as in geometric means ± 95% CI. Statistical comparison were determined between 17D AB6 and 17D AGB6. (*: $p<0.05$, ** $p<0.01$, *** $p<0.005$; multiple t-test, corrected by Holm-Sidak method; n=3-5.)

2.3.5 IFN-γ is secreted by NK cells early during 17D infection

IFN-γ has been shown to upregulate and activate cellular and humoral immunity, but it can also exhibit direct antiviral activity against YFV in many cell types through upregulation of genes that encode antiviral effector proteins, such as IFN-stimulated genes (ISGs). Since IFN-γ inhibition of 17D-204 occurred at early times after infection of AGB6 mice, we attempted to determine if differences in tissue-specific IFN-γ or ISGs expression could be detected in the absence of IFN-γ. Because we observed inhibition of 17D-204 replication and dissemination

before 4dpi, we examined IFN-γ transcript induction from 1dpi to 4dpi. Robust upregulation of the IFN-γ gene was observed as early as 2dpi in lymph nodes but not spleens of both AB6 and AGB6 mice (Fig. 9A). Using flow cytometry (Fig. 9B-D), we observed induction of IFN-γ in $NK1.1^+$ cells in the DLN, similar to a previous report that used immunocompetent B6 and BALB/c mice (160). Despite the lack of IFN-γ induction in the spleen, various antiviral genes including IGTP, IFIT1, and IFIT2 were upregulated in the spleens of 17D-204-infected AB6 to higher levels mice than in spleens of AGB6 mice, indicative of IFN-γ-dependent gene induction and likely a systemic antiviral effect of IFN-γ production (Fig. 10).

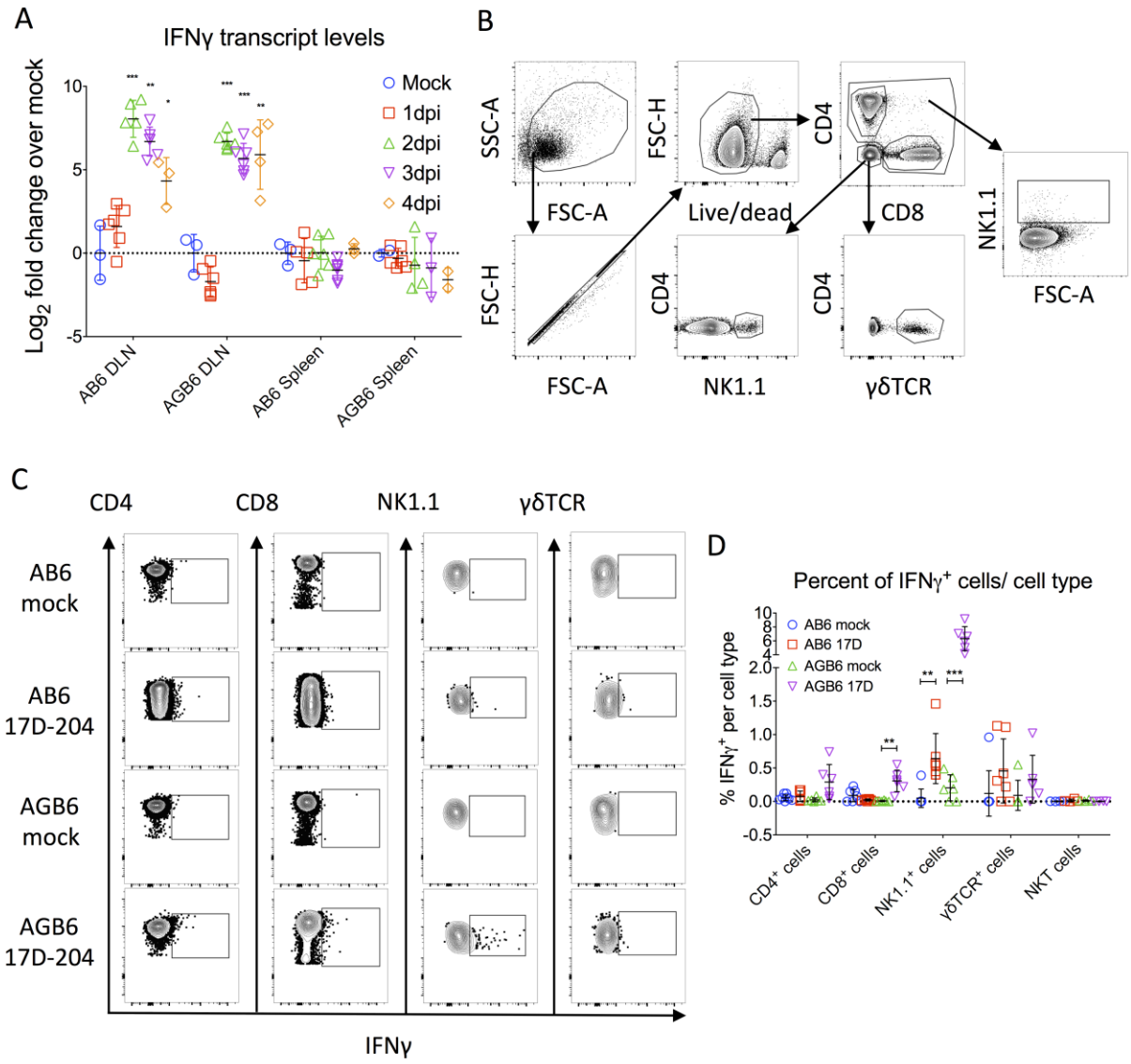

Figure 9: IFN-γ is produced locally at draining lymph node by NK1.1+ cells

Tissues from 17D-204-infected animals were harvested in Tri-reagent, followed by RNA isolation, reverse transcription, and quantitative PCR. (A) Kinetics of IFN-γ induction from 1-4dpi. (B-D) Flow cytometry analysis demonstrating early IFN-γ production at 3dpi in DLN by NK cells. (B) Gating strategy for cell types of interest. (C) Representative flow plots for IFN-γ staining for indicated cell types. (D) Proportion of indicated cells type positive of IFN-γ. In (A), data are presented as geometric means ± 95% CI. In (D) Data are presented in mean ± SD (*: $p<0.05$, ** $p<0.01$, *** $p<0.005$, **** $p<0.001$; multiple t-test, corrected by Holm-Sidak method.) (A-D) $n \geq 5$.

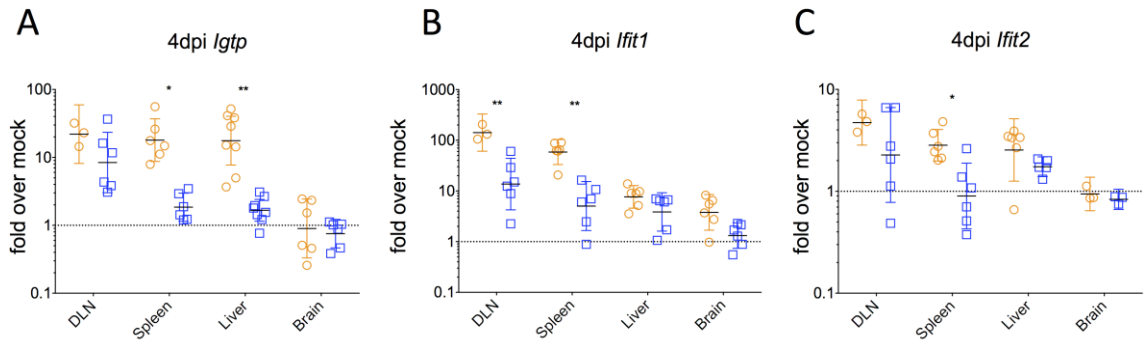

Figure 10. IFN-γ induces antiviral genes in tissues.

Tissues from 17D-204-infected animals were harvested in Tri-reagent, followed by RNA isolation, reverse transcription, and quantitative PCR. Expression of (A) *Igtp*, (B) *Ifit1*, and (C) *Ifit2* at 4dpi is shown here. Data are presented as geometric means ± 95% CI. (*: $p<0.05$, ** $p<0.01$; multiple t-test, corrected by Holm-Sidak method.) $n>3$.

To confirm the role of NK cells in IFN-γ production *in vivo*, we performed antibody-mediated depletion of $NK1.1^+$, $CD4^+$, or $CD8^+$ T cells in 17D-infected mice. In both AB6 and AGB6 mice, $NK1.1^+$ cell depletion led to a reduction in serum IFN-γ levels at 4dpi (Fig. 11B), supporting the flow cytometry data identifying $NK1.1^+$ cells as a primary source of IFN-γ. Depletion of $CD8^+$ T cells in AGB6, but not AB6, animals also led to reduction in serum IFN-γ levels. $NK1.1^+$ cell depletion also resulted in enhanced 17D replication in AB6 mice (Fig. 11C), likely due to less IFN-γ production. However, depletion of $NK1.1^+$ cells resulted in reduced virus titer in AGB6 mice, which may be due to the recently documented replication of 17D in $NK1.1^+$ cells in the absence of IFN-α/β and IFN-γ signaling (335).

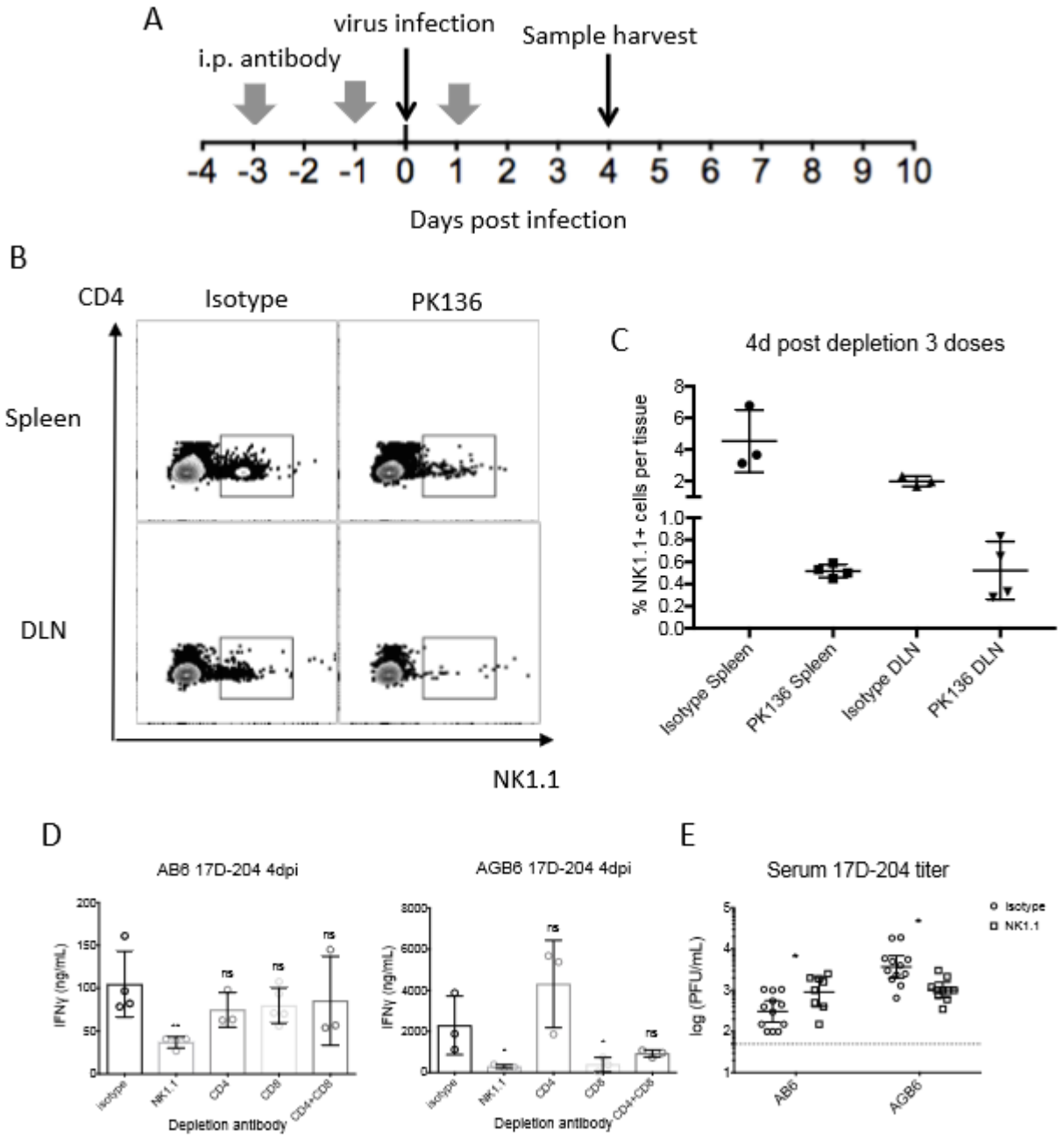

Figure 11: NK cells are important for IFN-γ production.

AB6 and AGB6 mice were injected with designated antibodies by the i.p. route and infected subcutaneously according to the experimental timeline in (A). (B-C) Depletion of NK1.1$^+$ cells was confirmed by flow cytometry. (D) ELISA quantification of serum IFN-γ at 4dpi. (E) Serum virus titer at 4dpi. Data are presented as mean ± SD in (B) and geometric mean ± 95% CI in (C) (*: $p<0.05$, ** $p<0.01$, *** $p<0.005$, **** $p<0.001$; multiple t-test, corrected by Holm-Sidak method.)

2.4 DISCUSSION

Despite the long-term success and widespread use of the 17D YFV vaccine substrains, the molecular mechanisms for attenuation of 17D remain unclear. One major restriction on understanding YF pathogenesis has been the lack of pathophysiologically relevant and cost-effective small animal models for studying YFV pathogenesis and attenuation. Previously, we reported that mice lacking type I interferon receptor ($IFNAR^{-/-}$) are susceptible to subcutaneous (s.c.) infection of wild-type YFV and display signs of viscerotropic disease similar to human YF, whereas 17D is avirulent in this model system (139). In addition, 17D-infection leads to protective immunity against wild-type YFV challenge for the life of the mouse (210). However, we and others have reported that 17D is virulent in mice lacking both type I and type II IFN receptors ($IFNAGR^{-/-}$), suggesting that type II IFN is a critical attenuation factor for 17D *in vivo*. In this study, we investigated the role of IFN-γ in controlling replication of 17D *in vitro* and *in vivo*. Our results indicate that type II IFN restricts 17D replication and spread *in vivo*.

By comparing 17D-204 pathogenesis in AB6 and AGB6 mice, we found that 17D-204 replication was largely restricted to lymphoid compartments by IFN-γ. In the absence of IFN-γ response, 17D-204 infection in AGB6 mice rapidly disseminated to tissues beyond DLN, spleen, and bone marrow. In addition to higher viral titers, we observed signs of liver stress and recovered infectious virus particles in the liver on 4dpi, indicative for a viscerotropic phase of 17D infection with the additional absence of IFN-γ responses. Despite viral clearance in the peripheral tissues, virus accumulated to high titer in the brain and was associated with signs of neurological disease including immune cell recruitment to brain and paralysis. Taking together our data and those of other reports (139, 318), we propose that 17D-infected AGB6 mice could be used to model neurotropic SAEs associated with 17D vaccination. Despite the presence of a

brief viscerotropic phase of 17D-204 infection in AGB6 mice, we did not observe cytokine storm comparable to Angola71-infected AB6 mice or extensive damage to the visceral organs (which can be found in viscerotropic SAE patients (227)), with the exception the spleen late during infection. These data indicate involvement of additional or alternative factors, such as host genetics (230, 336) and/or 17D genetic variants, both of which have been proposed as sources of SAE (231).

Consistent with other studies of 17D vaccination in mice (160) and non-human primates (NHP) (337), we observed an early induction of IFN-γ after 17D-204 vaccination in our mouse model. Such early induction of IFN-γ resulted in contemporaneous restriction of 17D-204 in AB6 mice. In both AB6 and AGB6 mice, $NK1.1^+$ cells were critical for IFN-γ production; however, in AGB6, $CD8^+$ T cells (CTL) were also involved. Lymphocyte activation is driven by antigen abundance, and the high virus titers in AGB6 mice may have contributed to more robust CTL activation and IFN-γ production than in AB6 mice. In addition, a recent report has shown that CTL and NK cells can be infected by 17D in the absence of STAT1 (335). In that report, deletion of STAT1 in the hematopoietic compartment rendered mice susceptible to intravenous 17D infection, and enhanced 17D replication in leukocytes from both myeloid and lymphoid lineages was detected in the spleen and the blood. Thus, we speculate that infection of both CTL and NK cells leads directly or indirectly to IFN-γ secretion. Whereas in AB6 mice, the presence of IFN-γ response partially protects T cells directly through inducing an antiviral state and/or indirectly through control of virus titer, leaving NK cells as the major IFN-γ producer.

Although deficiency in IFN-γ receptor led to early virus dissemination and uncontrolled replication, peripheral clearance is also observed in AGB6 mice by 12dpi, which is suggestive of a type II IFN-independent viral clearance mechanism. The nature of this response also needs to

be investigated, as it may be important in minimizing pathological consequences of 17D immunization such as SAEs. It should be noted that despite the lack of both type I and type II IFN responses, some antiviral genes were upregulated in our model, especially in the DLN and spleen. These genes may be induced directly without type I or type II through RIG-I and MDA5 (124), toll-like receptors (129, 338), or type III IFN (149, 339), which may aid eventual viral clearance from the periphery even in AGB6 mice. However, it was recently reported that mice lacking both type I and type III IFN receptors had higher 17D titers in the brain but not other tissues when compared to mice lacking IFNAR1 alone, suggestive of a neuroprotective role for type III IFN (151).

One major criticism of the AB6 model is the lack of a type I IFN response. However, evidence suggests that infection of these mice recapitulates important aspects of YFV infection and vaccination of human, namely, viscerotropic disease during WT virus infection and long-term protective immunity after 17D vaccination (139, 210). Indeed, robust, protective B and T cell responses to 17D are present in these animals (210). In human vaccinees, the presence of type I IFN does not prevent 17D replication and establishment of serum viremia or mild reactions at the site of vaccination. Whereas in C57BL/6 mice, the presence of type I IFN suppressed 17D replication to the point that replicating viruses cannot be detected by conventional assays, and infected mice do not have local reactions such as footpad swelling after infection. This suggests that YFV is more resistant to, or more capable of suppressing, the human type I IFN system than the murine counterpart. In fact, dengue and Zika virus are more effective in antagonizing human innate immune signaling molecules (STAT2 and STING) than murine homologs (78, 91, 92). Together, these observations suggest that the type I IFN receptor-deficient mouse is a pathophysiologically relevant model that is valuable in exploring the

immunogenicity, pathogenicity, and attenuation mechanisms of different YFV strains. However, clearly, type I IFN very likely has a role in controlling YFV in humans (193, 340).

The cause for the severe adverse events (SAEs) following 17D vaccination is still unknown. Despite the adaptation of monkey neurovirulence test to ensure safety of each vaccine lot, SAEs still occur, suggesting additional factors are contributing to virulence of 17D in SAE patients. In terms of host genetics, single nucleotide polymorphisms (SNPs) in CCR5 and RANTES genes were found in one viscerotropic SAE case (230), while SNPs in OAS1 were found in another (336). These polymorphisms are implicated in aberrant immune response upon 17D vaccination. In terms of virus genetics, mutations were found in some clinical isolates from SAE patients, and some, but not all of the viruses demonstrated enhanced virulence in animal models (341).

Our data suggest that IFN-γ is an attenuating factor against 17D *in vivo*, leading us to hypothesize that variability of host IFN-γ signaling is one potential underlying causes for SAEs. In humans, genetic differences that disturb IFN-γ production or signaling have been shown to enhance susceptibility to infections. For instances, heritable mutations in the IL-12 receptors, which are critical for IFN-γ induction, and IFN-γ receptors that reduce receptor expression or signaling efficacy render individuals susceptible to *Salmonella* and disseminated *Mycobacterium* infections (342–344); importantly, these individuals are also susceptible to the disease cause by the generally safe *M. bovis* BCG vaccine strain (343). This evidence indicates that primary immunodeficiency in IFN-γ signaling efficacy may influence the ability to control some pathogens. This may explain some 17D SAEs. NK cells are important early producer for IFN-γ (160), and NK cells are robustly activated in vaccines by three days post-vaccination (159). Since flaviviruses upregulate MHC-I early during infection to suppress activation of NK cells

(166, 345), it is tempting to speculate that defects in NK cell activation of the vaccinees due to genetics or environmental factors may delay virus control and increase risk of SAE.

These studies have revealed that the murine IFN-γ-mediated response protects $IFNAR^{-/-}$ mice from disease and promotes the eventual development of robust and long-lived protective immunity against wild-type YFV challenge (170) similar to human vaccination. In contrast, the lack of an IFN-γ response renders 17D virulent and leads to viscerotropic and neurologic disease and eventual death, potentially similar to human SAEs. Enhanced sensitivity to IFN or particular ISGs has been documented in several arbovirus LAVs (346–348). Thus, the deliberate creation of an IFN-γ sensitive phenotype may be a productive approach to rational design of new live attenuated vaccine (LAV) candidates against arboviruses. This will require identification of the mutations in 17D that underlie this phenotype.

3.0 YELLOW FEVER VIRUS 17D IS MORE SENSITIVE THAN WT YFV TO ANTIVIRAL ACTIVITIES INDUCED BY GAMMA-IFN IN MYELOID CELLS

3.1 PREFACE

Most of the work described in this chapter is adapted from a published study (LK Metthew Lam, Alan M. Watson, Kate D. Ryman, William B. Klimstra, 2018, *NPJ Vaccines* **3**, article number 5).

3.2 INTRODUCTION

Interferons are innate immune cytokines that exert important roles on restriction and clearance of invading pathogens. The three types of IFN are critical for controlling various pathogens, including flaviviruses. Sensitivity of pathogen to IFN responses can influence the pathologic outcome of an infected host, and some attenuated pathogens or live attenuated vaccine candidates are more sensitive to IFNs (346–348). Conversely, many pathogenic flaviviruses are equipped with multiple mechanisms to subvert the IFN response, by suppressing IFN induction and signaling and interfering with downstream antiviral effectors (91, 92, 121, 144). Different cell types have different responsiveness to IFN due to such factor as their steady-state gene expression, expression of IFN receptor, gene regulation pathways, and local environment,

rendering some more susceptible to virus infection (149, 349). Type II IFN has important roles in triggering TH1-biased adaptive immunity, and at the innate level, it has been shown to be directly antiviral to DENV, WNV, and TBEV (143, 144, 146). In addition, IFN-γ activates and enhances the antimicrobial response of macrophages by inducing iNOS, pro-inflammatory cytokines, and respiratory burst, which are important for clearance of many intracellular pathogens.

Based on our work on characterizing the role of IFN-γ in the IFNAR$^{-/-}$ mouse model, we observed that IFN-γ restricts 17D dissemination and replication as early as 2dpi, prior to activation of adaptive immunity. Thus, we hypothesize that 17D is inhibited by the innate antiviral activities of IFN-γ. In the current studies, we have compared virus replication of YFV *in vitro* in various cell types treated with IFN-γ or IFN-α/β. We found that both interferons inhibit replication of both 17D-204 and Angola71; however, 17D-204 is more sensitive to the antiviral activities induced by IFN-γ. In addition, such differential inhibition of YFV by IFN-γ occurs in myeloid, but not non-myeloid cells, suggestive of cell type-dependent IFN antiviral activities.

3.3 RESULTS

3.3.1 17D-204 is more sensitive to the IFN-γ-induced antiviral state than WT-YFV in myeloid cells but not non-myeloid cells

Based on our observations that 1) AGB6 mice succumbed to 17D-204 infection but not AB6 mice (Fig. 3A); 2) 17D-204 replicated to higher titer and disseminated faster in AGB6 mice than AB6 (Fig. 4); 3) IFN-γ induction in infected AB6 and AGB6 mice occurred as early as 2dpi

(Fig. 9); 4) Angola71-infected AB6 produced higher levels of serum IFN-γ than 17D-infected AB6 (Fig. 8), yet virus infection was not controlled in the Angola71-infected mice; 5) Angola71-related mortality was delayed in AB6 versus AGB6 mice (Fig. 3A); and 6) reports that IFN-γ inhibited flavivirus infection *in vitro* (143, 144, 146), we hypothesized that IFN-γ induces an antiviral state that can generally inhibit YFV replication *in vitro* and *in vivo* and that enhanced sensitivity to the IFN-γ antiviral state is a prominent attenuation mechanism of 17D. To test this hypothesis, we compared virus replication of 17D-204 and Angola71 in various relevant cell types treated with IFN-γ or IFN-α/β. Consistent with the hypothesis, we observed a dose-dependent inhibition of 17D-204 and Angola71 virus replication by IFN-γ in bone marrow-derived macrophages (BMMΦ) and dendritic cells (BMDC) derived from C57BL/6 mice (Fig. 12). In addition, 17D-204 was significantly more inhibited than Angola71 by an equivalent dose of IFN-γ or IFN-α/β. Since basal replication, which may be different between the viruses, can potentially induce different levels of IFN-α/β in cultured cells and alter sensitivity measurements, we performed the same experiments using cells that lack the ability to produce (IRF3x5x7$^{-/-}$ cells, Fig. 12B, E, I, L) or respond to (AB6 cells) IFN-α/β (Fig. 12C, F). Cells derived from AGB6 mice, which cannot respond to either type of IFN, were also included as negative controls (Fig. 12G, J). While 17D-204 and Angola71 multiply to higher titers in IRF3x5x7$^{-/-}$ and AB6 BMMΦ than BMMΦ derived from C57BL/6 mice, 17D-204 is still significantly more inhibited by IFN-γ than Angola71. To determine if IFN-γ has a broad-spectrum effect on YFV replication, we also measured the IFN-γ sensitivity of YFVs in immortalized mouse embryonic fibroblasts (MEFs) or a human hepatoma line (Huh7). We did not observe significant differences between the viruses to either IFN-α/β or IFN-γ treatment (Fig. 13), suggesting that 17D-204 and Angola71 are differentially inhibited by IFN-γ-induced antiviral state in a cell-specific manner.

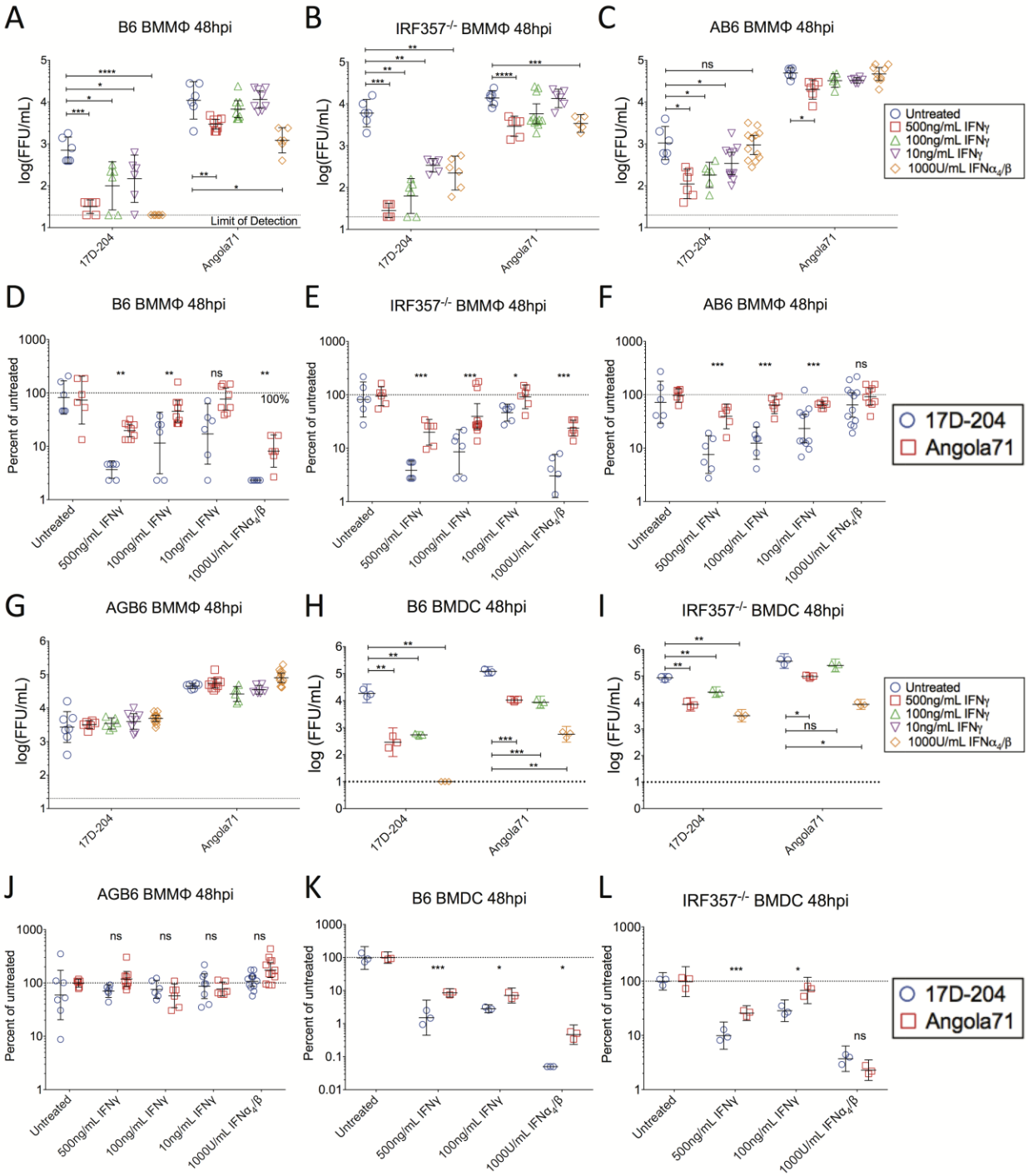

Figure 12: YFV-17D is more sensitive to IFN-γ-induced antiviral states than wild-type strain Angola71 in myeloid cells.

Indicated cells were treated with IFN 12hrs prior to infection. Cells were infected with 17D-204 or Angola71 at MOI=0.1. At 48hpi, supernatants were harvested and infectious virus particles were quantified by focus forming assay on Vero cells. (A-C, G-I) Foci data are presented as geometric mean ± 95% CI. (D-F, J-L) Corresponding foci data were normalized to untreated cells and presented in percentage, mean ± SD. (*: p<0.05, ** p <0.01, *** p<0.005, **** p<0.001; multiple t-test, corrected by Holm-Sidak method. Each dot represent data obtained each well. Macrophages from each mice were seeded in two duplicate wells, whereas each well of DCs are derived from one mice.)

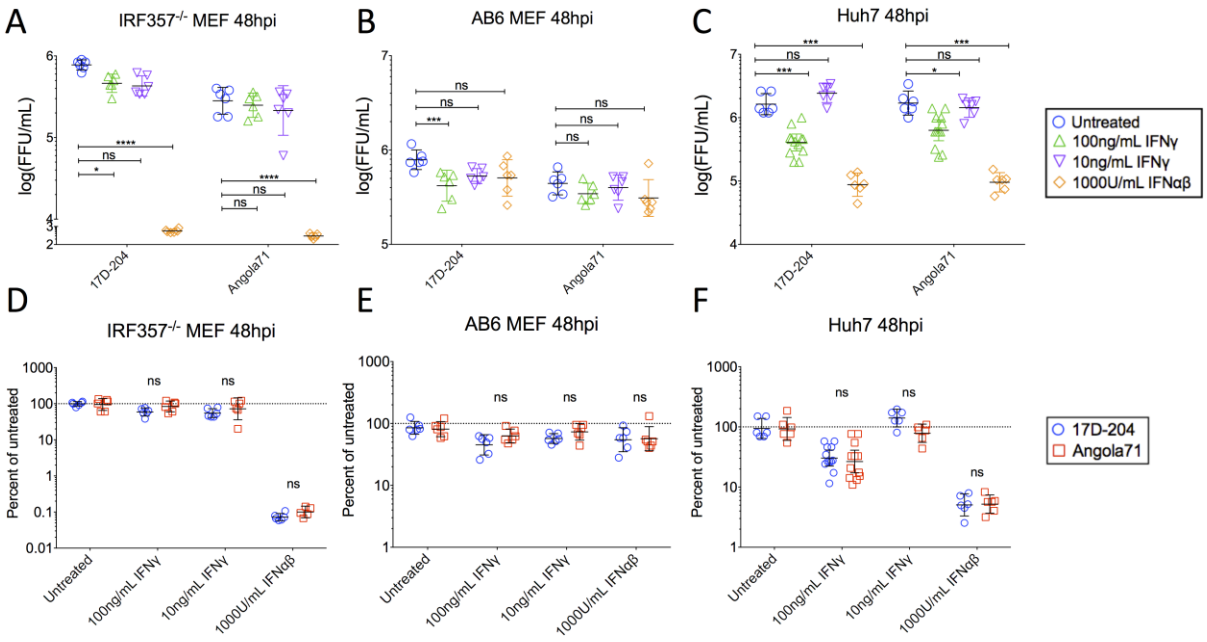

Figure 13: YFV-17D and Angola are similarly sensitive to the IFN-induced antiviral state in non-myeloid cells.

Indicated cell types were treated with the indicated IFN 12hrs prior to infection. Cells were infected with 17D-204 or Angola71 at MOI=0.1. At 48hpi, supernatants were harvested and infectious virus particles were quantified by focus forming assay on Vero cells. (A and D) IRF3x5x7$^{-/-}$ mouse embryonic fibroblast (MEFs) and (B and E) AB6 MEFs, and (C and F) Huh7. (A-C) Foci data are presented as geometric mean ± 95% CI. (B-F) Foci data from (A-C) are normalized to untreated cells and are presented as percentage, mean ± SD. (*: p<0.05, ** p <0.01, *** p<0.005, **** p<0.001; multiple t-test, corrected by Holm-Sidak method.)

3.3.2 IFN-γ treatment of myeloid cells induces antiviral genes that are upregulated in 17D-infected AB6 mice

Our data suggest that myeloid cells are responsible for IFN-γ-mediated restriction of 17D. Thus, we compared antiviral gene expression in 17D-204-infected animals and myeloid cells. Antiviral genes such as *Igtp* and *Ifit2* were selected because they are robustly induced by IFN-γ (350), and *Ifit2* has been shown to protect mice from WNV infection (351). These genes were upregulated similarly in DLN of both AB6 and AGB6 mice; however, in tissues like the spleens *Igtp* and *Ifit2* are preferentially upregulated the presence of IFN-γ response (Fig. 14A-B). This may be attributed to a combination of viral induction and IFN-γ-mediated induction of *Igtp* and *Ifit2*. IFN-γ treatment in BMMΦ and BMDC derived from C57BL/6, IRF3x5x7$^{-/-}$, and AB6 mice resulted in induction of *Igtp* and *Ifit2* but not from AGB6 mice (Fig. 14C-F). These results suggest myeloid cell activation by IFN-γ may contribute to restriction of 17D *in vivo*.

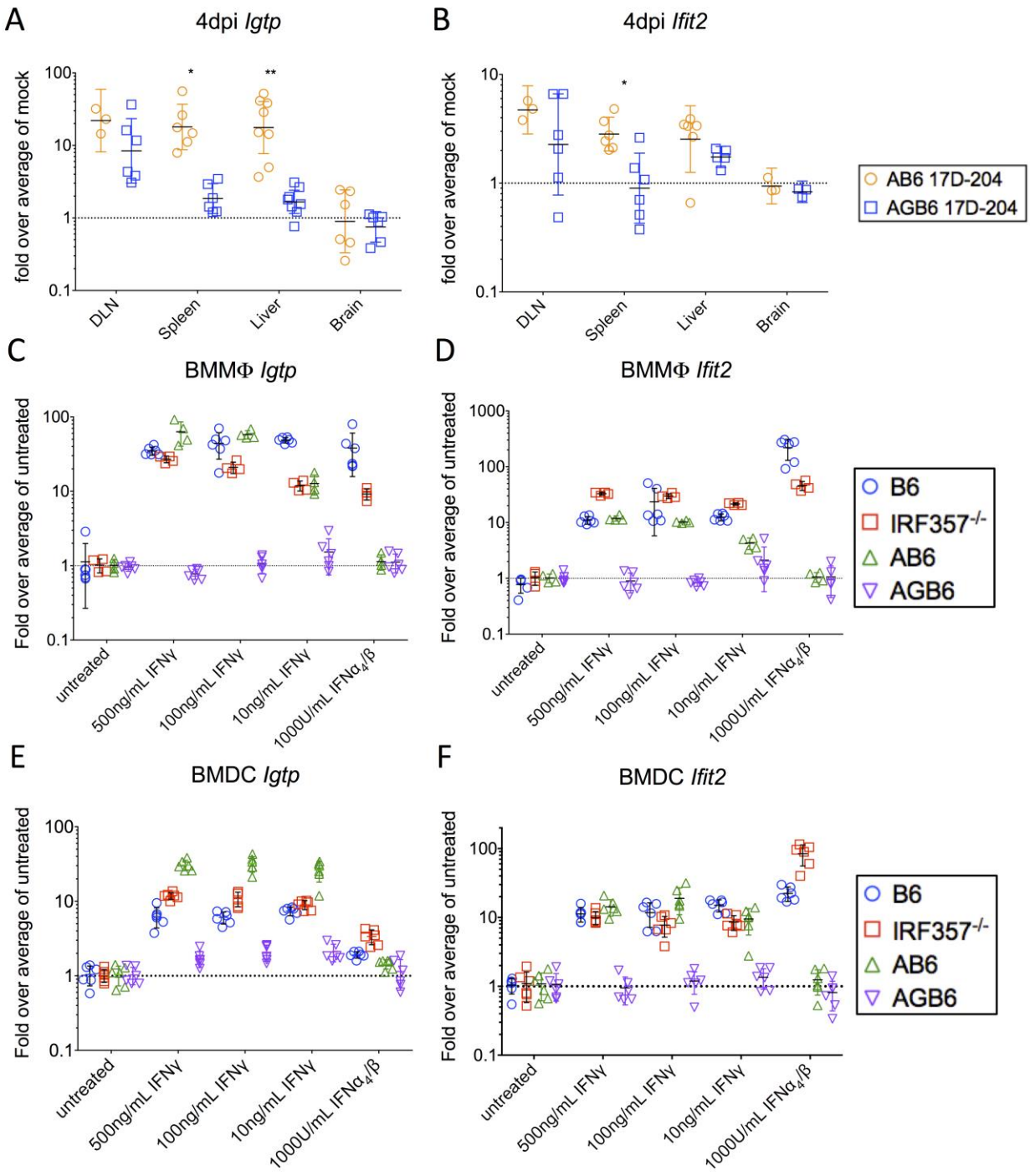

Figure 14: IFN-γ treatment *in vitro* induces antiviral genes that are upregulated in 17D-infected AB6 mice.

(A-B) 6-week-old mice were infected with 17D-204. At 4dpi, tissues were harvested and indicated gene transcripts were quantified using qPCR. Data are also presented in Fig. 10. (C-F) Indicated myeloid cells were treated with

indicated concentrations of IFN for 12hr. Cells were harvested. RNA was isolated, and indicated transcripts were analyzed by qPCR. (*: $p<0.05$, ** $p<0.01$; multiple t-test, corrected by Holm-Sidak method.)

3.4 DISCUSSION

To provide insight into the mechanism for IFN-γ-mediated attenuation of 17D, we compared sensitivity of WT and 17D viruses to IFN-γ. We found that 17D-204 is more sensitive to the antiviral activities of IFN-γ than wild-type YFV in myeloid, but not non-myeloid, cells *in vitro*. While the role that IFN-γ plays in inducing protective immunity against 17D requires further study, our data suggest one mechanism by which IFN-γ controls 17D is through inducing a direct antiviral response, especially in macrophages and DCs. Correspondingly, antiviral genes upregulated in 17D-204-infected AB6 mice, such as *Igtp* and *Ifit2* are also upregulated in myeloid cells treated with IFN-γ. This leads us to speculate that myeloid cells act as a gateway for restricting 17D *in vivo* through an IFN-γ-dependent mechanism. Because IFN-γ induces a large network of antiviral genes (350), it is very likely that multiple ISGs are participating in inhibition of YFV replication cycle. Since we also observe the lack of viral antigens in the liver of 17D-204-infected AB6 mice, genes differentially upregulated in the presence of IFN-γ response, such as *Igtp*, may be important downstream effectors to IFN-γ in attenuation of 17D and protection of visceral organs like the liver.

Cell-type specific effects of IFN-γ have been previously observed. In mice, an IFN-γ-induced antiviral state inhibits murine cytomegalovirus more robustly in macrophages than in MEF (349). IFN-γ induces different gene expression profiles in human DCs and macrophages

(352). Furthermore, the maturation state of macrophages affects the binding of STAT1 to IFN-γ-activated promoter sites (353). Clearly, further work is needed to elucidate the role of specific IFN-γ-induced antiviral effectors in suppression of 17D replication. In addition to ISG induction, specific innate antiviral activities in myeloid cells have been documented for IFN-γ. IFN-γ-induced nitric oxide inhibits replication of JEV in macrophages *in vitro* (145). The function of nitric oxide in the context of flavivirus infection is currently unknown. Nitric oxide is a potent radical species that modifies biomolecules (306), which may modify viral proteins (354), nucleic acid (355), or host factors (356) and interfere the virus replication cycle (145). Pathogens that modify host lipid membranes, such as murine norovirus and *Toxoplasma gondii*, are inhibited by IFN-γ-induced GTPases in macrophages (242). As flaviviruses modify the host membrane extensively for replication and polyprotein processing, YFV is likely also sensitive to these membrane-modulatory GTPases. Myeloid cells derived from mice lacking iNOS and/or immune-related GTPases can be useful to determine whether these factors attenuate17D.

In addition to IFN-γ-dependent antiviral activities in the host, the specific mutations in 17D responsible for the increased IFN-γ sensitivity, and how these mutations increase susceptibility to individual antiviral effectors, need to be identified. Other than mutations in E protein that confer increased GAGs binding (27), the effects of mutations in 17D have yet to be characterized. The mutations M-L36F and NS4B-I95M that differentiate between WT strains and attenuated strains (17D substrains and French neurotropic vaccine strain) are possible candidates for influencing IFN-γ sensitivity (212). For M-L36F, substitution of the analogous amino acid in JEV resulted in a mutant deficient in virion maturation and virus particle production (213). NS4B from various flaviviruses is an antagonist of IFN signaling and inhibits STAT1 translocation (84) and is also critical for usurping the host membrane to generate sites for virus

replication and polyprotein processing. The mutation E-G52R is also a potential candidate as it is also mutated in cell culture-adapted JEV and contributes to reduction of peripheral virulence and altered entry kinetics (213). E-G52R is located at the hinge region important for conformational changes during fusion; however, substitution of the analogous mutation in DENV2 does not alter fusion kinetics, suggestive of virus-specific role of this residue (220). Another potentially important mutation is the poorly characterized NS5-P901L, which is present in the attenuated strains 17D and HeLa-p6. This mutation is located at the C-terminus tail of NS5 and does not a have known regulatory function in viral replication. It is possible that these mutations, alone or in combination with other 17D mutations, could influence sensitivity to IFN-γ.

4.0 CONCLUDING REMARKS AND FUTURE DIRECTIONS

The YFV live attenuated vaccine strain 17D is arguably one of the best LAVs available. In addition to offering long-term protection, the genetic backbone of 17D has been used to develop vaccine candidates against other pathogens (326–328). However, our understanding of the mechanisms of YFV 17D attenuation remains incomplete. Understanding the factors contributing to attenuation and immunogenicity will also be valuable for future rational design of LAV candidates for other flaviviruses or pathogens. In addition, potentially lethal severe adverse events after 17D vaccination and the concerns of YFV re-emergence beyond current geographical boundaries highlight the need to further understand attenuation of 17D.

In contrast to primates, WT mice are highly resistant to peripheral infection of YFV, which complicates the studying of YFV pathogenesis and immunology in a pathophysiologically relevant context. To understand YFV-host interaction, we used mice lacking the type I IFN response (AB6), which are susceptible to s.c. infection of wild-type YFV but resistant to 17D infection. Wild-type virus causes viscerotropic disease in AB6 mice while 17D infection results in long-term immunity. Such similarity to human-YFV interactions prompted us to investigate host factors important in YFV attenuation. In this study, we have characterized the role of the host type II IFN system as an attenuation factor against 17D in a pathophysiologically relevant mouse model.

Our study revealed the importance of IFN-γ in controlling 17D *in vivo* (summarized in Fig. 15). By comparing 17D replication kinetics and pathogenesis in AB6 and AGB6 mice, we conclude that IFN-γ restricts 17D replication and dissemination early during infection. In the absence of the IFN-γ response, 17D replicated in and caused stress or inflammation in the liver and the brain, indicative of both viscerotropic and neurotropic disease. IFN-γ may play a role in virus clearance as clearance was observed within eight days in AB6 mice, whereas in AGB6 mice, virus clearance only occurred in the periphery but in a delayed manner. Deficiency in IFN-γ signaling resulted in poor cytokine responses and less robust induction of antiviral genes when compared to AB6 mice, indicative of a central role for cytokine upregulation and antiviral function of IFN-γ against 17D. We also determined that NK cells were a primary source of IFN-γ early during infection in our model. *In vitro*, we also demonstrated that, IFN-γ inhibits replication of both YFV strains 17D and Angola71 in a dose-dependent manner; however, 17D was more robustly inhibited by IFN-γ treatment than the WT strain in myeloid (macrophage and DC) but not fibroblastic cells. This prompted us to conclude that one mechanism for 17D attenuation is enhanced sensitivity to innate antiviral activities of IFN-γ in myeloid cells.

One important knowledge gap that should be addressed in future studies is the exact molecular mechanism(s) for enhanced sensitivity of 17D to IFN-γ. IFN-γ, like other IFN types, can induce a plethora of immune-modulatory genes. Among these gene products, iNOS and immune-related GTPases have been demonstrated to inhibit viruses from different families in myeloid cells (145, 242). It would be of interest to determine if these genes are also inhibitory to YFV replication. For instance, myeloid cells derived from mice deficient in iNOS and specific immune-related GTPases can be used to evaluate if these proteins are restricting 17D downstream to IFN-γ. In addition, comparative analysis on genes induced in myeloid and non-

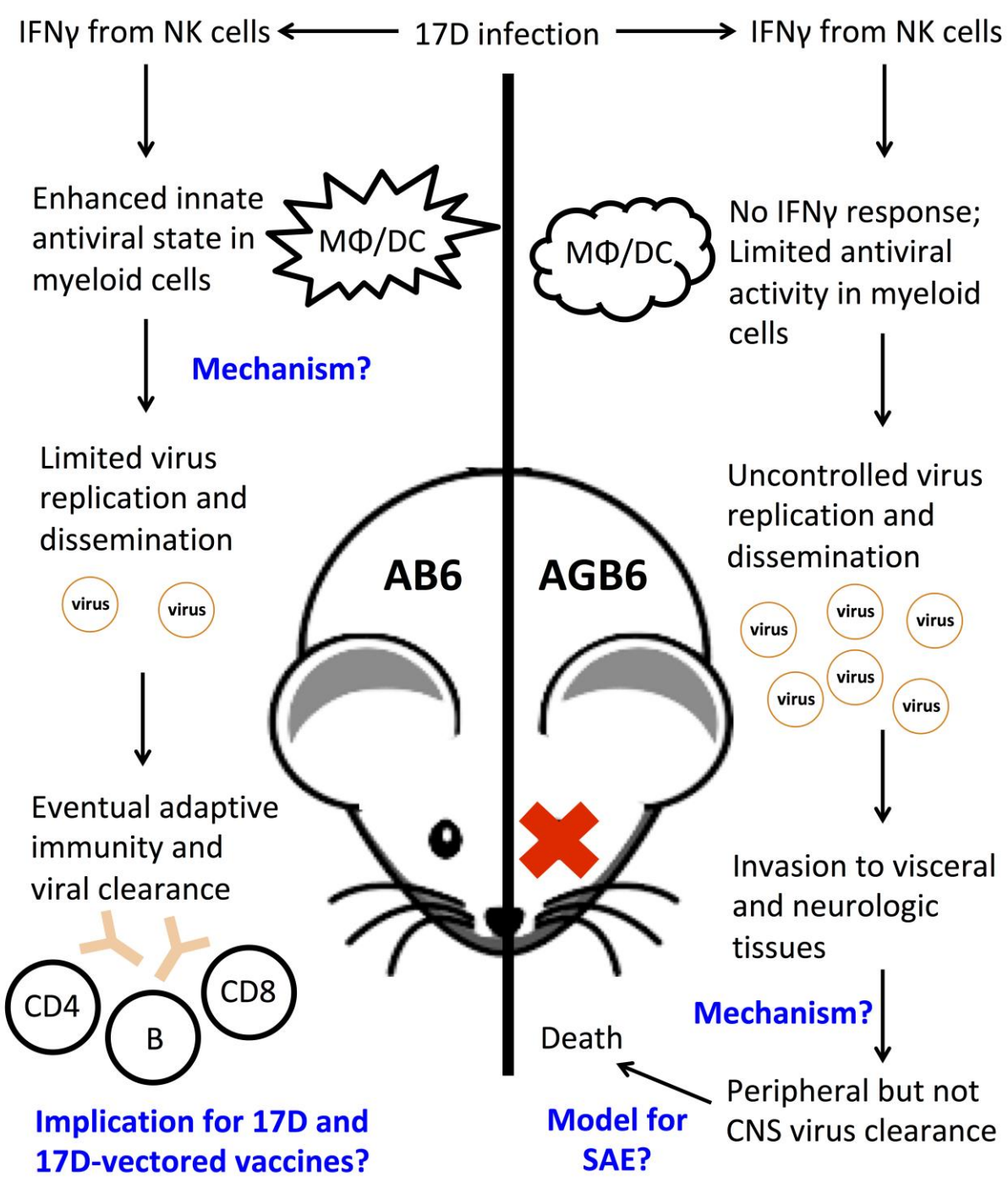

Figure 15. Model of IFN-γ interaction with 17D in mice.

17D infection results in early IFN-γ primarily by NK cells. In the presence of IFN-γ receptor (AB6 mice, left), myeloid cells are at a heightened antiviral state, leading to effective control of 17D replication and dissemination in vivo, and subsequent development of adaptive immunity. In contrast, in the absence of IFN-γ receptor (AGB6 mice,

right), myeloid cells possess limited antiviral activity, leading to unrestricted 17D replication and dissemination. The virus invades visceral tissues such as the liver and neurologic tissues such as the brain, causing stress and damage, eventually leading to death. Our study has highlighted some important questions and future direction (blue) on understanding YFV biology, which are discussed in text.

myeloid cells upon IFN-γ treatment can potentially identify factors that restrict 17D in myeloid cells at a global level. Alternatively, shRNA-mediated knockdown of host factors can be used to screen for the attenuating factors. In addition to identifying host factors contributing to restriction of 17D, the specific amino acid and/or nucleotide changes in the 17D genome leading to enhanced sensitivity to IFN-γ should be characterized. Chimeric viruses containing parts of 17D and parts of WT strains have been used in the literature to understand the role of genetic changes in YFV-mosquito interactions (357, 358). By comparing sensitivity of the chimeras to IFN-γ in myeloid cells, we can evaluate the contribution of individual or groups of mutation(s) to sensitivity to IFN-γ.

Prior to implementation of the monkey neurovirulence test, enhanced virulence due to post-vaccination mutations in 17D has been proposed to cause encephalitis in vaccinees. 17D mutants bearing unique mutations not present in the parent stock or in Asibi were isolated from a viscerotropic SAE case and were suspected to have enhanced virulence (231). It is possible that these unique mutations are compensatory and partially restore virulence of the resulting virus. A thorough understanding of how mutations in 17D alter virulence will aid prediction of the propensity of an individual vaccine batch to result in SAEs and facilitate informed design of a 17D vaccine that can accommodate more at-risk populations without sacrificing effectiveness. Moreover, 17D-vectored chimeric vaccines (326–328) retain the majority of the 17D genome (except structural proteins in the ChimeriVax platform (328)). As a result, these vaccine

candidates may retain the ability to cause SAEs and thus stand to benefit from advances in 17D safety.

Understanding the molecular mechanism of IFN-γ-mediated 17D attenuation can provide important insights into the host factors that enhance the risk of SAE. Based on our data, we speculate that variation in host IFN-γ response can be a potential risk factor for SAEs; however, IFN-γ signaling efficacy can be influenced by factors such as recent infections and on-going therapy. A better understanding of the factors upstream and downstream of IFN-γ can provide us direction for screening potential high-risk individuals prior to vaccination or closely monitor them after vaccination, which may reduce incidence and/or severity of SAEs.

Despite the lack of type I and type II IFN responses, virus clearance was also achieved in the periphery of 17D-infected AGB6 mice by 8dpi. This suggests alternative mechanisms are involved in controlling 17D at a later phase of infection. The role of other innate immunity components, such as TLR signaling and proinflammatory cytokines should be evaluated in our model because these molecules have been implicated in influencing the outcome of flavivirus infection (123, 230, 338). In addition, due to the timing of virus clearance, components of the adaptive immune system such as T cells and antibodies likely contribute to peripheral clearance.

In our model, 17D invasion and replication in CNS likely contribute to disease and ultimate death. However, it remains unclear whether virus and/or host immune responses are responsible for the death of AGB6 mice. Because the brain is an immune privileged site, viruses that invaded the brain may not be as well controlled when compared to the periphery (359). Characterization of the immune response in the brain after neuroinvasion of 17D could provide a clearer picture on pathogenesis and aid in development of therapeutic approaches. The role of glial cells and immune infiltrating cells, such as T cells, need to be investigated. Microglial cells

are resident immune cells that are susceptible to flavivirus infection *in vitro* (32, 360). Interestingly, JEV replicated in primary human microglial cells without secreting infectious particles, and infection induced expression of pro-inflammatory cytokines and chemokines (360). It will be of interest to determine if microglial cells are critical mediators of anti-17D activities in the CNS, or potentially, pathological processes, and whether IFN-γ is important for its these activities and whether or not IFN-α/β controls whether microglia are protective or disease-promoting. Lymphocytes, especially $CD8^+$ T cells have been implicated in controlling flavivirus infections in the CNS (211, 246). In DENV infected AGB6 mice, adoptive transfer of $CD8^+$ T cells from AB6 mice resulted in reduction of virus replication, indicating $CD8^+$ T cells restricts DENV in CNS in an IFN-γ-dependent manner (246). As with microglia, it will be of interest to determine if T cells are protective or disease-promoting in the absence of IFN-α/β.

Our results also suggest that enhanced sensitivity to IFN-γ can lead to attenuation of virus and that live attenuated vaccine candidates can be generated by deliberately enhancing viral sensitivity to IFN-γ (and reasonably, other host immune mechanisms). In fact, several arbovirus LAV candidates have enhanced sensitivity to IFN or particular ISGs (346–348). With the recent global emergence of arboviruses such as Chikungunya, Zika, and dengue virus (361–363), a rational approach for generating vaccine candidates will likely be beneficial to the public.

5.0 MATERIALS AND METHODS

Ethics Statement

Animals were maintained and procedures were performed in accordance with the recommendations in the Guide for the Care and Use of Laboratory Animals of the National Research Council. Protocols 1103456 and 14033545 were approved by the University of Pittsburgh's IACUC committee. Approved euthanasia criteria were based on weight loss and morbidity.

Cells lines

Vero (ATCC-CCL-81), Huh7 (Charles M. Rice, The Rockefeller University), PH5CH8 (Michael R. Holbrook, NIH) and mouse embryonic fibroblasts (MEFs, derived based on (348)) were maintained in DMEM supplemented with 10% fetal bovine serum (FBS), 100U/mL penicillin, 0.05mg/mL streptomycin, 0.29mg/mL L-glutamine, and 1mM sodium pyruvate unless otherwise specified. All cell incubation were performed at 37°C in 5% CO_2 unless otherwise specified.

Virus Stocks

Stocks of 17D-204 and Angola71 were generated from infectious clones by electroporating *in vitro* transcribed RNA into Vero cells as described previously (210). Virus-containing supernatant were harvested after incubation for 4 (Angola71) or 7 days (17D-204), followed by

clarification by centrifugation at 875g for 30min and stored at -80°C. Brazil75 stocks were obtained from Alan T. Barett Virus stock titers were quantified by plaque assay on Huh7. Viruses were diluted to appropriate titer using virus diluent – PBS supplemented with 1% donor bovine serum, 100U/mL penicillin, and 0.05mg/mL streptomycin.

Mouse experiments

AB6 and AGB6 mice were bred in-house. C57BL/6 mice were purchased from Charles River. Groups of randomized 6-week-old sex-matched mice were infected subcutaneously with $1x10^4$ PFU or mock at the hind-limb footpad after isoflurane anesthesia. Weight and swelling of footpad were monitored daily for at least 21 days. Animal experiments were not blinded. To harvest tissues, anesthetized mice were bled at submandibular vein and then sacrificed with isoflurane overdose, followed by cardiac perfusion with virus diluent. Blood were collected in Microtainer serum separator tube (BD, Cat.: 365967) and serum were obtained by centrifugation at 13523g for 5min at 4°C. Tissues were stored in virus diluent or Tri Reagent-LS (Invitrogen) at -80°C until further usage. For histology, mice were perfused with virus diluent and 4% paraformaldehyde (PFA), followed by 24hr fixation in 4% PFA at 4°C, prior to processing for sectioning. For antibody depletion experiments, 3 doses of 75µg of mouse IgG2a (C1.18.4) or NK1.1 (PK136, BioXCell) or 3 doses of 150µg of CD4 (GK1.5) or CD8 (2.43) at -3, -1, and 1dpi were injected to animals by intraperitoneal route. IgG2a, CD4, and CD8 antibodies were generated from the corresponding hybridomas (ATCC) using CELLine bioreactors (Argos Technologies) according to manufacture's protocol and purified with ammonium sulfate precipitation as described previously (364).

Flow Cytometry

Popliteal (draining) lymph node were harvested from infected animals at 3dpi, minced, and strained through 70μm cell strainer (Falcon). Single cell suspensions were cultured in media – RPMI 1640 supplemented with 10% FBS, 100U/mL penicillin, 0.05mg/mL streptomycin, 20μM β-mercaptoethanol (Sigma), and 5μg/mL Brefeldin A (Tonbo bioscience) for 6hr. Cells were stained as previously described (210). Antibody and dyes used in this study were: Fixable Viability dye UV Blue (eBioscience), anti-mouse CD16/32 (93, eBioscience), APC-Cy7-anti-CD8 (2.43, Tonbo bioscience), PerCP-Cy5.5-anti-CD4 (GK1.5, Tonbo bioscience), APC-anti-NK1.1 (PK136, Tonbo bioscience), PE-anti-γδTCR (GL3, eBioscience), and FITC-anti-IFN-γ (XMG1.2, Tonbo bioscience). FITC-rat IgG1 (MOPC-21, Tonbo bioscience) is used as isotype control. Stained cells were fixed in 1% PFA and analyzed using BD LSRFortessa (BD Bioscience) and FlowJo software (Tree Star).

Plaque assay

Huh7 cells were infected with serially diluted inoculum for 1hr. For quantification of virus in mouse organs, tissues were homogenized in sterile pestles (Bel-Art), and the virus-containing supernatant were clarified by centrifugation at 13523g for 15min at 4°C and used as inoculum. Infected Huh7 were overlaid with media supplemented with 0.5% carboxymethocellulose (CMC, high viscosity, Sigma). At 4dpi (virus stocks) or 5dpi (tissues), plaques were visualized by staining with 0.5% crystal violet in 2% PFA.

Cytokine and gene expression analyses

Serum cytokines were quantified by the Cytokine 20-plex Mouse Panel (Invitrogen) according to manufacturer protocol. To analyze gene expression in different organs, RNA from tissues was isolated using Tri reagent-LS (Invitrogen) following the manufacturer protocol. Polyacryl carrier was added to serum and lymph node samples only. Reverse transcription of 100ng of purified RNA were performed using random hexamer and TaqMan reverse transcription reagent (AB) under the following condition: 25°C for 10min, followed by extension at 48°C for 30min, and inactivation of enzymes at 95°C for 5min. Quantitation of 18S cDNA and antiviral genes was performed in Maxima Probe qPCR Master Mix (Thermo) and Maxima SYBR Green/Rox qPCR mix, respectively. Fluorescent intensity data were collected on a 7900HT Real-Time PCR System (AB). Thermocycling conditions were as follow: denaturing and polymerase activation at 95°C for 10min, followed by 40 cycles of denaturing at 95°C for 15s and extension at 60°C for 1min with fluorescent intensity data collection. An additional melting curve cycle was added for quality controls for antiviral genes. Primers and probes used in PCR were listed in table 2.

Table 2. qPCR primer and probe sequences used in this study.

Primer/probes	Sequence
18S-S	CGCCGCTAGAGGTGAAATTCT
18S-AS	CGAACCTCCGACTTTCGTTCT
18S probe (HEX)	/5HEX/CAA GAC GGA /ZEN/CCA GAG CGA AAG CAT TTG /3IABkFQ/
mIFIT1-S	GTGGCTCACATAGAGCAGGA
mIFIT1-AS	AGTTTCCTCCAAGCAAAGGA
mIFIT2-S	AGAATTCACCTCTGGATGGG
mIFIT2-AS	GTCAAGCTTCAGTGCCAAGA
mIGTP-S	TCTGAGCAGGTTCTGAAGGA
mIGTP-AS	TCCTCGGCTTCTTTCTTCTC
mIFNg-S	CAAAAGGATGGTGACATGAA
mIFNg-AS	TTGGCAATACTCATGAATGC

Histology

For Hematoxylin & Eosin (H&E) staining, PBS- and PFA-perfused mouse organs were harvested. Sectioning and staining were performed by the Histology Core at the McGowan Institute of Regenerative Medicine at the University of Pittsburgh. For Immunostaining, PBS-perfused mouse organs were harvested fresh, sunk in 30% sucrose at 4°C, and frozen in O.C.T. medium. For Angola71-infected mice, PFA perfusion and fixation were performed prior to sucrose treatment. Frozen tissues were stored at -80°C until cryosection. 7μm (spleen and liver) or 20μm (brain) sections were permeabilized in 100% methanol at -20°C, rehydrated in PBS with 0.05% Tween20 (PBST), antigen retrieved by proteinase K digest, and blocked in 2% BSA, 1:200 anti-CD16/32, 5% normal rat serum and goat serum, followed by incubation in M.O.M. reagent (VectorLab). YFV proteins were stained using heat-inactivated immune sera from immunized AB6 mice at 21dpi or normal serum as isotype control at 1:50 dilution, followed by AlexaFluor488- or AlexaFluor594-conjugated goat-anti-mouse antibody. For staining liver, tissues sections were treated with normal mouse serum prior to incubation in M.O.M. reagent. Specific cell types were probed with antibodies against F4/80 (BM8, Tonbo Bioscience), CD169 (MOMA-1, Acris Antibodies, Cat.: SM066B), LYVE-1 (Goat polyclonal, R&D systems, Cat.: AF2125), and GFAP (Chicken polyclonal, Abcam, Cat.: Ab4674). Stained slides were mounted on DAPI in SlowFade Gold (Invitrogen) and imaged using FluoView 1000 confocal microscope (Olympus).

IFN-γ ELISA

ELISA for IFN-γ was performed using the ELISA Ready-Set-Go kit (eBioscience) according to manufacture directions.

Generation of bone marrow-derived cells

Bone marrow-derived macrophages (BMMΦ) and dendritic cells (BMDC) were generated as described previously (118). After 6 days of maturation, DCs were collected from supernatant and macrophages were scraped from plates. Cells were washed, counted, and seeded on U-bottom 96-well plates for DC or 24-well plates for macrophages, followed by treatment with IFNs and virus infection.

Virus infection

Mouse embryonic fibroblasts (MEFs), macrophages, and dendritic cells were treated with various concentrations of IFN-γ (Peprotech) or IFN-α_4/β (made in-house as described previously (365)) for 12hr. Media containing IFNs were removed prior to infection with YFVs at designated MOI for 1hr. Cells were washed three times after infection. For BMDC, cells were pelleted at 219g for 5min at 4°C between washes. Infected cells were maintained in their corresponding media. Supernatant were harvested daily for focus-forming assay.

Focus-forming assay

$1x10^4$ Vero cells were seeded on 96-well plate, followed by infection with serially diluted virus inoculum. After 1hr infection, cells were washed and overlaid with media supplemented with 0.5% CMC for 96hr. Cell monolayers were washed in PBS and fixed in 4% PFA for 24hr. Fixed cells were washed and permeabilized with 100% methanol at -20°C for 10min, followed by washes in PBS containing 0.05% tween20 (PBST). Nonspecific protein binding was blocked by incubation in PBST with 1% BSA and 5% normal goat serum for 1hr at room temperature. YFV proteins were stained using heat-inactivated immune sera from immunized AB6 mice at 21dpi at

1:100 dilution for 24hr at 4°C, followed by probing with HRP-goat anti-mouse antibody for 1hr at room temperature. Foci were visualized by 3,3'-diaminobenzidine as substrate (ThermoFisher, cat.: 34065).

Immunofluorescence staining for STAT proteins 654321

$2x10^4$ PH5CH8 cells were seeded on glass slides (VWR Cat. #48312-003), followed by infection with viruses at MOI=2. After 1hr infection, cells were washed and overlaid with media supplemented with 20μM zVAD-fmk, zFA-fmk, or an equivalent volume of DMSO. At 48hpi, cells were washed and fixed in 4% PFA, followed by immunofluorescence staining using the same procedure as focus-forming assay. The following antibodies were used. Primary: STAT1 (M-22), STAT2 (H-190), and YFV (mouse ascites fluid, ATCC). Secondary: AlexaFluor488-conjugated donkey anti-mouse and AlexaFluor594-conjugated donkey-anti-rabbit. Stained slides were mounted on DAPI in SlowFade Gold (Invitrogen) and imaged using Olympus CKX41 microscope.

Statistical analysis

All data were analyzed with GraphPad Prism software. Log-rank test was performed on survival studies. Multiple t-test with Holm-Sidak correction was performed whenever appropriate. No statistical methods were used to ensure adequate power. Sample sizes were chosen based on experience on morbidity and mortality of YFV in mice to achieve statistical significance yet utilize fewest animals.

APPENDIX A

PRELIMINARY DATA RELATED TO THIS WORK

STAT1-degradation may contribute to enhanced virulence of WT YFV

Experiments in chapter 3 demonstrated that 17D is more sensitive to the antiviral state induced by IFN-γ than WT virus strain Angola71. Because virulent virus strains are more capable of antagonizing host antiviral activities than attenuated strains (346, 347), we sought to determine if WT YFV interferes with signaling molecules downstream of IFN-γ more efficiently than 17D. Inhibition of the JAK-STAT pathway is a prominent mechanism employed by virulent viruses to dampen IFN signaling. Flavivirus NS5, including that of YFV, suppresses IFN signaling by sequestration and/or degradation STAT2 (91, 92, 366). NS5 also inhibits phosphorylation of STAT1 (367). To determine if YFV also interferes with STAT1 signaling, we evaluated STAT1 protein levels in PH5CH8 human hepatocytes. PH5CH8 cells were used because they retain functional IFN responses, and different antiviral genes were induced when these cells were infected with YFV strains 17D or Asibi (368).

Infection in PH5CH8 cells with 17D or Angola71 virus resulted in a loss of STAT2 staining, as expected. Interestingly, while 17D-infected cells largely remained STAT1-positive, STAT1 protein levels were significantly lower in Angola71-infected cells (Fig. 16A-B).

Flavivirus infection has been shown to result in activation of caspases and apoptosis *in vitro* (44, 369–371). Because of STAT1 has been reported to be cleaved by caspase-3 and -7, leading to its degradation (372), we evaluated if caspase inhibition could rescue STAT1 protein levels. Treatment of cells with caspase inhibitors or vehicle did not affect virus replication (Fig. 16C). However, treatment of Angola71-infected cells with the pan-caspase inhibitor zVAD-fmk partially restored STAT1 protein levels (Fig. 16D), indicating caspase activation is involved in degradation of STAT1 by WT YFV.

These preliminary studies suggest that one potential mechanism for enhanced IFN-γ sensitivity by 17D is failure to degrade STAT1. However, more detailed and in-depth studies are required to elucidate the role of caspase activation in STAT1 degradation and the relative impact of differential degradation on 17D and WT YFV replication. Based on our model, IFN-γ signaling in myeloid cells, but not non-myeloid cells contributes to attenuation of 17D. The effects of caspase inhibition in YFV-infected myeloid cells and the subsequent effects on IFN-γ-mediated immunity should be evaluated. In addition, the viral factor(s) and the corresponding mechanism(s) contributing to caspase-mediated degradation of STAT1 should be identified, as it can aid development of pharmacological intervention in YF and/or SAE patients. The C-terminus of M protein of flaviviruses activates caspases, and M protein from Asibi induces apoptosis more robustly than 17D (44). In addition, the E protein, which possesses most of the genetic differences between 17D and Asibi, and the viral protease NS3 has also been reported to activate caspases (369–371). Thus, it will be of interest to determine if these proteins differentially activate caspases to degrade STAT1 and subvert host IFN responses.

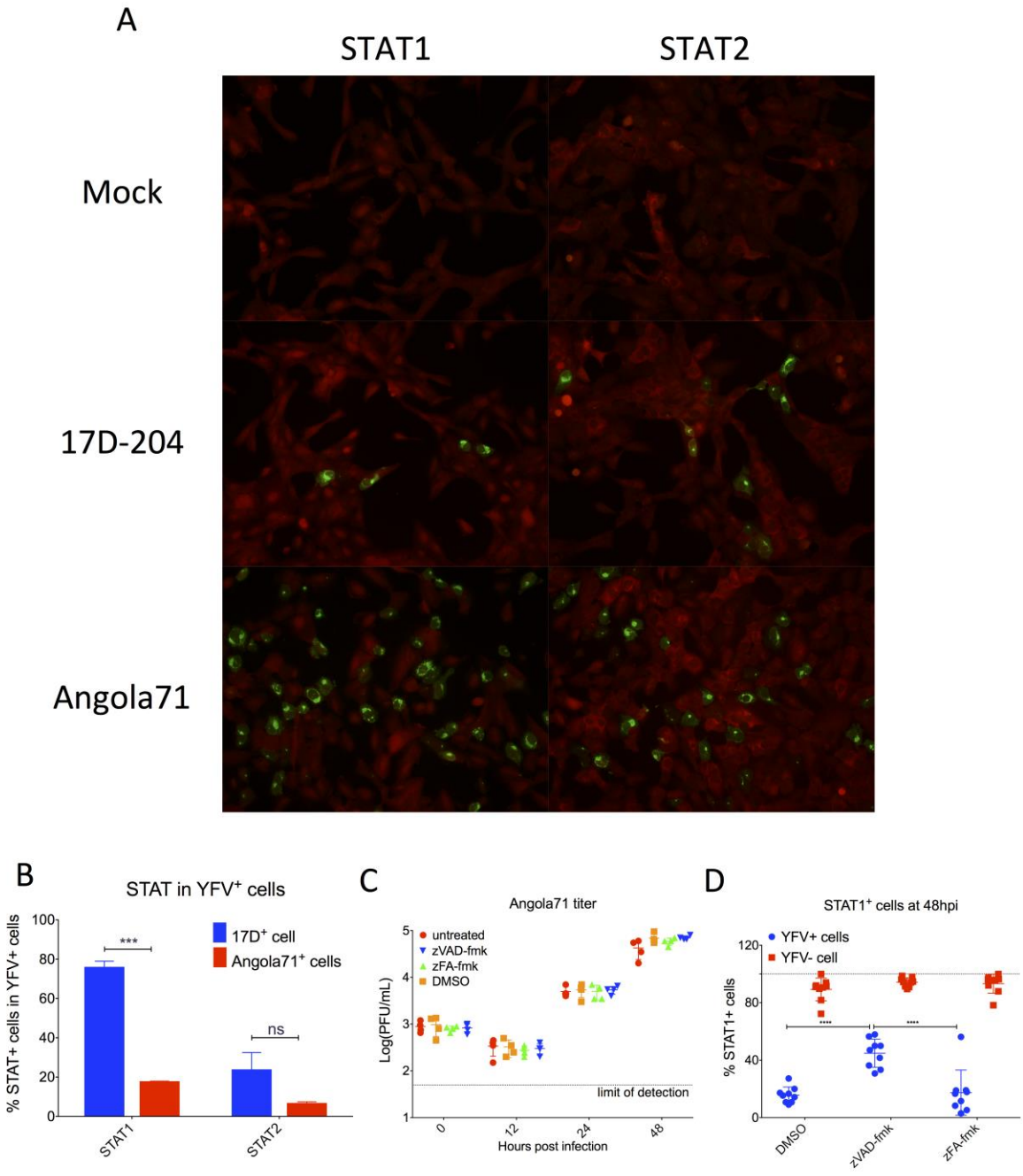

Figure 16. Wild-type YFV but not 17D-204 downregulates STAT1 in a caspase-dependent manner.

$2x10^4$ PH5CH8 cells were infected at MOI=2 on glass slides. At 48hpi, cells were washed and fixed in 4% PFA, followed by immunofluorescence staining. Red=STAT protein and green=virus. (A) representative staining for STAT1 and STAT2 in YFV-infected cells. (B) quantified data from (A). (C-D) Experiment was performed as in (A) except only Angola71 was used and after infection, cells were incubated in media containing DMSO or 20μM

indicated compounds. (C) Virus replication kinetics were not affected by chemical treatments. (D) Pan-caspase inhibitor zVAD-fmk partially restored STAT1 level in Angola71-infected cells. (***: $p<0.001$, multiple t-test corrected with Sidak-Holm method. $n\geq4$)

A YEL-AVD clinical isolate, Brazil75 shows enhanced virulence in AGB6 mice

In addition to host variation in IFN-γ responses, mutations in 17D have been hypothesized to be associated with incidence of SAE (231, 232). One YEL-AVD SAE clinical isolate, strain Brazil75 (B75) contains two mutations (M-I49L and NS4B-Y240F) when compared to its parent strain 17DD (231). These mutations are unique and not reversions to WT residues. Engel et al. reported that B75 and 17DD are similarly virulent in immortalized kidney and hepatocyte cell lines and the hamster infection model (231); however, in this study, the B75 virus was not adapted to hamster prior to infection, which may explain the lack of enhanced virulence. To investigate the contribution of viral genetics to SAEs, we evaluated the virulence of B75 in our mouse model. In AB6 mice, B75 infection did not result in any discernable disease, including footpad swelling (data not shown). However, in AGB6 mice, B75-infected mice succumbed to disease significantly earlier (AST 9.17±0.98) than 17D-204-infected animals (11.2±0.45, Fig. 17A). B75 also resulted in more rapid weigh-loss in infected animals (Fig. 17B). Interestingly, in contrast to 17D, no footpad swelling was observed in B75-infected AGB6 mice (Fig. 17C). We determined virus replication levels at 8dpi, when B75-infected animals started to succumb to infection. Virus titers in most sampled tissues were similar between B75 and 17D-204 except in the serum and the brain (Fig. 17D), where viremia remained detectable in B75-infected mice at 8dpi but not in 17D-204-infected mice, suggesting B75 remained in the circulation longer. Virus titer was also significantly higher in the brains of B75-infected AGB6 mice (up to 10^8 PFU/mg), indicative of higher neurovirulence than 17D-204.

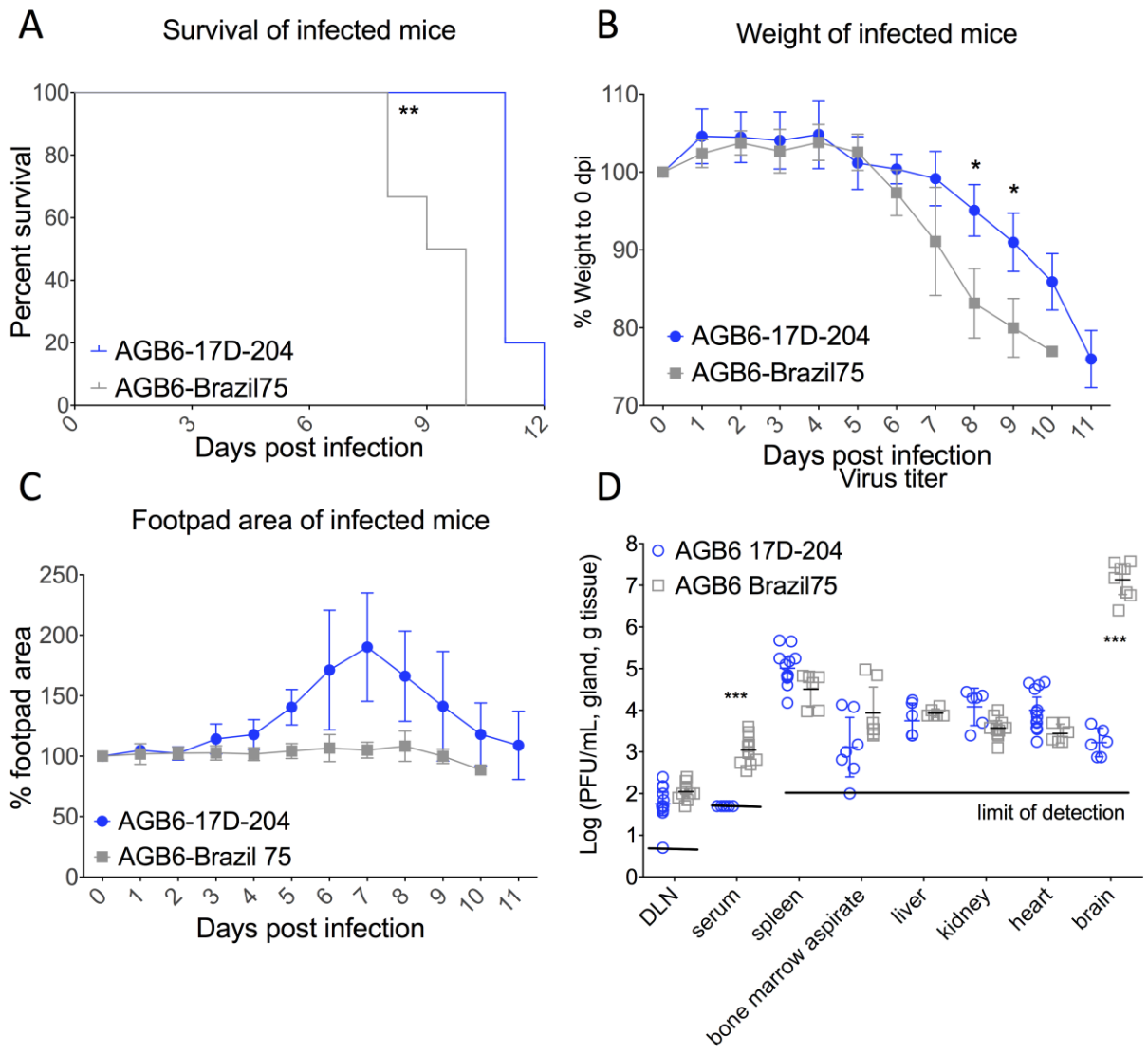

Figure 17. A YEL-AVD SAE clinical isolate, strain Brazil75 is more virulent than 17D-204 in AGB6 mice.

6-week-old AGB6 mice were infected subcutaneously with $1x10^4$ PFU of virus. (A) Survival, (B) weight, and (C) footpad swelling were monitored daily. (D) Infected animals were sacrificed on 8dpi. Tissues were harvested and virus titers were quantified as described in materials and methods. (**: $p<0.01$, Log-rank test in A, *: $p<0.05$ and ***: $p<0.001$ in B and D, multiple t-test with Sidak-Holm correction. $n\geq6$)

Our data suggest that mutation(s) in 17D that occur during replication in vaccinees can contribute to enhanced virulence. However, some important questions and caveats need to be addressed. B75 is derived from the substrain 17DD but not 17D-204 (231). Therefore, 17DD will be a better control for future experiments. The observation that B75-infected mice showed no footpad swelling is interesting. It remains to be determined if virus mutations are contributing to the lack of swelling or local reaction at the site of infection or if it is simply due to differences in genetic background of 17DD and 17D-204. A more in-depth analysis of virus replication kinetics and immune response are necessary to determine how those genetic changes influence virus pathogenicity. It is also intriguing that B75, a YEL-AVD clinical isolate replicated to high titer in the brain, suggesting a potential for two mutations (M-I49L and NS4B-Y240F) in causing encephalitic disease and/or the AGB6 mice are more prone to experiencing neurologic disease after 17D infection. Nevertheless, histological studies are needed to determine the likely cause of disease and death.

APPENDIX B

TABLE OF ABBREVIATION

AB6: B6 mice lacking type I interferon receptor

AGB6: B6 mice lacking type I and type II interferon receptors

Axl: AXL Receptor Tyrosine Kinase

BMDC: Bone marrow-derived dendritic cell

BMMΦ: Bone marrow-derived macrophage

C: Capsid

CAPRIN1: Cell cycle associated protein 1

CCL: CC Chemokine ligand

cGAS: Cyclic GMP-AMP synthase

CIITA: class II, major histocompatibility complex, transactivator

CNS: Central nervous system

CPE: Cytopathic effects

CrkL: Crk-like protein

CS: Circularization sequence

DC-SIGN: Dendritic Cell-Specific Intercellular adhesion molecule-3-Grabbing Non-integrin

DENV: Dengue virus

DNase: Deoxyribonuclease

Dpi: Day(s) post-infection

dsRNA: double-stranded RNA

E: Envelope

ERK1/2: extracellular signal–regulated kinases 1/2

FBS: Fetal bovine serum

G3BP: Ras GTPase-activating protein-binding protein

GAGs: Glycosaminoglycan

H&E: Hematoxylin & Eosin

Hlx: Homeobox Protein HB24

i.c.: intracerebral

i.p.: intra-peritoneal

IFIT: IFN-induced protein with tetratricopeptide repeats

IFN: Interferon

IfngCNS: conserved noncoding sequences around *Ifng* gene locus

IL: Interleukin

iNOS: inducible nitric oxide synthases

IP-10: Interferon gamma-induced protein 10

IRF: Interferon regulatory factor

ISG: Interferon-stimulated genes

ITAM: immunoreceptor tyrosine-based activation motif

ITIM: immunoreceptor tyrosine-based inhibition motif

JAK: Janus Kinase

JEV: Japanese encephalitis virus

JNK1: Mitogen-activated protein kinase 8

LAV: Live attenuated vaccine

MAPK: mitogen-activated protein kinase

MAVS: Mitochondrial antiviral-signaling protein

MDA5: Melanoma Differentiation-Associated protein 5

MHC: Major histocompatibility complex

MICA: MHC class I polypeptide-related sequence A

MTase: Methyltransferase

mTOR: Mechanistic target of rapamycin

MVEV: Murray Valley encephalitis virus

MyD88: Myeloid differentiation primary response 88

NFκB: nuclear factor kappa-light-chain-enhancer of activated B cells

NHP: Non-human primate

NK: Natural killer

NS1: nonstructural protein 1

NS2A: nonstructural protein 2A

NTPase: Nucleoside triphosphatase

OAS: 2'-5'-oligoadenylate synthetase

PAMPs: Pathogen-associated molecular patterns

PBS: Phosphate-buffered saline

PFU: Plaque forming unit

PKC: Protein kinase C

PMN: Polymorphonuclear leukocyte

PrM: precursor-membrane

PRR: Pattern recognition receptor

qRT-PCR: quantitative real time reverse-transcription-polymerase chain reaction

RC: Replicative complex

RI: Replicative intermediate

RIG-I: retinoic acid-inducible gene I

RLR: RIG-I-like receptor

RNase: Ribonuclease

Runx3: Runt-related transcription factor 3

s.c.: subcutaneous

SeV: Sendai virus

sfRNA: subgenomic flavivirus RNA

SHP: Src homology region 2 domain-containing phosphatase

SLA: stem loop A

SNP: Single nucleotide polymorphism

SOCS: Suppressor of cytokine signaling

STAT: Signal transducer and activator of transcription

STING: Stimulator of Interferon Genes

Syk: Spleen tyrosin kinase

T-bet: T-box transcription factor TBX21

TBEV: Tick-borne encephalitis virus

TBK1: TANK-binding kinase 1

T_{CM}: Central memory T cell

T_{EM}: Effector memory T cell

T_{EMRA}: Effector memory T cell re-expressing CD45RA

TLR: Toll-like receptor

TNF: Tumor necrosis factor

UAR: upstream ATG region

UTR: untranslated region

WT: wild-type

WNV: West Nile virus

XRN1: 5'-3' exoribonuclease

YFV: Yellow fever virus

APPENDIX B

BIBLIOGRAPHY

1. Kuno G, Chang G-JJ, Tsuchiya KR, Karabatsos N, Cropp CB (1998) Phylogeny of the Genus Flavivirus. *J Virol* 72(1):73–83.

2. Cigarroa-Toledo N, et al. (2016) Serologic Evidence of Flavivirus Infections in Peridomestic Rodents in Merida, Mexico. *J Wildl Dis* 52(1):168–172.

3. Sf L, et al. (2015) Flavivirus Infection in Wild Birds from Brazilian Amazon. *Entomol Ornithol Herpetol Curr Res* 4(3):1–4.

4. Almeida MAB, et al. (2014) Surveillance for Yellow Fever Virus in Non-Human Primates in Southern Brazil, 2001–2011: A Tool for Prioritizing Human Populations for Vaccination. *PLoS Negl Trop Dis* 8(3). doi:10.1371/journal.pntd.0002741.

5. Morales MA, et al. (2017) Detection of the mosquito-borne flaviviruses, West Nile, Dengue, Saint Louis Encephalitis, Ilheus, Bussuquara, and Yellow Fever in free-ranging black howlers (Alouatta caraya) of Northeastern Argentina. *PLoS Negl Trop Dis* 11(2). doi:10.1371/journal.pntd.0005351.

6. Kading RC, Schountz T (2016) Flavivirus Infections of Bats: Potential Role in Zika Virus Ecology. *Am J Trop Med Hyg* 95(5):993–996.

7. Tajima S, Takasaki T, Matsuno S, Nakayama M, Kurane I (2005) Genetic characterization of Yokose virus, a flavivirus isolated from the bat in Japan. *Virology* 332(1):38–44.

8. Machain-Williams C, et al. (2013) Serologic Evidence of Flavivirus Infection in Bats in the Yucatan Peninsula of Mexico. *J Wildl Dis* 49(3). doi:10.7589/2012-12-318.

9. Nofchissey RA, et al. (2013) Seroprevalence of Powassan virus in New England deer, 1979-2010. *Am J Trop Med Hyg* 88(6):1159–1162.

10. Lin S-R, et al. (2004) Study of Sequence Variation of Dengue Type 3 Virus in Naturally Infected Mosquitoes and Human Hosts: Implications for Transmission and Evolution. *J Virol* 78(22):12717–12721.

11. Sim S, et al. (2015) Tracking Dengue Virus Intra-host Genetic Diversity during Human-to-Mosquito Transmission. *PLoS Negl Trop Dis* 9(9):e0004052.

12. Ciota AT, et al. (2007) Cell-specific adaptation of two flaviviruses following serial passage in mosquito cell culture. *Virology* 357(2):165–174.

13. Billoir F, et al. (2000) Phylogeny of the genus flavivirus using complete coding sequences of arthropod-borne viruses and viruses with no known vector. *J Gen Virol* 81(Pt 3):781–790.

14. Clifford CM, Yunker CE, Thomas LA, Easton ER, Corwin D (1971) Isolation of a Group B arbovirus from Ixodes uriae collected on Three Arch Rocks National Wildlife Refuge, Oregon. *Am J Trop Med Hyg* 20(3):461–468.

15. Lawrie CH, Uzcátegui NY, Armesto M, Bell-Sakyi L, Gould EA (2004) Susceptibility of mosquito and tick cell lines to infection with various flaviviruses. *Med Vet Entomol* 18(3):268–274.

16. Lawrie CH, Uzcátegui NY, Gould EA, Nuttall PA (2004) Ixodid and argasid tick species and west nile virus. *Emerg Infect Dis* 10(4):653–657.

17. Gaunt MW, et al. (2001) Phylogenetic relationships of flaviviruses correlate with their epidemiology, disease association and biogeography. *J Gen Virol* 82(8):1867–1876.

18. Calisher CH, et al. (1989) Antigenic Relationships between Flaviviruses as Determined by Cross-neutralization Tests with Polyclonal Antisera. *J Gen Virol* 70(1):37–43.

19. Kuhn RJ, et al. (2002) Structure of Dengue Virus: Implications for Flavivirus Organization, Maturation, and Fusion. *Cell* 108(5):717–725.

20. Zhang X, et al. (2013) Cryo-EM structure of the mature dengue virus at 3.5-Å resolution. *Nat Struct Mol Biol* 20(1):105–110.

21. Allison SL, et al. (2003) Two Distinct Size Classes of Immature and Mature Subviral Particles from Tick-Borne Encephalitis Virus. *J Virol* 77(21):11357–11366.

22. Dong H, et al. (2007) Distinct RNA Elements Confer Specificity to Flavivirus RNA Cap Methylation Events. *J Virol* 81(9):4412–4421.

23. Asghar N, et al. (2016) The role of the poly(A) tract in the replication and virulence of tick-borne encephalitis virus. *Sci Rep* 6:39265.

24. Mandl CW, Kunz C, Heinz FX (1991) Presence of poly(A) in a flavivirus: significant differences between the 3' noncoding regions of the genomic RNAs of tick-borne encephalitis virus strains. *J Virol* 65(8):4070–4077.

25. Tassaneetrithep B, et al. (2003) DC-SIGN (CD209) mediates dengue virus infection of human dendritic cells. *J Exp Med* 197(7):823–829.

26. Shimojima M, Takenouchi A, Shimoda H, Kimura N, Maeda K (2014) Distinct usage of three C-type lectins by Japanese encephalitis virus: DC-SIGN, DC-SIGNR, and LSECtin. *Arch Virol* 159(8):2023–2031.

27. Lee E, Lobigs M (2008) E Protein Domain III Determinants of Yellow Fever Virus 17D Vaccine Strain Enhance Binding to Glycosaminoglycans, Impede Virus Spread, and Attenuate Virulence. *J Virol* 82(12):6024–6033.

28. Chen S-T, et al. (2008) CLEC5A is critical for dengue-virus-induced lethal disease. *Nature* 453(7195):672–676.

29. Chen S-T, et al. (2012) CLEC5A Regulates Japanese Encephalitis Virus-Induced Neuroinflammation and Lethality. *PLOS Pathog* 8(4):e1002655.

30. Meertens L, et al. (2012) The TIM and TAM Families of Phosphatidylserine Receptors Mediate Dengue Virus Entry. *Cell Host Microbe* 12(4):544–557.

31. Jemielity S, et al. (2013) TIM-family Proteins Promote Infection of Multiple Enveloped Viruses through Virion-associated Phosphatidylserine. *PLOS Pathog* 9(3):e1003232.

32. Meertens L, et al. (2017) Axl Mediates ZIKA Virus Entry in Human Glial Cells and Modulates Innate Immune Responses. *Cell Rep* 18(2):324–333.

33. Smit JM, Bittman R, Wilschut J (1999) Low-pH-Dependent Fusion of Sindbis Virus with Receptor-Free Cholesterol- and Sphingolipid-Containing Liposomes. *J Virol* 73(10):8476–8484.

34. Randolph VB, Stollar V (1990) Low pH-induced Cell Fusion in Flavivirus-infected Aedes Albopictus Cell Cultures. *J Gen Virol* 71(8):1845–1850.

35. Corver J, et al. (2000) Membrane Fusion Activity of Tick-Borne Encephalitis Virus and Recombinant Subviral Particles in a Liposomal Model System. *Virology* 269(1):37–46.

36. Gollins SW, Porterfield JS (1986) PH-dependent Fusion between the Flavivirus West Nile and Liposomal Model Membranes. *J Gen Virol* 67(1):157–166.

37. Stiasny K, Koessl C, Heinz FX (2003) Involvement of Lipids in Different Steps of the Flavivirus Fusion Mechanism. *J Virol* 77(14):7856–7862.

38. Haslwanter D, Blaas D, Heinz FX, Stiasny K (2017) A novel mechanism of antibody-mediated enhancement of flavivirus infection. *PLOS Pathog* 13(9):e1006643.

39. Dowd KA, Pierson TC (2011) Antibody-mediated neutralization of flaviviruses: A reductionist view. *Virology* 411(2):306–315.

40. Assenberg R, et al. (2009) Crystal Structure of a Novel Conformational State of the Flavivirus NS3 Protein: Implications for Polyprotein Processing and Viral Replication. *J Virol* 83(24):12895–12906.

41. Jones CT, et al. (2003) Flavivirus Capsid Is a Dimeric Alpha-Helical Protein. *J Virol* 77(12):7143–7149.

42. Ma L, Jones CT, Groesch TD, Kuhn RJ, Post CB (2004) Solution structure of dengue virus capsid protein reveals another fold. *Proc Natl Acad Sci U S A* 101(10):3414–3419.

43. Samuel GH, Wiley MR, Badawi A, Adelman ZN, Myles KM (2016) Yellow fever virus capsid protein is a potent suppressor of RNA silencing that binds double-stranded RNA. *Proc Natl Acad Sci* 113(48):13863–13868.

44. Catteau A, et al. (2003) Dengue virus M protein contains a proapoptotic sequence referred to as ApoptoM. *J Gen Virol* 84(10):2781–2793.

45. Bhardwaj S, Holbrook M, Shope RE, Barrett AD, Watowich SJ (2001) Biophysical characterization and vector-specific antagonist activity of domain III of the tick-borne flavivirus envelope protein. *J Virol* 75(8):4002–4007.

46. Thullier P, et al. (2001) Mapping of a dengue virus neutralizing epitope critical for the infectivity of all serotypes: insight into the neutralization mechanism. *J Gen Virol* 82(Pt 8):1885–1892.

47. Crill WD, Roehrig JT (2001) Monoclonal antibodies that bind to domain III of dengue virus E glycoprotein are the most efficient blockers of virus adsorption to Vero cells. *J Virol* 75(16):7769–7773.

48. Rey FA, Heinz FX, Mandl C, Kunz C, Harrison SC (1995) The envelope glycoprotein from tick-borne encephalitis virus at 2 A resolution. *Nature* 375(6529):291–298.

49. Adams SC, et al. (1995) Glycosylation and antigenic variation among Kunjin virus isolates. *Virology* 206(1):49–56.

50. Chambers TJ, Halevy M, Nestorowicz A, Rice CM, Lustig S (1998) West Nile virus envelope proteins: nucleotide sequence analysis of strains differing in mouse neuroinvasiveness. *J Gen Virol* 79 (Pt 10):2375–2380.

51. Post PR, et al. (1992) Heterogeneity in envelope protein sequence and N-linked glycosylation among yellow fever virus vaccine strains. *Virology* 188(1):160–167.

52. Roehrig JT, Bolin RA, Kelly RG (1998) Monoclonal Antibody Mapping of the Envelope Glycoprotein of the Dengue 2 Virus, Jamaica. *Virology* 246(2):317–328.

53. Crill WD, Chang G-JJ (2004) Localization and Characterization of Flavivirus Envelope Glycoprotein Cross-Reactive Epitopes. *J Virol* 78(24):13975–13986.

54. Goncalvez AP, Men R, Wernly C, Purcell RH, Lai C-J (2004) Chimpanzee Fab Fragments and a Derived Humanized Immunoglobulin G1 Antibody That Efficiently Cross-Neutralize Dengue Type 1 and Type 2 Viruses. *J Virol* 78(23):12910–12918.

55. Chambers TJ, Nickells M (2001) Neuroadapted Yellow Fever Virus 17D: Genetic and Biological Characterization of a Highly Mouse-Neurovirulent Virus and Its Infectious Molecular Clone. *J Virol* 75(22):10912–10922.

56. Nickells M, Chambers TJ (2003) Neuroadapted Yellow Fever Virus 17D: Determinants in the Envelope Protein Govern Neuroinvasiveness for SCID Mice. *J Virol* 77(22):12232–12242.

57. van der Most RG, Corver J, Strauss JH (1999) Mutagenesis of the RGD Motif in the Yellow Fever Virus 17D Envelope Protein. *Virology* 265(1):83–95.

58. Hung J-J, et al. (2004) An External Loop Region of Domain III of Dengue Virus Type 2 Envelope Protein Is Involved in Serotype-Specific Binding to Mosquito but Not Mammalian Cells. *J Virol* 78(1):378–388.

59. Chu JJ, Ng M-L (2004) Interaction of West Nile Virus with αvβ3 Integrin Mediates Virus Entry into Cells. *J Biol Chem* 279(52):54533–54541.

60. Lindenbach BD, Rice CM (1997) trans-Complementation of yellow fever virus NS1 reveals a role in early RNA replication. *J Virol* 71(12):9608–9617.

61. Lindenbach BD, Rice CM (1999) Genetic Interaction of Flavivirus Nonstructural Proteins NS1 and NS4A as a Determinant of Replicase Function. *J Virol* 73(6):4611–4621.

62. Muylaert IR, Chambers TJ, Galler R, Rice CM (1996) Mutagenesis of the N-linked glycosylation sites of the yellow fever virus NS1 protein: effects on virus replication and mouse neurovirulence. *Virology* 222(1):159–168.

63. Youn S, Cho H, Fremont DH, Diamond MS (2010) A Short N-Terminal Peptide Motif on Flavivirus Nonstructural Protein NS1 Modulates Cellular Targeting and Immune Recognition. *J Virol* 84(18):9516–9532.

64. Avirutnan P, et al. (2010) Antagonism of the complement component C4 by flavivirus nonstructural protein NS1. *J Exp Med* 207(4):793–806.

65. Chung KM, et al. (2006) West Nile virus nonstructural protein NS1 inhibits complement activation by binding the regulatory protein factor H. *Proc Natl Acad Sci* 103(50):19111–19116.

66. Puerta-Guardo H, Glasner DR, Harris E (2016) Dengue Virus NS1 Disrupts the Endothelial Glycocalyx, Leading to Hyperpermeability. *PLOS Pathog* 12(7):e1005738.

67. Henchal EA, Henchal LS, Schlesinger JJ (1988) Synergistic Interactions of Anti-NS1 Monoclonal Antibodies Protect Passively Immunized Mice from Lethal Challenge with Dengue 2 Virus. *J Gen Virol* 69(8):2101–2107.

68. Schlesinger JJ, Brandriss MW, Cropp CB, Monath TP (1986) Protection against yellow fever in monkeys by immunization with yellow fever virus nonstructural protein NS1. *J Virol* 60(3):1153–1155.

69. Schlesinger JJ, Foltzer M, Chapman S (1993) The Fc Portion of Antibody to Yellow Fever Virus NS1 Is a Determinant of Protection against YF Encephalitis in Mice. *Virology* 192(1):132–141.

70. Xie X, Zou J, Puttikhunt C, Yuan Z, Shi P-Y (2015) Two Distinct Sets of NS2A Molecules Are Responsible for Dengue Virus RNA Synthesis and Virion Assembly. *J Virol* 89(2):1298–1313.

71. Kümmerer BM, Rice CM (2002) Mutations in the yellow fever virus nonstructural protein NS2A selectively block production of infectious particles. *J Virol* 76(10):4773–4784.

72. Muñoz-Jordan JL, Sánchez-Burgos GG, Laurent-Rolle M, García-Sastre A (2003) Inhibition of interferon signaling by dengue virus. *Proc Natl Acad Sci U S A* 100(24):14333–14338.

73. Liu WJ, et al. (2006) A single amino acid substitution in the West Nile virus nonstructural protein NS2A disables its ability to inhibit alpha/beta interferon induction and attenuates virus virulence in mice. *J Virol* 80(5):2396–2404.

74. Chang Y-S, et al. (1999) Membrane Permeabilization by Small Hydrophobic Nonstructural Proteins of Japanese Encephalitis Virus. *J Virol* 73(8):6257–6264.

75. León-Juárez M, et al. (2016) Recombinant Dengue virus protein NS2B alters membrane permeability in different membrane models. *Virol J* 13. doi:10.1186/s12985-015-0456-4.

76. Aguirre S, et al. (2017) Dengue virus NS2B protein targets cGAS for degradation and prevents mitochondrial DNA sensing during infection. *Nat Microbiol* 2(5):nmicrobiol201737.

77. Chambers TJ, et al. (1990) Evidence that the N-terminal domain of nonstructural protein NS3 from yellow fever virus is a serine protease responsible for site-specific cleavages in the viral polyprotein. *Proc Natl Acad Sci U S A* 87(22):8898–8902.

78. Aguirre S, et al. (2012) DENV Inhibits Type I IFN Production in Infected Cells by Cleaving Human STING. *PLOS Pathog* 8(10):e1002934.

79. Nunes Duarte dos Santos C, et al. (2000) Determinants in the Envelope E Protein and Viral RNA Helicase NS3 That Influence the Induction of Apoptosis in Response to Infection with Dengue Type 1 Virus. *Virology* 274(2):292–308.

80. Mackenzie JM, Khromykh AA, Jones MK, Westaway EG (1998) Subcellular localization and some biochemical properties of the flavivirus Kunjin nonstructural proteins NS2A and NS4A. *Virology* 245(2):203–215.

81. Bartenschlager R, Lohmann V, Wilkinson T, Koch JO (1995) Complex formation between the NS3 serine-type proteinase of the hepatitis C virus and NS4A and its importance for polyprotein maturation. *J Virol* 69(12):7519–7528.

82. Shiryaev SA, Chernov AV, Aleshin AE, Shiryaeva TN, Strongin AY (2009) NS4A regulates the ATPase activity of the NS3 helicase: a novel cofactor role of the non-structural protein NS4A from West Nile virus. *J Gen Virol* 90(9):2081–2085.

83. Miller S, Sparacio S, Bartenschlager R (2006) Subcellular localization and membrane topology of the Dengue virus type 2 Non-structural protein 4B. *J Biol Chem* 281(13):8854–8863.

84. Muñoz-Jordán JL, et al. (2005) Inhibition of alpha/beta interferon signaling by the NS4B protein of flaviviruses. *J Virol* 79(13):8004–8013.

85. Lee Y-R, et al. (2008) Autophagic machinery activated by dengue virus enhances virus replication. *Virology* 374(2):240–248.

86. Liang Q, et al. (2016) Zika Virus NS4A and NS4B Proteins Deregulate Akt-mTOR Signaling in Human Fetal Neural Stem Cells to Inhibit Neurogenesis and Induce Autophagy. *Cell Stem Cell* 19(5):663–671.

87. McLean JE, Wudzinska A, Datan E, Quaglino D, Zakeri Z (2011) Flavivirus NS4A-induced Autophagy Protects Cells against Death and Enhances Virus Replication. *J Biol Chem* 286(25):22147–22159.

88. Zou G, et al. (2009) A single-amino acid substitution in West Nile virus 2K peptide between NS4A and NS4B confers resistance to lycorine, a flavivirus inhibitor. *Virology* 384(1):242–252.

89. Egloff M-P, Benarroch D, Selisko B, Romette J-L, Canard B (2002) An RNA cap (nucleoside-2′-O-)-methyltransferase in the flavivirus RNA polymerase NS5: crystal structure and functional characterization. *EMBO J* 21(11):2757–2768.

90. Yap TL, et al. (2007) Crystal Structure of the Dengue Virus RNA-Dependent RNA Polymerase Catalytic Domain at 1.85-Angstrom Resolution. *J Virol* 81(9):4753–4765.

91. Ashour J, et al. (2010) Mouse STAT2 Restricts Early Dengue Virus Replication. *Cell Host Microbe* 8(5):410–421.

92. Grant A, et al. (2016) Zika Virus Targets Human STAT2 to Inhibit Type I Interferon Signaling. *Cell Host Microbe* 19(6):882–890.

93. Pijlman GP, Kondratieva N, Khromykh AA (2006) Translation of the flavivirus kunjin NS3 gene in cis but not its RNA sequence or secondary structure is essential for efficient RNA packaging. *J Virol* 80(22):11255–11264.

94. Sun M, et al. (2013) Global Analysis of Eukaryotic mRNA Degradation Reveals Xrn1-Dependent Buffering of Transcript Levels. *Mol Cell* 52(1):52–62.

95. Chapman EG, Moon SL, Wilusz J, Kieft JS (2014) RNA structures that resist degradation by Xrn1 produce a pathogenic Dengue virus RNA. *eLife* 3:e01892.

96. Moon SL, et al. (2012) A noncoding RNA produced by arthropod-borne flaviviruses inhibits the cellular exoribonuclease XRN1 and alters host mRNA stability. *RNA N Y N* 18(11):2029–2040.

97. Silva ML, et al. (2010) Clinical and Immunological Insights on Severe, Adverse Neurotropic and Viscerotropic Disease following 17D Yellow Fever Vaccination. *Clin Vaccine Immunol CVI* 17(1):118–126.

98. Funk A, et al. (2010) RNA Structures Required for Production of Subgenomic Flavivirus RNA. *J Virol* 84(21):11407–11417.

99. Schuessler A, et al. (2012) West Nile Virus Noncoding Subgenomic RNA Contributes to Viral Evasion of the Type I Interferon-Mediated Antiviral Response. *J Virol* 86(10):5708–5718.

100. Donald CL, et al. (2016) Full Genome Sequence and sfRNA Interferon Antagonist Activity of Zika Virus from Recife, Brazil. *PLoS Negl Trop Dis* 10(10):e0005048.

101. Manokaran G, et al. (2015) Dengue subgenomic RNA binds TRIM25 to inhibit interferon expression for epidemiological fitness. *Science* 350(6257):217–221.

102. Bidet K, Dadlani D, Garcia-Blanco MA (2014) G3BP1, G3BP2 and CAPRIN1 Are Required for Translation of Interferon Stimulated mRNAs and Are Targeted by a Dengue Virus Non-coding RNA. *PLOS Pathog* 10(7):e1004242.

103. Chu PWG, Westaway EG (1992) Molecular and ultrastructural analysis of heavy membrane fractions associated with the replication of Kunjin virus RNA. *Arch Virol* 125(1–4):177–191.

104. Zou J, et al. (2015) Mapping the Interactions between the NS4B and NS3 Proteins of Dengue Virus. *J Virol* 89(7):3471–3483.

105. Tay MYF, et al. (2014) The C-terminal 50 amino acid residues of Dengue NS3 protein are important for NS3-NS5 interaction and viral replication. *J Biol Chem*:jbc.M114.607341.

106. Klema VJ, Padmanabhan R, Choi KH (2015) Flaviviral Replication Complex: Coordination between RNA Synthesis and 5′-RNA Capping. *Viruses* 7(8):4640–4656.

107. Cleaves GR, Ryan TE, Schlesinger RW (1981) Identification and characterization of type 2 dengue virus replicative intermediate and replicative form RNAs. *Virology* 111(1):73–83.

108. Fan Y-H, et al. (2011) Small noncoding RNA modulates japanese encephalitis virus replication and translation in trans. *Virol J* 8:492.

109. Filomatori CV, et al. (2006) A 5′ RNA element promotes dengue virus RNA synthesis on a circular genome. *Genes Dev* 20(16):2238–2249.

110. Selisko B, et al. (2012) Molecular Basis for Nucleotide Conservation at the Ends of the Dengue Virus Genome. *PLOS Pathog* 8(9):e1002912.

111. Selisko B, Wang C, Harris E, Canard B (2014) Regulation of Flavivirus RNA synthesis and replication. *Curr Opin Virol* 9:74–83.

112. Leung JY, et al. (2008) Role of Nonstructural Protein NS2A in Flavivirus Assembly. *J Virol* 82(10):4731–4741.

113. Plevka P, et al. (2011) Maturation of flaviviruses starts from one or more icosahedrally independent nucleation centres. *EMBO Rep* 12(6):602–606.

114. Wu B, et al. (2013) Structural basis for dsRNA recognition, filament formation, and antiviral signal activation by MDA5. *Cell* 152(1–2):276–289.

115. Dixit E, et al. (2010) Peroxisomes Are Signaling Platforms for Antiviral Innate Immunity. *Cell* 141(4):668–681.

116. Devarkar SC, et al. (2016) Structural basis for m7G recognition and 2'-O-methyl discrimination in capped RNAs by the innate immune receptor RIG-I. *Proc Natl Acad Sci U S A* 113(3):596–601.

117. Kato H, et al. (2006) Differential roles of MDA5 and RIG-I helicases in the recognition of RNA viruses. *Nature* 441(7089):101–105.

118. Kato H, et al. (2008) Length-dependent recognition of double-stranded ribonucleic acids by retinoic acid-inducible gene-I and melanoma differentiation-associated gene 5. *J Exp Med* 205(7):1601–1610.

119. Gitlin L, et al. (2006) Essential role of mda-5 in type I IFN responses to polyriboinosinic:polyribocytidylic acid and encephalomyocarditis picornavirus. *Proc Natl Acad Sci U S A* 103(22):8459–8464.

120. Sato M, et al. (2000) Distinct and essential roles of transcription factors IRF-3 and IRF-7 in response to viruses for IFN-alpha/beta gene induction. *Immunity* 13(4):539–548.

121. Fredericksen BL, Gale M (2006) West Nile virus evades activation of interferon regulatory factor 3 through RIG-I-dependent and -independent pathways without antagonizing host defense signaling. *J Virol* 80(6):2913–2923.

122. Fredericksen BL, Keller BC, Fornek J, Katze MG, Gale M (2008) Establishment and maintenance of the innate antiviral response to West Nile Virus involves both RIG-I and MDA5 signaling through IPS-1. *J Virol* 82(2):609–616.

123. Nasirudeen AMA, et al. (2011) RIG-I, MDA5 and TLR3 Synergistically Play an Important Role in Restriction of Dengue Virus Infection. *PLoS Negl Trop Dis* 5(1):e926.

124. Errett JS, Suthar MS, McMillan A, Diamond MS, Gale M (2013) The Essential, Nonredundant Roles of RIG-I and MDA5 in Detecting and Controlling West Nile Virus Infection. *J Virol* 87(21):11416–11425.

125. Bruni D, et al. (2015) Viral entry route determines how human plasmacytoid dendritic cells produce type I interferons. *Sci Signal* 8(366):ra25.

126. Parthiban P, Mahendra J (2015) Toll-Like Receptors: A Key Marker for Periodontal Disease and Preterm Birth – A Contemporary Review. *J Clin Diagn Res JCDR* 9(9):ZE14-ZE17.

127. Tsai Y-T, Chang S-Y, Lee C-N, Kao C-L (2009) Human TLR3 recognizes dengue virus and modulates viral replication in vitro. *Cell Microbiol* 11(4):604–615.

128. Wang JP, et al. (2006) Flavivirus activation of plasmacytoid dendritic cells delineates key elements of TLR7 signaling beyond endosomal recognition. *J Immunol Baltim Md 1950* 177(10):7114–7121.

129. Querec T, et al. (2006) Yellow fever vaccine YF-17D activates multiple dendritic cell subsets via TLR2, 7, 8, and 9 to stimulate polyvalent immunity. *J Exp Med* 203(2):413–424.

130. Wang T, et al. (2004) Toll-like receptor 3 mediates West Nile virus entry into the brain causing lethal encephalitis. *Nat Med* 10(12):1366–1373.

131. Daffis S, Samuel MA, Suthar MS, Gale M, Diamond MS (2008) Toll-Like Receptor 3 Has a Protective Role against West Nile Virus Infection. *J Virol* 82(21):10349–10358.

132. Szretter KJ, et al. (2010) The Innate Immune Adaptor Molecule MyD88 Restricts West Nile Virus Replication and Spread in Neurons of the Central Nervous System. *J Virol* 84(23):12125–12138.

133. Shipley JG, Vandergaast R, Deng L, Mariuzza RA, Fredericksen BL (2012) Identification of multiple RIG-I-specific pathogen associated molecular patterns within the West Nile virus genome and antigenome. *Virology* 432(1):232–238.

134. Chan YK, Gack MU (2016) A phosphomimetic-based mechanism of dengue virus to antagonize innate immunity. *Nat Immunol* 17(5):523–530.

135. Platanias LC (2005) Mechanisms of type-I- and type-II-interferon-mediated signalling. *Nat Rev Immunol* 5(5):nri1604.

136. Leyssen P, et al. (2003) Interferons, Interferon Inducers, and Interferon-Ribavirin in Treatment of Flavivirus-Induced Encephalitis in Mice. *Antimicrob Agents Chemother* 47(2):777–782.

137. Govero J, et al. (2016) Zika virus infection damages the testes in mice. *Nature* 540(7633):438.

138. Sheehan KCF, Lazear HM, Diamond MS, Schreiber RD (2015) Selective Blockade of Interferon-α and -β Reveals Their Non-Redundant Functions in a Mouse Model of West Nile Virus Infection. *PLoS ONE* 10(5). doi:10.1371/journal.pone.0128636.

139. Meier KC, Gardner CL, Khoretonenko MV, Klimstra WB, Ryman KD (2009) A Mouse Model for Studying Viscerotropic Disease Caused by Yellow Fever Virus Infection. *PLOS Pathog* 5(10):e1000614.

140. Lobigs M, Mullbacher A, Wang Y, Pavy M, Lee E (2003) Role of type I and type II interferon responses in recovery from infection with an encephalitic flavivirus. *J Gen Virol*. doi:10.1099/vir.0.18654-0.

141. Weber E, et al. (2014) Type I Interferon Protects Mice from Fatal Neurotropic Infection with Langat Virus by Systemic and Local Antiviral Responses. *J Virol* 88(21):12202–12212.

142. Pinto AK, et al. (2011) A Temporal Role Of Type I Interferon Signaling in CD8+ T Cell Maturation during Acute West Nile Virus Infection. *PLOS Pathog* 7(12):e1002407.

143. Diamond MS, et al. (2000) Modulation of Dengue Virus Infection in Human Cells by Alpha, Beta, and Gamma Interferons. *J Virol* 74(11):4957–4966.

144. Best SM, et al. (2005) Inhibition of Interferon-Stimulated JAK-STAT Signaling by a Tick-Borne Flavivirus and Identification of NS5 as an Interferon Antagonist. *J Virol* 79(20):12828–12839.

145. Lin YL, et al. (1997) Inhibition of Japanese encephalitis virus infection by nitric oxide: antiviral effect of nitric oxide on RNA virus replication. *J Virol* 71(7):5227–5235.

146. Shrestha B, et al. (2006) Gamma Interferon Plays a Crucial Early Antiviral Role in Protection against West Nile Virus Infection. *J Virol* 80(11):5338–5348.

147. Arroyo JI, et al. (1988) Effect of human gamma interferon on yellow fever virus infection. *Am J Trop Med Hyg* 38(3):647–650.

148. Ma D, et al. (2009) Antiviral effect of interferon lambda against West Nile virus. *Antiviral Res* 83(1):53–60.

149. Lazear HM, et al. (2015) Interferon-λ restricts West Nile virus neuroinvasion by tightening the blood-brain barrier. *Sci Transl Med* 7(284):284ra59.

150. Corry J, Arora N, Good CA, Sadovsky Y, Coyne CB (2017) Organotypic models of type III interferon-mediated protection from Zika virus infections at the maternal-fetal interface. *Proc Natl Acad Sci U S A* 114(35):9433–9438.

151. Douam F, et al. (2017) Type III Interferon-Mediated Signaling Is Critical for Controlling Live Attenuated Yellow Fever Virus Infection In Vivo. *mBio* 8(4):e00819-17.

152. Silverman RH (2007) Viral Encounters with 2′,5′-Oligoadenylate Synthetase and RNase L during the Interferon Antiviral Response. *J Virol* 81(23):12720–12729.

153. Elbahesh H, Jha BK, Silverman RH, Scherbik SV, Brinton MA (2011) The Flvr-encoded murine oligoadenylate synthetase 1b (Oas1b) suppresses 2-5A synthesis in intact cells. *Virology* 409(2):262–270.

154. Mertens E, et al. (2010) Viral determinants in the NS3 helicase and 2K peptide that promote West Nile virus resistance to antiviral action of 2′,5′-oligoadenylate synthetase 1b. *Virology* 399(1):176–185.

155. Lin R-J, et al. (2009) Distinct Antiviral Roles for Human 2′,5′-Oligoadenylate Synthetase Family Members against Dengue Virus Infection. *J Immunol* 183(12):8035–8043.

156. Kurane I, Hebblewaite D, Brandt WE, Ennis FA (1984) Lysis of dengue virus-infected cells by natural cell-mediated cytotoxicity and antibody-dependent cell-mediated cytotoxicity. *J Virol* 52(1):223–230.

157. Reefman E, et al. (2010) Cytokine Secretion Is Distinct from Secretion of Cytotoxic Granules in NK Cells. *J Immunol* 184(9):4852–4862.

158. Mariani E, et al. (2002) RANTES and MIP-1α production by T lymphocytes, monocytes and NK cells from nonagenarian subjects. *Exp Gerontol* 37(2):219–226.

159. Marquardt N, et al. (2015) The Human NK Cell Response to Yellow Fever Virus 17D Is Primarily Governed by NK Cell Differentiation Independently of NK Cell Education. *J Immunol Baltim Md 1950* 195(7):3262–3272.

160. Neves PCC, Santos JR, Tubarão LN, Bonaldo MC, Galler R (2013) Early IFN-Gamma Production after YF 17D Vaccine Virus Immunization in Mice and Its Association with Adaptive Immune Responses. *PLoS ONE* 8(12):e81953.

161. Shresta S, et al. (2004) Interferon-Dependent Immunity Is Essential for Resistance to Primary Dengue Virus Infection in Mice, Whereas T- and B-Cell-Dependent Immunity Are Less Critical. *J Virol* 78(6):2701–2710.

162. Blom K, et al. (2016) NK Cell Responses to Human Tick-Borne Encephalitis Virus Infection. *J Immunol* 197(7):2762–2771.

163. Cheng Y, King NJC, Kesson AM Major Histocompatibility Complex Class I (MHC-I) Induction by West Nile Virus: Involvement of 2 Signaling Pathways in MHC-I Up-Regulation. *J Infect Dis*:658–668.

164. Müllbacher A, Lobigs M (1995) Up-regulation of MHC class I by flavivirus-induced peptide translocation into the endoplasmic reticulum. *Immunity* 3(2):207–214.

165. Lobigs M, Müllbacher A, Lee E (2004) Evidence that a mechanism for efficient flavivirus budding upregulates MHC class I. *Immunol Cell Biol*. Available at: https://www.nature.com/articles/icb200429 [Accessed January 4, 2018].

166. Hershkovitz O, et al. (2008) Dengue Virus Replicon Expressing the Nonstructural Proteins Suffices To Enhance Membrane Expression of HLA Class I and Inhibit Lysis by Human NK Cells. *J Virol* 82(15):7666–7676.

167. Hershkovitz O, et al. (2009) NKp44 Receptor Mediates Interaction of the Envelope Glycoproteins from the West Nile and Dengue Viruses with NK Cells. *J Immunol* 183(4):2610–2621.

168. García G, et al. (2006) Antibodies from patients with dengue viral infection mediate cellular cytotoxicity. *J Clin Virol* 37(1):53–57.

169. Gardner CL, Ryman KD (2010) Yellow Fever: A Reemerging Threat. *Clin Lab Med* 30(1):237–260.

170. Huang Y-JS, Higgs S, Horne KM, Vanlandingham DL (2014) Flavivirus-Mosquito Interactions. *Viruses* 6(11):4703–4730.

171. Wee LK, et al. (2013) Relationship between rainfall and Aedes larval population at two insular sites in Pulau Ketam, Selangor, Malaysia. *Southeast Asian J Trop Med Public Health* 44(2):157–166.

172. Nasir S, Jabeen F, Abbas S, Nasir I, Debboun M (2017) Effect of Climatic Conditions and Water Bodies on Population Dynamics of the Dengue Vector, Aedes aegypti (Diptera: Culicidae). *J Arthropod-Borne Dis* 11(1):50–59.

173. Black WC, Rai KS, Turco BJ, Arroyo DC (1989) Laboratory study of competition between United States strains of Aedes albopictus and Aedes aegypti (Diptera: Culicidae). *J Med Entomol* 26(4):260–271.

174. World Health Organization (2011) Yellow fever in Africa and Central and South America, 2008–2009. *Releve Epidemiol Hebd* 86(4):25–36.

175. World Health Organization (2013) Yellow fever in Africa and South America, 2011–2012. *Releve Epidemiol Hebd* 88(28):285–296.

176. World Health Organization (2014) Yellow fever in Africa and South America, 2013. *Releve Epidemiol Hebd* 89(27):297–306.

177. World Health Organization (2016) Yellow fever in Africa and South America, 2015. *Releve Epidemiol Hebd* 91(32):381–388.

178. World Health Organization WHO | Yellow fever – Brazil. *WHO*. Available at: http://www.who.int/csr/don/27-january-2017-yellow-fever-brazil/en/ [Accessed November 1, 2017].

179. Romano APM, et al. (2014) Yellow Fever outbreaks in unvaccinated populations, Brazil, 2008-2009. *PLoS Negl Trop Dis* 8(3):e2740.

180. Wasserman S, Tambyah PA, Lim PL (2016) Yellow fever cases in Asia: primed for an epidemic. *Int J Infect Dis* 48:98–103.

181. Agampodi SB, Wickramage K (2013) Is There a Risk of Yellow Fever Virus Transmission in South Asian Countries with Hyperendemic Dengue? *BioMed Res Int* 2013:e905043.

182. Johansson MA, Vasconcelos PFC, Staples JE (2014) The whole iceberg: estimating the incidence of yellow fever virus infection from the number of severe cases. *Trans R Soc Trop Med Hyg* 108(8):482–487.

183. Monath TP, et al. (1980) Yellow fever in the Gambia, 1978--1979: epidemiologic aspects with observations on the occurrence of orungo virus infections. *Am J Trop Med Hyg* 29(5):912–928.

184. Staples JE, Gershman M, Fischer M, Centers for Disease Control and Prevention (CDC) (2010) Yellow fever vaccine: recommendations of the Advisory Committee on Immunization Practices (ACIP). *MMWR Recomm Rep Morb Mortal Wkly Rep Recomm Rep* 59(RR-7):1–27.

185. Stokes A, Bauer JH, Hudson NP (1928) THE TRANSMISSION OF YELLOW FEVER TO MACACUS RHESUS: PRELIMINARY NOTE. *J Am Med Assoc* 90(4):253–254.

186. Sellards AW, Hindle E (1928) THE PRESERVATION OF YELLOW FEVER VIRUS. *Br Med J* 1(3512):713–714.

187. Berry GP, Kitchen SF (1931) Yellow Fever Accidentally Contracted in the Laboratory. *Am J Trop Med Hyg* s1-11(6):365–434.

188. Lloyd W, Theiler M, Ricci NI (1936) Modification of the virulence of yellow fever virus by cultivation in tissues in vitro. *Trans R Soc Trop Med Hyg* 29(5):481–529.

189. Barrett ADT (1987) Yellow Fever Vaccines. *Bull Inst Pasteur* 85:103–124.

190. World Health Organization (1998) Requirements for yellow fever vaccine, Annex 2. *WHO Tech Rep Ser* 872.

191. Campi-Azevedo AC, et al. (2014) Subdoses of 17DD yellow fever vaccine elicit equivalent virological/immunological kinetics timeline. *BMC Infect Dis* 14:391.

192. Barba-Spaeth G, Longman RS, Albert ML, Rice CM (2005) Live attenuated yellow fever 17D infects human DCs and allows for presentation of endogenous and recombinant T cell epitopes. *J Exp Med* 202(9):1179–1184.

193. Querec TD, et al. (2009) Systems biology approach predicts immunogenicity of the yellow fever vaccine in humans. *Nat Immunol* 10(1):116–125.

194. Kohler S, et al. (2012) The early cellular signatures of protective immunity induced by live viral vaccination. *Eur J Immunol* 42(9):2363–2373.

195. Gibney KB, et al. (2012) Detection of Anti-Yellow Fever Virus Immunoglobulin M Antibodies at 3–4 Years Following Yellow Fever Vaccination. *Am J Trop Med Hyg* 87(6):1112–1115.

196. Poland JD, Calisher CH, Monath TP, Downs WG, Murphy K (1981) Persistence of neutralizing antibody 30-35 years after immunization with 17D yellow fever vaccine. *Bull World Health Organ* 59(6):895–900.

197. Niedrig M, Lademann M, Emmerich P, Lafrenz M (1999) Assessment of IgG antibodies against yellow fever virus after vaccination with 17D by different assays: neutralization test, haemagglutination inhibition test, immunofluorescence assay and ELISA. *Trop Med Int Health* 4(12):867–871.

198. Wieten RW, et al. (2016) A Single 17D Yellow Fever Vaccination Provides Lifelong Immunity; Characterization of Yellow-Fever-Specific Neutralizing Antibody and T-Cell Responses after Vaccination. *PLOS ONE* 11(3):e0149871.

199. Hepburn MJ, et al. (2006) Neutralizing antibody response to booster vaccination with the 17d yellow fever vaccine. *Vaccine* 24(15):2843–2849.

200. Hayakawa K, et al. (2015) Persistent seropositivity for yellow fever in a previously vaccinated autologous hematopoietic stem cell transplantation recipient. *Int J Infect Dis* 37(Supplement C):9–10.

201. Avelino-Silva VI, et al. (2015) Persistence of Yellow Fever vaccine-induced antibodies after cord blood stem cell transplant. *Hum Vaccines Immunother* 12(4):937–938.

202. Martínez MJ, et al. (2011) Persistence of yellow fever vaccine RNA in urine. *Vaccine* 29(18):3374–3376.

203. Blom K, et al. (2013) Temporal Dynamics of the Primary Human T Cell Response to Yellow Fever Virus 17D As It Matures from an Effector- to a Memory-Type Response. *J Immunol* 190(5):2150–2158.

204. Akondy RS, et al. (2015) Initial viral load determines the magnitude of the human CD8 T cell response to yellow fever vaccination. *Proc Natl Acad Sci* 112(10):3050–3055.

205. Miller JD, et al. (2008) Human effector and memory CD8+ T cell responses to smallpox and yellow fever vaccines. *Immunity* 28(5):710–722.

206. Silva ML, et al. (2011) Characterization of main cytokine sources from the innate and adaptive immune responses following primary 17DD yellow fever vaccination in adults. *Vaccine* 29(3):583–592.

207. Campi-Azevedo AC, et al. (2012) 17DD and 17D-213/77 Yellow Fever Substrains Trigger a Balanced Cytokine Profile in Primary Vaccinated Children. *PLOS ONE* 7(12):e49828.

208. James EA, et al. (2013) Yellow Fever Vaccination Elicits Broad Functional CD4+ T Cell Responses That Recognize Structural and Nonstructural Proteins. *J Virol* 87(23):12794–12804.

209. Santos AP, Matos DCS, Bertho AL, Mendonça SCF, Marcovistz R (2008) Detection of TH1/TH2 cytokine signatures in yellow fever 17DD first-time vaccinees through ELISpot assay. *Cytokine* 42(2):152–155.

210. Watson AM, Lam LKM, Klimstra WB, Ryman KD (2016) The 17D-204 Vaccine Strain-Induced Protection against Virulent Yellow Fever Virus Is Mediated by Humoral Immunity and CD4+ but not CD8+ T Cells. *PLOS Pathog* 12(7):e1005786.

211. Bassi MR, et al. (2015) CD8+ T Cells Complement Antibodies in Protecting against Yellow Fever Virus. *J Immunol* 194(3):1141–1153.

212. Beck AS, Barrett ADT (2015) Current status and future prospects of yellow fever vaccines. *Expert Rev Vaccines* 14(11):1479–1492.

213. de Wispelaere M, Khou C, Frenkiel M-P, Desprès P, Pardigon N (2016) A Single Amino Acid Substitution in the M Protein Attenuates Japanese Encephalitis Virus in Mammalian Hosts. *J Virol* 90(5):2676–2689.

214. Zmurko J, Neyts J, Dallmeier K (2015) Flaviviral NS4b, chameleon and jack-in-the-box roles in viral replication and pathogenesis, and a molecular target for antiviral intervention. *Rev Med Virol* 25(4):205–223.

215. Dunster LM, et al. (1999) Molecular and Biological Changes Associated with HeLa Cell Attenuation of Wild-Type Yellow Fever Virus. *Virology* 261(2):309–318.

216. McArthur MA, Suderman MT, Mutebi J-P, Xiao S-Y, Barrett ADT (2003) Molecular Characterization of a Hamster Viscerotropic Strain of Yellow Fever Virus. *J Virol* 77(2):1462–1468.

217. Fernandez-Garcia MD, et al. (2016) Vaccine and Wild-Type Strains of Yellow Fever Virus Engage Distinct Entry Mechanisms and Differentially Stimulate Antiviral Immune Responses. *mBio* 7(1):e01956-15.

218. Hasegawa H, Yoshida M, Shiosaka T, Fujita S, Kobayashi Y (1992) Mutations in the envelope protein of Japanese encephalitis virus affect entry into cultured cells and virulence in mice. *Virology* 191(1):158–165.

219. Morita K, et al. (2001) Locus of a Virus Neutralization Epitope on the Japanese Encephalitis Virus Envelope Protein Determined by Use of Long PCR-Based Region-Specific Random Mutagenesis. *Virology* 287(2):417–426.

220. Butrapet S, et al. (2011) Amino acid changes within the E protein hinge region that affect dengue virus type 2 infectivity and fusion. *Virology* 413(1):118–127.

221. Lindsey NP, Rabe IB, Miller ER, Fischer M, Staples JE (2016) Adverse event reports following yellow fever vaccination, 2007–13. *J Travel Med* 23(5):taw045.

222. Merlo C, Steffen R, Landis T, Tsai T, Karabatsos N (1993) Possible association of encephalitis and 17D yellow fever vaccination in a 29-year-old traveller. *Vaccine* 11(6):691.

223. Kengsakul K, Sathirapongsasuti K, Punyagupta S (2002) Fatal myeloencephalitis following yellow fever vaccination in a case with HIV infection. *J Med Assoc Thail Chotmaihet Thangphaet* 85(1):131–134.

224. Monath TP, Barrett AD (2003) Pathogenesis and pathophysiology of yellow fever. *Adv Virus Res* 60:343–395.

225. Martin M, et al. (2001) Fever and multisystem organ failure associated with 17D-204 yellow fever vaccination: a report of four cases. *The Lancet* 358(9276):98–104.

226. Chan RC, et al. (2001) Hepatitis and death following vaccination with 17D-204 yellow fever vaccine. *The Lancet* 358(9276):121–122.

227. Vasconcelos PF, et al. (2001) Serious adverse events associated with yellow fever 17DD vaccine in Brazil: a report of two cases. *The Lancet* 358(9276):91–97.

228. Whittembury A, et al. (2009) Viscerotropic disease following yellow fever vaccination in Peru. *Vaccine* 27(43):5974–5981.

229. Seligman SJ, Cohen JE, Itan Y, Casanova J-L, Pezzullo JC (2014) Defining Risk Groups to Yellow Fever Vaccine-Associated Viscerotropic Disease in the Absence of Denominator Data. *Am J Trop Med Hyg* 90(2):267–271.

230. Pulendran B, et al. (2008) Case of Yellow Fever Vaccine-associated Viscerotropic Disease with Prolonged Viremia, Robust Adaptive Immune Responses, and Polymorphisms in CCR5 and RANTES Genes. *J Infect Dis* 198(4):500–507.

231. Engel AR, C Vasconcelos PF, McArthur MA, T. Barrett AD (2006) Characterization of a viscerotropic yellow fever vaccine variant from a patient in Brazil. *Vaccine* 24(15):2803–2809.

232. Galler R, et al. (2001) Phenotypic and Molecular Analyses of Yellow Fever 17DD Vaccine Viruses Associated with Serious Adverse Events in Brazil. *Virology* 290(2):309–319.

233. Nascimento Silva JR, et al. (2011) Mutual interference on the immune response to yellow fever vaccine and a combined vaccine against measles, mumps and rubella. *Vaccine* 29(37):6327–6334.

234. Lieberman LA, Hunter CA (2002) Regulatory pathways involved in the infection-induced production of IFN-gamma by NK cells. *Microbes Infect* 4(15):1531–1538.

235. Tato CM, et al. (2004) Cutting Edge: Innate Production of IFN-γ by NK Cells Is Independent of Epigenetic Modification of the IFN-γ Promoter. *J Immunol* 173(3):1514–1517.

236. Eberl G, Colonna M, Santo JPD, McKenzie ANJ (2015) Innate lymphoid cells: A new paradigm in immunology. *Science* 348(6237):aaa6566.

237. Darwich L, et al. (2009) Secretion of interferon-γ by human macrophages demonstrated at the single-cell level after costimulation with interleukin (IL)-12 plus IL-18. *Immunology* 126(3):386–393.

238. Pan J, et al. (2004) Interferon-γ is an autocrine mediator for dendritic cell maturation. *Immunol Lett* 94(1):141–151.

239. Moretto MM, Weiss LM, Combe CL, Khan IA (2007) IFN-γ-Producing Dendritic Cells Are Important for Priming of Gut Intraepithelial Lymphocyte Response Against Intracellular Parasitic Infection. *J Immunol* 179(4):2485–2492.

240. Ethuin F, et al. (2004) Human neutrophils produce interferon gamma upon stimulation by interleukin-12. *Lab Invest* 84(10):1363–1371.

241. Bao Y, et al. (2014) Identification of IFN-γ-producing innate B cells. *Cell Res* 24(2):161–176.

242. Biering SB, et al. (2017) Viral Replication Complexes Are Targeted by LC3-Guided Interferon-Inducible GTPases. *Cell Host Microbe* 22(1):74–85.e7.

243. Herrero C, Marqués L, Lloberas J, Celada A (2001) IFN-γ–dependent transcription of MHC class II IA is impaired in macrophages from aged mice. *J Clin Invest* 107(4):485–493.

244. Flynn JL, et al. (1993) An essential role for interferon gamma in resistance to Mycobacterium tuberculosis infection. *J Exp Med* 178(6):2249–2254.

245. Lane TE, Wu-Hsieh BA, Howard DH (1991) Iron limitation and the gamma interferon-mediated antihistoplasma state of murine macrophages. *Infect Immun* 59(7):2274–2278.

246. Prestwood TR, et al. (2012) Gamma Interferon (IFN-γ) Receptor Restricts Systemic Dengue Virus Replication and Prevents Paralysis in IFN-α/β Receptor-Deficient Mice. *J Virol* 86(23):12561–12570.

247. Takács AC, Swierzy IJ, Lüder CGK (2012) Interferon-γ Restricts Toxoplasma gondii Development in Murine Skeletal Muscle Cells via Nitric Oxide Production and Immunity-Related GTPases. *PLOS ONE* 7(9):e45440.

248. Schoenborn JR, Wilson CB (2007) Regulation of interferon-gamma during innate and adaptive immune responses. *Adv Immunol* 96:41–101.

249. Collier SP, Collins PL, Williams CL, Boothby MR, Aune TM (2012) Cutting Edge: Influence of Tmevpg1, a Long Intergenic Noncoding RNA, on the Expression of Ifng by Th1 Cells. *J Immunol* 189(5):2084–2088.

250. Schoenborn JR, et al. (2007) Comprehensive epigenetic profiling identifies multiple distal regulatory elements directing transcription of the gene encoding interferon-γ. *Nat Immunol* 8(7):ni1474.

251. Winders BR, Schwartz RH, Bruniquel D (2004) A Distinct Region of the Murine IFN-γ Promoter Is Hypomethylated from Early T Cell Development through Mature Naive and Th1 Cell Differentiation, but Is Hypermethylated in Th2 Cells. *J Immunol* 173(12):7377–7384.

252. Szabo SJ, et al. (2000) A Novel Transcription Factor, T-bet, Directs Th1 Lineage Commitment. *Cell* 100(6):655–669.

253. Tato CM, et al. (2006) Opposing roles of NF-κB family members in the regulation of NK cell proliferation and production of IFN-γ. *Int Immunol* 18(4):505–513.

254. Rahman MM, McFadden G (2011) Modulation of NF-κB signalling by microbial pathogens. *Nat Rev Microbiol* 9(4):291–306.

255. Corn RA, et al. (2003) T Cell-Intrinsic Requirement for NF-κB Induction in Postdifferentiation IFN-γ Production and Clonal Expansion in a Th1 Response. *J Immunol* 171(4):1816–1824.

256. Tato CM, Villarino A, Caamaño JH, Boothby M, Hunter CA (2003) Inhibition of NF-κB Activity in T and NK Cells Results in Defective Effector Cell Expansion and Production of IFN-γ Required for Resistance to Toxoplasma gondii. *J Immunol* 170(6):3139–3146.

257. Corn RA, Hunter C, Liou H-C, Siebenlist U, Boothby MR (2005) Opposing Roles for RelB and Bcl-3 in Regulation of T-Box Expressed in T Cells, GATA-3, and Th Effector Differentiation. *J Immunol* 175(4):2102–2110.

258. Gomez JA, et al. (2013) NeST, a long noncoding RNA, controls microbial susceptibility and epigenetic activation of the Ifng locus. *Cell* 152(4):743–754.

259. Collier SP, Henderson MA, Tossberg JT, Aune TM (2014) Regulation of the Th1 Genomic Locus from Ifng through Tmevpg1 by T-bet. *J Immunol* 193(8):3959–3965.

260. Long EO, Kim HS, Liu D, Peterson ME, Rajagopalan S (2013) Controlling NK Cell Responses: Integration of Signals for Activation and Inhibition. *Annu Rev Immunol* 31. doi:10.1146/annurev-immunol-020711-075005.

261. Ma X, et al. (2015) Regulation of IL-10 and IL-12 production and function in macrophages and dendritic cells. *F1000Research* 4. doi:10.12688/f1000research.7010.1.

262. de Groen RA, et al. (2015) IFN-λ-mediated IL-12 production in macrophages induces IFN-γ production in human NK cells. *Eur J Immunol* 45(1):250–259.

263. Xing Z, Zganiacz A, Santosuosso M (2000) Role of IL-12 in macrophage activation during intracellular infection: IL-12 and mycobacteria synergistically release TNF-α and nitric oxide from macrophages via IFN-γ induction. *J Leukoc Biol* 68(6):897–902.

264. Heufler C, et al. (1996) Interleukin-12 is produced by dendritic cells and mediates T helper 1 development as well as interferon-γ production by T helper 1 cells. *Eur J Immunol* 26(3):659–668.

265. Henry CJ, Ornelles DA, Mitchell LM, Brzoza-Lewis KL, Hiltbold EM (2008) IL-12 Produced by Dendritic Cells Augments CD8+ T cell Activation through the Production of the Chemokines CCL1 and CCL17. *J Immunol Baltim Md 1950* 181(12):8576–8584.

266. Bliss SK, Marshall AJ, Zhang Y, Denkers EY (1999) Human polymorphonuclear leukocytes produce IL-12, TNF-alpha, and the chemokines macrophage-inflammatory protein-1 alpha and -1 beta in response to Toxoplasma gondii antigens. *J Immunol Baltim Md 1950* 162(12):7369–7375.

267. Cassatella MA, et al. (1995) Interleukin-12 production by human polymorphonuclear leukocytes. *Eur J Immunol* 25(1):1–5.

268. Luque I, Reyburn H, Strominger JL (2000) Expression of the CD80 and CD86 molecules enhances cytotoxicity by human natural killer cells. *Hum Immunol* 61(8):721–728.

269. Wilson JL, et al. (1999) NK Cell Triggering by the Human Costimulatory Molecules CD80 and CD86. *J Immunol* 163(8):4207–4212.

270. Wang KS, Ritz J, Frank DA (1999) IL-2 Induces STAT4 Activation in Primary NK Cells and NK Cell Lines, But Not in T Cells. *J Immunol* 162(1):299–304.

271. Hunter CA, Gabriel KE, Radzanowski T, Neyer LE, Remington JS (1997) Type I interferons enhance production of IFN-gamma by NK cells. *Immunol Lett* 59(1):1–5.

272. Hunter CA, et al. (1997) Comparison of the effects of interleukin-1α, interleukin-lβ and interferon-γ-inducing factor on the production of interferon-γ by natural killer. *Eur J Immunol* 27(11):2787–2792.

273. Okamura H, et al. (1995) Cloning of a new cytokine that induces IFN-gamma production by T cells. *Nature* 378(6552):88–91.

274. Cooper MA, et al. (2002) In vivo evidence for a dependence on interleukin 15 for survival of natural killer cells. *Blood* 100(10):3633–3638.

275. Koka R, et al. (2003) Interleukin (IL)-15Rα–deficient Natural Killer Cells Survive in Normal but Not IL-15Rα–deficient Mice. *J Exp Med* 197(8):977–984.

276. Carson WE, et al. (1995) The functional characterization of interleukin-10 receptor expression on human natural killer cells. *Blood* 85(12):3577–3585.

277. D'Andrea A, et al. (1993) Interleukin 10 (IL-10) inhibits human lymphocyte interferon gamma-production by suppressing natural killer cell stimulatory factor/IL-12 synthesis in accessory cells. *J Exp Med* 178(3):1041–1048.

278. Yu J, et al. (2006) Pro- and antiinflammatory cytokine signaling: reciprocal antagonism regulates interferon-gamma production by human natural killer cells. *Immunity* 24(5):575–590.

279. Trotta R, et al. (2008) TGF-beta utilizes SMAD3 to inhibit CD16-mediated IFN-gamma production and antibody-dependent cellular cytotoxicity in human NK cells. *J Immunol Baltim Md 1950* 181(6):3784–3792.

280. Afkarian M, et al. (2002) T-bet is a STAT1-induced regulator of IL-12R expression in naïve CD4+ T cells. *Nat Immunol* 3(6):549–557.

281. Agarwal S, Rao A (1998) Modulation of Chromatin Structure Regulates Cytokine Gene Expression during T Cell Differentiation. *Immunity* 9(6):765–775.

282. Mullen AC, et al. (2002) Hlx is induced by and genetically interacts with T-bet to promote heritable T_H1 gene induction. *Nat Immunol* 3(7):652.

283. Djuretic IM, et al. (2007) Transcription factors T-bet and Runx3 cooperate to activate Ifng and silence Il4 in T helper type 1 cells. *Nat Immunol* 8(2):145–153.

284. Cho BK, Wang C, Sugawa S, Eisen HN, Chen J (1999) Functional differences between memory and naive CD8 T cells. *Proc Natl Acad Sci* 96(6):2976–2981.

285. Krämer OH, et al. (2009) A phosphorylation-acetylation switch regulates STAT1 signaling. *Genes Dev* 23(2):223–235.

286. Choudhury GG (2004) A Linear Signal Transduction Pathway Involving Phosphatidylinositol 3-Kinase, Protein Kinase Cϵ, and MAPK in Mesangial Cells

Regulates Interferon-γ-induced STAT1α Transcriptional Activation. *J Biol Chem* 279(26):27399–27409.

287. Uddin S, et al. (2002) Protein Kinase C-δ (PKC-δ) Is Activated by Type I Interferons and Mediates Phosphorylation of Stat1 on Serine 727. *J Biol Chem* 277(17):14408–14416.

288. Wen Z, Zhong Z, Darnell JE (1995) Maximal activation of transcription by statl and stat3 requires both tyrosine and serine phosphorylation. *Cell* 82(2):241–250.

289. Beurel E, Jope RS (2009) Glycogen synthase kinase-3 promotes the synergistic action of interferon-γ on lipopolysaccharide-induced IL-6 production in RAW264.7 cells1. *Cell Signal* 21(6):978–985.

290. Valledor AF, et al. (2008) Selective Roles of MAPKs during the Macrophage Response to IFN-γ. *J Immunol* 180(7):4523–4529.

291. Wang Z, et al. (2015) Interferon-γ Inhibits Nonopsonized Phagocytosis of Macrophages via an mTORC1-c/EBPβ Pathway. *J Innate Immun* 7(2):165–176.

292. Su X, et al. (2015) Interferon-γ regulates cellular metabolism and mRNA translation to potentiate macrophage activation. *Nat Immunol* 16(8):838.

293. Kroczynska B, et al. (2016) Interferon γ (IFNγ) Signaling via Mechanistic Target of Rapamycin Complex 2 (mTORC2) and Regulatory Effects in the Generation of Type II Interferon Biological Responses. *J Biol Chem* 291(5):2389–2396.

294. Alsayed Y, et al. (2000) IFN-γ Activates the C3G/Rap1 Signaling Pathway. *J Immunol* 164(4):1800–1806.

295. Gatto L, et al. (2004) Analysis of SOCS-3 Promoter Responses to Interferon γ. *J Biol Chem* 279(14):13746–13754.

296. Lesinski GB, et al. (2010) Modulation of SOCS protein expression influences the interferon responsiveness of human melanoma cells. *BMC Cancer* 10:142.

297. Liang Y, Xu W-D, Peng H, Pan H-F, Ye D-Q (2014) SOCS signaling in autoimmune diseases: Molecular mechanisms and therapeutic implications. *Eur J Immunol* 44(5):1265–1275.

298. Chong MMW, Thomas HE, Kay TWH (2001) γ-Interferon Signaling in Pancreatic β-Cells Is Persistent but Can Be Terminated by Overexpression of Suppressor of Cytokine Signaling-1. *Diabetes* 50(12):2744–2751.

299. Haspel RL, Salditt-Georgieff M, Darnell JE (1996) The rapid inactivation of nuclear tyrosine phosphorylated Stat1 depends upon a protein tyrosine phosphatase. *EMBO J* 15(22):6262–6268.

300. Endo TA, et al. (1997) A new protein containing an SH2 domain that inhibits JAK kinases. *Nature* 387(6636):921–924.

301. Sakamoto H, Kinjyo I, Yoshimura A (2000) The Janus Kinase Inhibitor, JAB/SOCS-1, Is an Interferon-γ Inducible Gene and Determines the Sensitivity to Interferons. *Leuk Lymphoma* 38(1–2):49–58.

302. Wormald S, et al. (2006) The comparative roles of suppressor of cytokine signaling-1 and -3 in the inhibition and desensitization of cytokine signaling. *J Biol Chem* 281(16):11135–11143.

303. Zhang J-G, et al. (1999) The conserved SOCS box motif in suppressors of cytokine signaling binds to elongins B and C and may couple bound proteins to proteasomal degradation. *Proc Natl Acad Sci* 96(5):2071–2076.

304. Jasmin J-F, Mercier I, Sotgia F, Lisanti MP (2006) SOCS proteins and caveolin-1 as negative regulators of endocrine signaling. *Trends Endocrinol Metab* 17(4):150–158.

305. Zhang X, Mosser D (2008) Macrophage activation by endogenous danger signals. *J Pathol* 214(2):161–178.

306. Eiserich JP, Patel RP, O'Donnell VB (1998) Pathophysiology of nitric oxide and related species: free radical reactions and modification of biomolecules. *Mol Aspects Med* 19(4–5):221–357.

307. Larena M, Regner M, Lobigs M (2013) Cytolytic effector pathways and IFN-γ help protect against Japanese encephalitis. *Eur J Immunol* 43(7):1789–1798.

308. Liu T, Chambers TJ (2001) Yellow Fever Virus Encephalitis: Properties of the Brain-Associated T-Cell Response during Virus Clearance in Normal and Gamma Interferon-Deficient Mice and Requirement for CD4+ Lymphocytes. *J Virol* 75(5):2107–2118.

309. Engelmann F, et al. (2014) Pathophysiologic and Transcriptomic Analyses of Viscerotropic Yellow Fever in a Rhesus Macaque Model. *PLoS Negl Trop Dis* 8(11):e3295.

310. Rosen L (1958) Experimental infection of New World monkeys with dengue and yellow fever viruses. *Am J Trop Med Hyg* 7(4):406–410.

311. Tesh RB, et al. (2001) Experimental Yellow Fever Virus Infection in the Golden Hamster (Mesocricetus auratus). I. Virologic, Biochemical, and Immunologic Studies. *J Infect Dis* 183(10):1431–1436.

312. Xiao S-Y, Zhang H, Guzman H, Tesh RB (2001) Experimental Yellow Fever Virus Infection in the Golden Hamster (Mesocricetus auratus). II. Pathology. *J Infect Dis* 183(10):1437–1444.

313. Julander JG, Shafer K, Smee DF, Morrey JD, Furuta Y (2009) Activity of T-705 in a Hamster Model of Yellow Fever Virus Infection in Comparison with That of a Chemically Related Compound, T-1106. *Antimicrob Agents Chemother* 53(1):202–209.

314. Julander JG, et al. (2014) BCX4430, a Novel Nucleoside Analog, Effectively Treats Yellow Fever in a Hamster Model. *Antimicrob Agents Chemother* 58(11):6607–6614.

315. Julander JG, Ennis J, Turner J, Morrey JD (2011) Treatment of Yellow Fever Virus with an Adenovirus-Vectored Interferon, DEF201, in a Hamster Model ▿. *Antimicrob Agents Chemother* 55(5):2067–2073.

316. Fitzgeorge R, Bradish CJ (1980) Differentiation of Strains of Yellow Fever Virus in γ-irradiated mice. *J Gen Virol* 50(2):345–356.

317. Fitzgeorge R, Bradish CJ (1980) The In Vivo Differentiation of Strains of Yellow Fever Virus in Mice. *J Gen Virol* 46(1):1–13.

318. Thibodeaux BA, et al. (2012) A small animal peripheral challenge model of yellow fever using interferon-receptor deficient mice and the 17D-204 vaccine strain. *Vaccine* 30(21):3180–3187.

319. Green A (2016) Yellow fever continues to spread in Angola. *The Lancet* 387(10037):2493.

320. Woodall JP, Yuill TM (2016) Why is the yellow fever outbreak in Angola a 'threat to the entire world'? *Int J Infect Dis* 48:96–97.

321. Lucey D, Gostin LO (2016) A yellow fever epidemic: A new global health emergency? *JAMA* 315(24):2661–2662.

322. Vasconcelos PFC, Monath TP (2016) Yellow Fever Remains a Potential Threat to Public Health. *Vector-Borne Zoonotic Dis* 16(8):566–567.

323. Gotuzzo E, Yactayo S, Córdova E (2013) Efficacy and Duration of Immunity after Yellow Fever Vaccination: Systematic Review on the Need for a Booster Every 10 Years. *Am J Trop Med Hyg* 89(3):434–444.

324. Barrett AD, Teuwen DE (2009) Yellow fever vaccine — how does it work and why do rare cases of serious adverse events take place? *Curr Opin Immunol* 21(3):308–313.

325. Breugelmans JG, et al. (2013) Adverse events following yellow fever preventive vaccination campaigns in eight African countries from 2007 to 2010. *Vaccine* 31(14):1819–1829.

326. Tao D, et al. (2005) Yellow fever 17D as a vaccine vector for microbial CTL epitopes protection in a rodent malaria model. *J Exp Med* 201(2):201–209.

327. Martins MA, et al. (2013) Immunogenicity of Seven New Recombinant Yellow Fever Viruses 17D Expressing Fragments of SIVmac239 Gag, Nef, and Vif in Indian Rhesus Macaques. *PLOS ONE* 8(1):e54434.

328. Monath TP, et al. (2002) Clinical proof of principle for ChimeriVax™: recombinant live, attenuated vaccines against flavivirus infections. *Vaccine* 20(7–8):1004–1018.

329. Guirakhoo F, et al. (2002) Viremia and Immunogenicity in Nonhuman Primates of a Tetravalent Yellow Fever–Dengue Chimeric Vaccine: Genetic Reconstructions, Dose Adjustment, and Antibody Responses against Wild-type Dengue Virus Isolates. *Virology* 298(1):146–159.

330. Theiler M, Smith HH (1937) The Effect of Prolonged Cultivation in Vitro Upon the Pathogenicity of Yellow Fever Virus. *J Exp Med* 65(6):767–786.

331. Galler R, Freire M da S, Jabor AV, Mann GF (1997) The yellow fever 17D vaccine virus: molecular basis of viral attenuation and its use as an expression vector. *Braz J Med Biol Res* 30(2):157–168.

332. Camacho LAB, et al. (2004) Immunogenicity of WHO-17D and Brazilian 17DD yellow fever vaccines: a randomized trial. *Rev Saúde Pública* 38(5):671–678.

333. Jennings AD, Whitby JE, Minor PD, Barrett ADT (1993) Comparison of the nucleotide and deduced amino acid sequences of the structural protein genes of the yellow fever 17DD vaccine strain from Senegal with those of other yellow fever vaccine viruses. *Vaccine* 11(6):679–681.

334. Hahn CS, Dalrymple JM, Strauss JH, Rice CM (1987) Comparison of the virulent Asibi strain of yellow fever virus with the 17D vaccine strain derived from it. *Proc Natl Acad Sci U S A* 84(7):2019–2023.

335. Douam F, et al. (2017) Single-cell tracking of flavivirus RNA uncovers species-specific interactions with the immune system dictating disease outcome. *Nat Commun* 8:14781.

336. Belsher JL, et al. (2007) Fatal multiorgan failure due to yellow fever vaccine-associated viscerotropic disease. *Vaccine* 25(50):8480–8485.

337. Neves PCC, et al. (2010) CD8+ gamma-delta TCR+ and CD4+ T cells produce IFN-γ at 5–7 days after yellow fever vaccination in Indian rhesus macaques, before the induction of classical antigen-specific T cell responses. *Vaccine* 28(51):8183–8188.

338. Mandl JN, et al. (2011) Distinctive TLR7 Signaling, Type I IFN Production, and Attenuated Innate and Adaptive Immune Responses to Yellow Fever Virus in a Primate Reservoir Host. *J Immunol* 186(11):6406–6416.

339. Bayer A, et al. (2016) Type III Interferons Produced by Human Placental Trophoblasts Confer Protection against Zika Virus Infection. *Cell Host Microbe* 19(5):705–712.

340. Gaucher D, et al. (2008) Yellow fever vaccine induces integrated multilineage and polyfunctional immune responses. *J Exp Med* 205(13):3119–3131.

341. Jennings AD, et al. (1994) Analysis of a Yellow Fever Virus Isolated from a Fatal Case of Vaccine-Associated Human Encephalitis. *J Infect Dis* 169(3):512–518.

342. Jong R de, et al. (1998) Severe Mycobacterial and Salmonella Infections in Interleukin-12 Receptor-Deficient Patients. *Science* 280(5368):1435–1438.

343. Jouanguy E, et al. (1997) Partial interferon-gamma receptor 1 deficiency in a child with tuberculoid bacillus Calmette-Guérin infection and a sibling with clinical tuberculosis. *J Clin Invest* 100(11):2658–2664.

344. Ramirez-Alejo N, Santos-Argumedo L (2014) Innate Defects of the IL-12/IFN-γ Axis in Susceptibility to Infections by Mycobacteria and Salmonella. *J Interferon Cytokine Res* 34(5):307–317.

345. Yossef R, Rosental B, Appel MY, Hershkovitz O, Porgador A (2012) Upregulation of MHC class I expression following dengue virus infection: the mechanism at the promoter level. *Expert Rev Anti Infect Ther* 10(3):285–287.

346. Gardner CL, Burke CW, Higgs ST, Klimstra WB, Ryman KD (2012) Interferon-alpha/beta deficiency greatly exacerbates arthritogenic disease in mice infected with wild-type chikungunya virus but not with the cell culture-adapted live-attenuated 181/25 vaccine candidate. *Virology* 425(2):103–112.

347. Liang J-J, Liao C-L, Liao J-T, Lee Y-L, Lin Y-L (2009) A Japanese encephalitis virus vaccine candidate strain is attenuated by decreasing its interferon antagonistic ability. *Vaccine* 27(21):2746–2754.

348. White LJ, Wang J-G, Davis NL, Johnston RE (2001) Role of Alpha/Beta Interferon in Venezuelan Equine Encephalitis Virus Pathogenesis: Effect of an Attenuating Mutation in the 5′ Untranslated Region. *J Virol* 75(8):3706–3718.

349. Presti RM, Popkin DL, Connick M, Paetzold S, Virgin HW (2001) Novel Cell Type–Specific Antiviral Mechanism of Interferon γ Action in Macrophages. *J Exp Med* 193(4):483–496.

350. Liu S-Y, Sanchez DJ, Aliyari R, Lu S, Cheng G (2012) Systematic identification of type I and type II interferon-induced antiviral factors. *Proc Natl Acad Sci U S A* 109(11):4239–4244.

351. Cho H, Shrestha B, Sen GC, Diamond MS (2013) A Role for Ifit2 in Restricting West Nile Virus Infection in the Brain. *J Virol* 87(15):8363–8371.

352. Riquelme P, et al. (2013) IFN-γ-induced iNOS Expression in Mouse Regulatory Macrophages Prolongs Allograft Survival in Fully Immunocompetent Recipients. *Mol Ther* 21(2):409–422.

353. Coccia EM, et al. (2002) Protein inhibitor of activated signal transducer and activator of transcription (STAT)-1 (PIAS-1) regulates the IFN-γ response in macrophage cell lines. *Cell Signal* 14(6):537–545.

354. Colasanti M, Persichini T, Venturini G, Ascenzi P (1999) S-nitrosylation of viral proteins: molecular bases for antiviral effect of nitric oxide. *IUBMB Life* 48(1):25–31.

355. Akaike T, et al. (2000) Viral mutation accelerated by nitric oxide production during infection in vivo. *FASEB J* 14(10):1447–1454.

356. Dunne KA, et al. (2013) Increased S-Nitrosylation and Proteasomal Degradation of Caspase-3 during Infection Contribute to the Persistence of Adherent Invasive Escherichia coli (AIEC) in Immune Cells. *PLOS ONE* 8(7):e68386.

357. McElroy KL, Tsetsarkin KA, Vanlandingham DL, Higgs S (2006) Manipulation of the yellow fever virus non-structural genes 2A and 4B and the 3'non-coding region to evaluate genetic determinants of viral dissemination from the Aedes aegypti midgut. *Am J Trop Med Hyg* 75(6):1158–1164.

358. McElroy KL, Tsetsarkin KA, Vanlandingham DL, Higgs S (2006) Role of the yellow fever virus structural protein genes in viral dissemination from the Aedes aegypti mosquito midgut. *J Gen Virol* 87(10):2993–3001.

359. Carson MJ, Doose JM, Melchior B, Schmid CD, Ploix CC (2006) CNS immune privilege: hiding in plain sight. *Immunol Rev* 213:48–65.

360. Lannes N, et al. (2017) Interactions of human microglia cells with Japanese encephalitis virus. *Virol J* 14:8.

361. Weaver SC (2014) Arrival of Chikungunya Virus in the New World: Prospects for Spread and Impact on Public Health. *PLoS Negl Trop Dis* 8(6). doi:10.1371/journal.pntd.0002921.

362. Gubler DJ, Vasilakis N, Musso D (2017) History and Emergence of Zika Virus. *J Infect Dis* 216(suppl_10):S860–S867.

363. Vasilakis N, Cardosa J, Hanley KA, Holmes EC, Weaver SC (2011) Fever from the forest: prospects for the continued emergence of sylvatic dengue virus and its impact on public health. *Nat Rev Microbiol* 9(7):532–541.

364. Cooper HM, Paterson Y (2001) Purification of immunoglobulin G fraction from antiserum, ascites fluid, or hybridoma supernatant. *Curr Protoc Mol Biol* Chapter 11:Unit11.14.

365. Yin J, Gardner CL, Burke CW, Ryman KD, Klimstra WB (2009) Similarities and Differences in Antagonism of Neuron Alpha/Beta Interferon Responses by Venezuelan Equine Encephalitis and Sindbis Alphaviruses. *J Virol* 83(19):10036–10047.

366. Laurent-Rolle M, et al. (2014) The Interferon Signaling Antagonist Function of Yellow Fever Virus NS5 Protein Is Activated by Type I Interferon. *Cell Host Microbe* 16(3):314–327.

367. Laurent-Rolle M, et al. (2010) The NS5 protein of the virulent West Nile virus NY99 strain is a potent antagonist of type I interferon-mediated JAK-STAT signaling. *J Virol* 84(7):3503–3515.

368. Woodson SE, Holbrook MR (2011) Infection of hepatocytes with 17-D vaccine-strain yellow fever virus induces a strong pro-inflammatory host response. *J Gen Virol* 92(10):2262–2271.

369. Yang T-C, et al. (2009) Japanese encephalitis virus NS2B-NS3 protease induces caspase 3 activation and mitochondria-mediated apoptosis in human medulloblastoma cells. *Virus Res* 143(1):77–85.

370. Prikhod'ko GG, Prikhod'ko EA, Pletnev AG, Cohen JI (2002) Langat Flavivirus Protease NS3 Binds Caspase-8 and Induces Apoptosis. *J Virol* 76(11):5701–5710.

371. Prikhod'ko GG, Prikhod'ko EA, Cohen JI, Pletnev AG (2001) Infection with Langat Flavivirus or expression of the envelope protein induces apoptotic cell death. *Virology* 286(2):328–335.

372. King P, Goodbourn S (1998) STAT1 Is Inactivated by a Caspase. *J Biol Chem* 273(15):8699–8704.